

**EVALUATION OF LOAD CARRYING CAPACITY OF  
PRECAST CONCRETE PILES BASED ON CPT**

**MD. MOMINUR RAHMAN**

DEPARTMENT OF CIVIL ENGINEERING  
BANGLADESH UNIVERSITY OF ENGINEERING AND TECHNOLOGY  
DHAKA-1000, BANGLADESH  
DECEMBER 27, 2014

**EVALUATION OF LOAD CARRYING CAPACITY OF  
PRECAST CONCRETE PILES BASED ON CPT**

A THESIS

SUBMITTED TO THE DEPARTMENT OF CIVIL ENGINEERING  
IN PARTIAL FULFILLMENT OF THE REQUIREMENTS FOR THE  
DEGREE

OF

MASTER OF ENGINEERING IN CIVIL ENGINEERING  
(GEOTECHNICAL)

**BY**

**MD. MOMINUR RAHMAN**

DEPARTMENT OF CIVIL ENGINEERING  
BANGLADESH UNIVERSITY OF ENGINEERING AND TECHNOLOGY  
DHAKA-1000, BANGLADESH  
DECEMBER 27, 2014

The thesis titled “Evaluation of Load Carrying Capacity of Precast Concrete Piles Based on CPT”, submitted by: Md. Mominur Rahman, Roll No: 0409042220, Session: April, 2009 has been accepted as satisfactory in partial fulfillment of the requirements for the degree of Master of Engineering in Civil Engineering(Geotechnical) on December 27, 2014.

### **BOARD OF EXAMINERS**

---

**Dr. Mehedi Ahmed Ansary**  
Professor,  
Department of Civil Engineering,  
BUET, Dhaka.

Chairman  
( Supervisor)

---

**Dr. Abu Siddique**  
Professor,  
Department of Civil Engineering,  
BUET, Dhaka.

Member

---

**Dr. Md. Jahangir Alam**  
Professor,  
Department of Civil Engineering,  
BUET, Dhaka.

Member

## **DEDICATION**

*I like to dedicate this work to my late mother who loved, raised and guided me in every single step of my life.*

## **DECLARATION**

It is hereby declared that, except where specific references are made, the work embodied in this thesis is the result of investigation carried out by the author under the supervision of Dr. Mehedi Ahmed Ansary, Professor, Department of Civil Engineering, BUET, Dhaka.

Neither this thesis nor any part of it is concurrently submitted to any other institution in candidature for any degree.

---

Md. Mominur Rahman

## **ACKNOWLEDGEMENT**

In the name of Almighty Allah, the most beneficent and most merciful, the author expresses his profound gratitude to Allah for giving him the opportunity to undergo the Masters program and complete this project. The author expresses his sincere gratitude to his honourable, esteemed supervisor, Dr. Mehedi Ahmed Ansary, Professor, Department of Civil Engineering, Bangladesh University of Engineering and Technology (BUET) for his exemplary support, motivation, guidance, and encouragement for this study and research.

Besides Dr. Mehedi Ahmed Ansary the supervisor, the author expresses his heartiest thanks to the rest of the Board of Examiners: Dr. Abu Siddique, Professor, Department of Civil Engineering, BUET, Dr. Md. Jahangir Alam, Professor, Department of Civil Engineering, BUET, for their encouragement and insightful comments.

## ABSTRACT

This thesis presents an evaluation of the performance of eight methods based on cone penetration test (CPT) for predicting the ultimate load carrying capacity of square precast RC concrete piles at a site in Siddhirganj. The following methods were used to predict the load carrying capacity of the piles using the CPT data: Schmertmann, Bustamante and Ganeselli (LCPC/LCP), de Ruyter and Beringen, Tumay and Fakhroo, Price and Wardle, Philipponnat, Aoki and De Alencar, and Penpile method. The ultimate load carrying capacity for each pile is also predicted using the traditional method based on SPT. The ultimate pile capacity obtained from CPT data is also compared graphically with the traditional method based on SPT data.

Prediction of pile capacity has been performed at seven locations within the site. However, Evaluation of the prediction methods was conducted using the statistical analysis based on the results of six friction piles and one end-bearing pile.

An evaluation scheme has been executed to evaluate the CPT methods based on their ability to predict the ultimate pile capacity. Only the criteria selected to evaluate the performance of the prediction methods is: the arithmetic mean and the standard deviation. Based on this evaluation, the Schmertmann method, de Ruyter and Beringen method and Philipponnat method show the best performance in predicting the load carrying capacity of square precast RC concrete piles. But Philipponnat method does not consider the consistency of cohesive soil (soft or hard) to determine the ultimate shaft friction capacity,  $Q_s$  of pile and assumes the same empirical factor for all types of clay. Aoki and De Alencar method exhibits moderate performance and Bustamante and Ganeselli (LCPC/LCP) method shows unsatisfactory performance to estimate the pile capacity. The worst prediction methods are Penpile method and Price and Wardle method, which are very conservative (underpredict the pile capacities) and the Tumay and Fakhroo method, which overpredicts the pile capacity excessively. The four CPT methods, which are de Ruyter and Beringen method, Philipponnat method, Schmertmann method and Aoki and De Alencar method show better performance than the currently used method based on SPT. The soil of this site is very erratic and the thickness of soil layers varies drastically throughout the site. SPT is not reliable for cohesive soil which is the predominant soil of the whole site.

## **TABLE OF CONTENTS**

---

	Page
DECLARATION	i
ACKNOWLEDGEMENT	ii
ABSTRACT	iii
TABLE OF CONTENTS	iv
LIST OF TABLES	vi
LIST OF FIGURES	vii
LIST OF ABBREVIATIONS	xi
<b>CHAPTER 1 :        INTRODUCTION</b>	
1.1 Background	1
1.2 Objective of the Study	2
1.3 Methodology	3
1.4 Outline of the Thesis	3
<b>CHAPTER 2:        LITERATURE REVIEW</b>	
2.1 General	4
2.2 Cone Penetration Test	5
2.3 Prediction of Pile Capacity by CPT	8
2.3.1 Schmertmann Method	8
2.3.2 de Ruiter and Beringen Method	10
2.3.3 Bustamante and Ganeselli Method (LCPC/LCP Method)	12
2.3.4 Tumay and Fakhroo Method (Cone-m Method)	19
2.3.5 Aoki and De Alencar Method	20



	Page	
2.3.6	Price and Wardle Method	22
2.3.7	Philipponnat Method	22
2.3.8	Penpile Method	24
2.4	Prediction of Pile Capacity by SPT	25
2.5	Soil Classification by CPT	29
2.6	Concluding Remarks	3
<b>CHAPTER 3:</b>	<b>DATA COLLECTION AND ANALYSIS</b>	
3.1	General	34
3.2	Geology of the Project	34
3.3	Subsoil Investigation Based on SPT	34
3.4	Subsoil Investigation Based on CPT	40
3.5	Interpretation of Soil Profile from CPT	40
3.6	Characterization of the Investigated Piles	48
3.7	Predicted Pile Capacity using CPT and SPT	49
3.8	Applicability of Methods used for Predicting Pile Capacity	69
3.9	Concluding Remarks	71
<b>CHAPTER 4:</b>	<b>CONCLUSIONS AND RECOMMENDATIONS</b>	
4.1	Conclusions	72
4.2	Recommendations for Further Study	73
<b>REFERENCES</b>		74
<b>APPENDICES</b>		79
Appendix A:	Spliced precast R.C. concrete piles	79
Appendix B:	Sample calculations	81
Appendix C:	CPT machine	89

## LIST OF TABLES

	Page
Table 2.1 LCPC bearing capacity factor ( $k_b$ ) (after Bustamante and Gianceselli, 1982)	13
Table 2.2 Pile categories for the LCPC method (after Bustamante and Gianceselli, 1982)	15
Table 2.3 Input parameters for clay and silt for LCPC method (after Bustamante and Gianceselli, 1982)	16
Table 2.4 Input parameters for sand and gravel for LCPC method (after Bustamante and Gianceselli, 1982)	17
Table 2.5 Empirical factors $F_b$ and $F_s$ (after Aoki and De Alencar, 1975)	20
Table 2.6 The empirical factor $\alpha_s$ values for different soil types (after Aoki and De Alencar, 1975)	21
Table 2.7 Bearing capacity factor (after Philipponnat, 1980)	24
Table 2.8 Empirical factor $F_s$ (after Philipponnat, 1980)	24
Table 2.9 Friction limit factors for concrete piles (after Bowels, 1982)	26
Table 3.1 Number of precast piles investigated based on pile type, soil type, and pile splicing	48
Table 3.2 Results of the analyses conducted on square reinforced concrete piles at a site in Siddhirganj	50

## LIST OF FIGURES

		Page
Figure 2.1	The electric cone penetrometer	7
Figure 2.2	Calculation of the average cone tip resistance in Schmertmann method(1978)	9
Figure 2.3	Penetration design curves for pile side friction in clay in Schmertmann method(1978)	11
Figure 2.4	Penetrometer design curve for side pile friction in sand in Schmertmann method(1978)	11
Figure 2.5	Calculation of the equivalent average tip resistance for LCPC method (after Bustamante and Gianceselli, 1982)	14
Figure 2.6	Maximum friction curves for LCPC method (after Briaud,1986)	18
Figure 2.7	Bearing capacity factor $N_c$ for foundations in clay (after Skempton,1951)	27
Figure 2.8	Limiting adhesion for piles in soft to stiff clays (after Tomlinson,1975)	27
Figure 2.9	Relationship between $\alpha$ -coefficient and angle of internal Friction for cohesionless soils (after Bowles,1982)	28
Figure 2.10	Estimating the bearing capacity factor $Nq'$ (after Bowles,1982 )	28
Figure 2.11	Relationship between the maximum unit pile point resistance and friction angle for cohesionless soils (after Bowles, 1982)	29
Figure 2.12	Soil classification chart for standard electric friction cone (after Douglas and Olsen,1981)	30
Figure 2.13	Soil classification using the probabilistic region method (after Zhang and Tumay,1999)	31
Figure 2.14	Simplified classification chart by Robertson and Campanella for standard electric friction cone (after Robertson and Campanella, 1984)	32

	Page	
Figure 3.1	Layout of bore holes and sections	35
Figure 3.2	Geotechnical Characterization, Section-AA	36
Figure 3.3	Geotechnical Characterization, Section-BB	37
Figure 3.4	Geotechnical Characterization, Section-CC	38
Figure 3.5	Geotechnical Characterization, Section-DD	39
Figure 3.6	Geotechnical Characterization, Section-EE	39
Figure 3.7	Cone Tip Resistance, Shaft Friction and Friction Ratio with Depth	41
Figure 3.8	Cone Tip Resistance, Shaft Friction and Friction Ratio with Depth	42
Figure 3.9	Cone Tip Resistance, Shaft Friction and Friction Ratio with Depth	43
Figure 3.10	Cone Tip Resistance, Shaft Friction and Friction Ratio with Depth	44
Figure 3.11	Cone Tip Resistance, Shaft Friction and Friction Ratio with Depth	45
Figure 3.12	Cone Tip Resistance, Shaft Friction and Friction Ratio with Depth	46
Figure 3.13	Cone Tip Resistance, Shaft Friction and Friction Ratio with Depth	47
Figure 3.14a	Comparison of ultimate end bearing capacity of pile predicted by Schmertmann method with the one predicted by SPT data	53
Figure 3.14b	Comparison of ultimate shaft friction capacity of pile predicted by Schmertmann method with the one predicted by SPT data	53
Figure 3.14c	Comparison of ultimate pile capacity predicted by Schmertmann method with the one predicted by SPT data	54
Figure 3.15a	Comparison of ultimate end bearing capacity of pile predicted by de Ruitter and Beringen method with the one predicted by SPT data	55

	Page	
Figure 3.15b	Comparison of ultimate shaft friction capacity of pile predicted by de Ruiter and Beringen method with the one predicted by SPT data	55
Figure 3.15c	Comparison of ultimate pile capacity predicted by de Ruiter and Beringen method with the one predicted by SPT data	56
Figure 3.16a	Comparison of ultimate end bearing capacity of pile predicted by LCPC method with the one predicted by SPT data	57
Figure 3.16b	Comparison of ultimate shaft friction capacity of pile predicted by LCPC method with the one predicted by SPT data	57
Figure 3.16c	Comparison of ultimate pile capacity predicted by LCPC method with the one predicted by SPT data	58
Figure 3.17a	Comparison of ultimate end bearing capacity of pile predicted by Tumay and Fakhroo method with the one predicted by SPT data	59
Figure 3.17b	Comparison of ultimate shaft friction capacity of pile predicted by Tumay and Fakhroo method with the one predicted by SPT data	59
Figure 3.17c	Comparison of ultimate pile capacity predicted by Tumay and Fakhroo method with the one predicted by SPT data	60
Figure 3.18a	Comparison of ultimate end bearing capacity of pile predicted by Aoki and De Alencar method with the one predicted by SPT data	61
Figure 3.18b	Comparison of ultimate shaft friction capacity of pile predicted by Aoki and De Alencar method with the one predicted by SPT data	61
Figure 3.18c	Comparison of ultimate pile capacity predicted by Aoki and De Alencar method with the one predicted by SPT data	62
Figure 3.19a	Comparison of ultimate end bearing capacity of pile predicted by Price and Wardle method with the one predicted by SPT data	63
Figure 3.19b	Comparison of ultimate shaft friction capacity of pile predicted by Price and Wardle method with the one predicted by SPT data	63

	Page	
Figure 3.19c	Comparison of ultimate pile capacity predicted by Price and Wardle method with the one predicted by SPT data	64
Figure 3.20a	Comparison of ultimate end bearing capacity of pile predicted by Philipponnat method with the one predicted by SPT data	65
Figure 3.20b	Comparison of ultimate shaft friction capacity of pile predicted by Philipponnat method with the one predicted by SPT data	65
Figure 3.20c	Comparison of ultimate pile capacity predicted by Philipponnat method with the one predicted by SPT data	66
Figure 3.21a	Comparison of ultimate end bearing capacity of pile predicted by Penpile method with the one predicted by SPT data	67
Figure 3.21b	Comparison of ultimate shaft friction capacity of pile predicted by Penpile method with the one predicted by SPT data	67
Figure 3.21c	Comparison of ultimate pile capacity predicted by Penpile method with the one predicted by SPT data	68
Figure A1	Spliced Precast RC Concrete Piles before driving	79
Figure A2	Spliced Precast RC Concrete Piles before casting and during driving	80
Figure C1	Hydraulic Pump	89
Figure C2	CPT Machine	90
Figure C3	Short beams inside the machine	91
Figure C4	Long beams on top of the short ones	91
Figure C5	Automatic locks on the auger rods.	92
Figure C6	Depth Sensor Wheel	92

## LIST OF ABBREVIATIONS

CPT	Cone Penetration Test	$\sigma'_{avg}$	average effective overburden pressure
FS	Factor of Safety	$\phi$	angle of internal friction
$Q_u$	Ultimate Axial Load Carrying Capacity of Pile	$K$	coefficient of lateral stress
$Q_t$	End-bearing Capacity of Pile	$\sigma'_v$	effective vertical stress
$Q_s$	Shaft Friction Capacity of Pile	$u$	pore water pressure
$A_t$	Area of Pile Tip	$c_a$	limiting pile/soil adhesion
$A_s$	Area of Pile Shaft	LTRC	Louisiana Transportation Research Center
$q_t$	Unit Tip Bearing Capacity		
$f_s$	Unit Skin Friction Capacity		
$Q_d$	Design Load Carrying Capacity		
D	Diameter of Pile		
$q_c$	Cone Tip Resistance		
psi	Pound per square inch		
mm	Millimeter		
3D	3 Dimensional		
l	Litres		
hrs	Hour		
kN	kilo Newton		
$R_f$	Friction Ratio		
SPT	Standard Penetration Test		
$S_u$	Undrained Shear Strength		
$N_c$	Bearing Capacity Factor		
$c$	cohesion		

# CHAPTER ONE

## INTRODUCTION

### 1.1 BACKGROUND

The prediction of axial pile capacity is a complex problem in geotechnical engineering. Traditional methods of data collection and subsequent analyses are frequently in error when compared to full-scale load tests of the piles. Cone penetration testing (CPT) provides a means by which continuous representative field data may be obtained. The CPT data are acquired by friction cone penetrometers and in these tests the total cone tip resistance and sleeve friction are recorded and pore water pressure is also measured.

Among the different in situ tests, cone penetration test (CPT) is considered the most frequently used method for characterization of geomedia. The CPT is basically advancing a cylindrical rod with a cone tip into the soil and measuring the tip resistance and sleeve friction due to this intrusion. The resistance parameters are used to classify soil strata and to estimate strength and deformation characteristics of soils. Different devices added to cone penetrometers made it possible to apply this test for a wide range of geotechnical applications.

The CPT is a simple, quick, and economical test that provides reliable in situ continuous soundings of subsurface soil. Due to the soft nature of soil deposits at Siddhirganj, the CPT is considered a perfect tool for site characterization.

Deep foundations are usually used when the conditions of the upper soil layers are weak and unable to support the superstructural loads. Piles carry these superstructural loads deep in the ground. Therefore, the safety and stability of pile supported structures depend on the behavior of piles. The square precast RC concrete piles are the most common piles used in Public Works Department.

Piles are expensive structural members, and pile projects are always costly. Soil properties are needed as input parameters for the static analysis. Therefore, it is necessary to conduct field and laboratory tests, which include soil boring, standard penetration test, unconfined compression test, soil classification, etc. Running these field and laboratory tests is expensive and time consuming.

Due to the uncertainties associated with pile design, load tests are usually conducted to verify the design loads and to evaluate the actual response of the pile under loading. Pile load tests



are also expensive. Moreover, pile load tests are a verification tool for pile design and they cannot be a substitute for the engineering analysis of the pile behavior.

Cone penetration test can be utilized for a wide range of geotechnical engineering applications. Implementation of the CPT is limited to identification of dense sand layers required to support the tip of the end-bearing piles. In subsurface exploration, the CPT can be effectively used to identify and classify soils and to evaluate the undrained shear strength. Implementation of the CPT can drastically decrease the number of soil borings and reduce the cost and time required for subsurface characterization. Therefore, implementation of the CPT technology in different engineering applications should be seriously considered.

Due to the similarity between the cone and the pile, the prediction of pile capacity utilizing the cone data is considered among the earliest applications of the CPT. Cone penetration tests can provide valuable and continuous information regarding the soil strength with depth. Therefore, the in situ characteristics of the soil are available to the design engineers at a particular point. The pile design methods that utilize the CPT data prove to predict the pile capacity within an acceptable accuracy.

Generally, pile design depends on soil conditions, pile characteristics, and driving and installation conditions. Local experience usually played an important role in design/analysis of piles. Therefore, it is essential to take advantage of this experience in the CPT technology to identify suitable CPT design methods. Implementation of the CPT (in conjunction with the currently used method) in the analysis/design of piles will foster confidence in the CPT technology. With time and experience, the role of the CPT can be increased while the role of traditional subsurface exploration is reduced.

## **1.2 OBJECTIVE OF THE STUDY**

The major objectives of this study are as follows:

1. To identify the most appropriate methods for estimating the ultimate axial load carrying capacity of precast RC concrete piles from the cone penetration test data.
2. To compare the ultimate pile capacity predicted by different methods utilizing the CPT data with the ultimate pile capacity calculated by the method using the SPT data.

### **1.3 OUTLINE OF THE THESIS**

The thesis is composed of total 4 chapters:

Chapter 2 highlights the different methods of predicting the pile capacity utilizing the CPT data and the method of predicting the pile capacity using the SPT data.

Chapter 3 elaborates the SPT and CPT data collection and analysis in detail and presents the results of the analyses conducted on square reinforced concrete piles for Siddhirganj, Narayanganj soils to predict the pile capacity from the CPT and SPT data.. This research effort is focused on the applicability of eight CPT methods to predict the ultimate axial compression load carrying capacity of piles from CPT data. Comparison of ultimate pile capacity predicted by various methods of CPT with the one predicted by SPT data is also presented graphically.

Chapter 4 presents the conclusion and the recommendations regarding the findings and the future projects.

## CHAPTER TWO LITERATURE REVIEW

### 2.1 GENERAL

Piles are relatively long and generally slender structural foundation members that transmit superstructure loads to deep soil layers. In geotechnical engineering, piles usually serve as foundations when soil conditions are not suitable for the use of shallow foundations. Moreover, piles have other applications in deep excavations and in slope stability. As presented in the literature, piles are classified according to:

- a. the nature of load support (friction and end-bearing piles),
- b. the displacement properties (full-displacement, partial-displacement, and non-displacement piles), and
- c. the composition of piles (timber, concrete, steel, and composite piles).

The behavior of the pile depends on many different factors, including pile characteristics, soil conditions and properties, installation method, and loading conditions. The performance of piles affects the serviceability of the structure they support.

The prediction of pile load carrying capacity can be achieved using different methods such as pile load test, dynamic analysis, static analysis based on soil properties from laboratory tests, and static analysis utilizing the results of in situ tests such as cone penetration test.

In the design and analysis of piles, it is important to identify piles based on the nature of support provided by the surrounding soil, i.e. to classify piles as end-bearing piles and friction piles. While end-bearing piles transfer most of their loads to an end-bearing stratum, friction piles resist a significant portion of their loads via the skin friction developed along the surface of the piles. The behavior of friction piles mainly depends on the interaction between the surrounding soil and the pile shaft.

The ultimate axial load carrying capacity of the pile ( $Q_u$ ) composed of the end-bearing capacity of the pile ( $Q_t$ ) and the shaft friction capacity ( $Q_s$ ). The general equation described in the literature is given by:

$$Q_u = Q_t + Q_s = q_t A_t + f A_s \quad (2.1)$$

where  $q_t$  is the unit tip bearing capacity,  $A_t$  is the area of the pile tip,  $f$  is the unit skin friction,

and  $A_s$  is the area of the pile shaft. In sands, the end-bearing capacity ( $Q_t$ ) dominates, while in soft clays the shaft friction capacity ( $Q_s$ ) dominates.

The design load carrying capacity ( $Q_d$ ) of the pile can be calculated by:

$$Q_d = \frac{Q_u}{F.S.} \quad (2.2)$$

where  $Q_u$  is the ultimate load carrying capacity and  $F.S.$  is the factor of safety.

## 2.2 CONE PENETRATION TEST

The cone penetration test has been recognized as one of the most widely used in situ tests. In Bangladesh, cone penetration testing is not popular. The cone penetration test consists of advancing a cylindrical rod with a conical tip into the soil and measuring the forces required to push this rod. The friction cone penetrometer measures two forces during penetration. These forces are: the total tip resistance ( $q_c$ ), which is the soil resistance to advance the cone tip and the sleeve friction ( $f_s$ ), which is the sleeve friction developed between the soil and the sleeve of the cone penetrometer. The friction ratio ( $R_f$ ) is defined as the ratio between the sleeve friction and tip resistance and is expressed in percent. A schematic of the electric cone penetrometer is depicted in Figure 2.1. The resistance parameters are used to classify soil strata and to estimate strength and deformation characteristics of soils.

The cone penetration test data has been used to predict the ultimate axial pile load carrying capacity. Several methods are available in the literature to predict the axial pile capacity utilizing the CPT data. These methods can be classified into two well-known approaches:

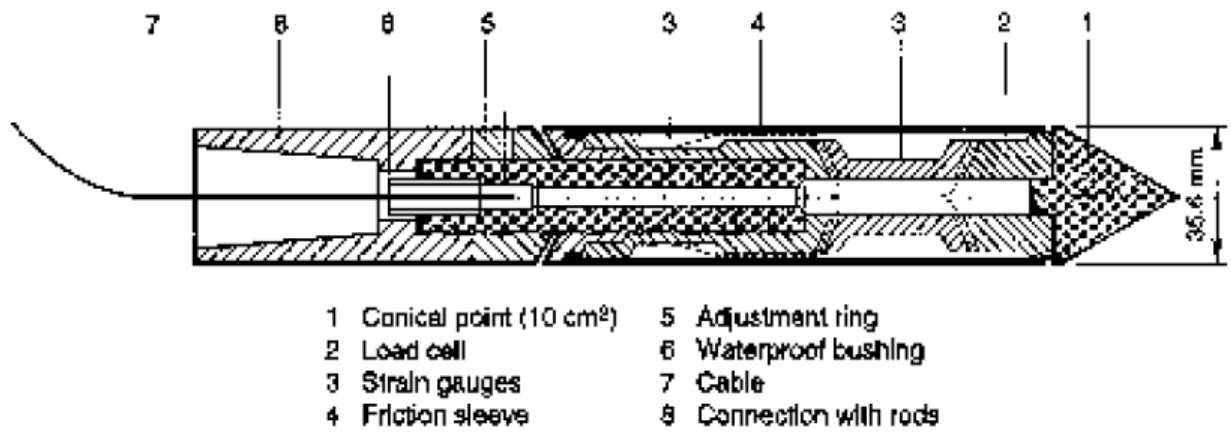
(1) Direct approach: in which

- The unit tip bearing capacity of the pile ( $q_t$ ) is evaluated from the cone tip resistance ( $q_c$ ) profile.
- The unit skin friction of the pile ( $f$ ) is evaluated from either the sleeve friction ( $f_s$ ) profile or the cone tip resistance ( $q_c$ ) profile.

(2) Indirect approach: in which the CPT data ( $q_c$  and  $f_s$ ) are first used to evaluate the soil strength parameters such as the undrained shear strength and the angle of internal friction.

These parameters are then used to evaluate the unit tip bearing capacity of the pile ( $q_t$ ) and the unit skin friction of the pile ( $f$ ) using formulas derived based on semi-empirical/theoretical methods.

In the current research, only the direct methods of predicting the pile capacity from cone penetration test data are investigated.



(a) Schematic of the electric friction cone penetrometer



(b) The 1.27, 2, 10, and 15 cm<sup>2</sup> cone penetrometers

Figure 2.1 The electric cone penetrometer ( after LTRC)

## 2.3 PREDICTION OF PILE CAPACITY BY CPT

In this project, the direct methods are described in detail. These methods are Schmertmann (1978), de Ruiter and Beringen (1979), Bustamante and Ganeselli (LCPC/LPC) (1982), Tumay and Fakhroo (cone-m) (1982), Aoki and De Alencar (1975), Price and Wardle (1982), Philipponnat (1980), and the Penpile (1978) method. The direct CPT methods evaluate the unit tip bearing capacity of the pile ( $q_t$ ) from the measured cone tip resistance ( $q_c$ ) by averaging the cone tip resistance over an assumed influence zone. The unit shaft resistance ( $f$ ) is either evaluated from the measured sleeve friction ( $f_s$ ) in some methods or from the measured cone tip resistance ( $q_c$ ) in others.

### 2.3.1 Schmertmann Method

Schmertmann (1978) proposed the following relationship to predict the unit tip bearing capacity of the pile ( $q_t$ ) from the cone tip resistance ( $q_c$ ):

$$q_t = \frac{q_{c1} + q_{c2}}{2} \quad (2.3)$$

where  $q_{c1}$  is the minimum of the average cone tip resistances of zones ranging from  $0.7D$  to  $4D$  below the pile tip (where  $D$  is the pile diameter) and  $q_{c2}$  is the average of minimum cone tip resistances over a distance  $8D$  above the pile tip. To determine  $q_{c1}$ , the minimum path rule is used as illustrated in Figure 2.2. The described zone (from  $8D$  above to  $0.7D$ - $4D$  below the pile tip) represents the failure surface, which is approximated by a logarithmic spiral. Schmertmann (1978) suggested an upper limit of 150 TSF (15 MPa) for the unit tip bearing capacity ( $q_t$ ).

According to Schmertmann's method (1978), the unit skin friction of the pile ( $f$ ) is given by:

$$f = \alpha_c f_s \quad (2.4)$$

Where  $\alpha_c$  is a reduction factor, which varies from 0.2 to 1.25 for clayey soil, and  $f_s$  is the sleeve friction. Figure 2.3 depicts the variation of  $\alpha_c$  with  $f_s$  for different pile types in clay.

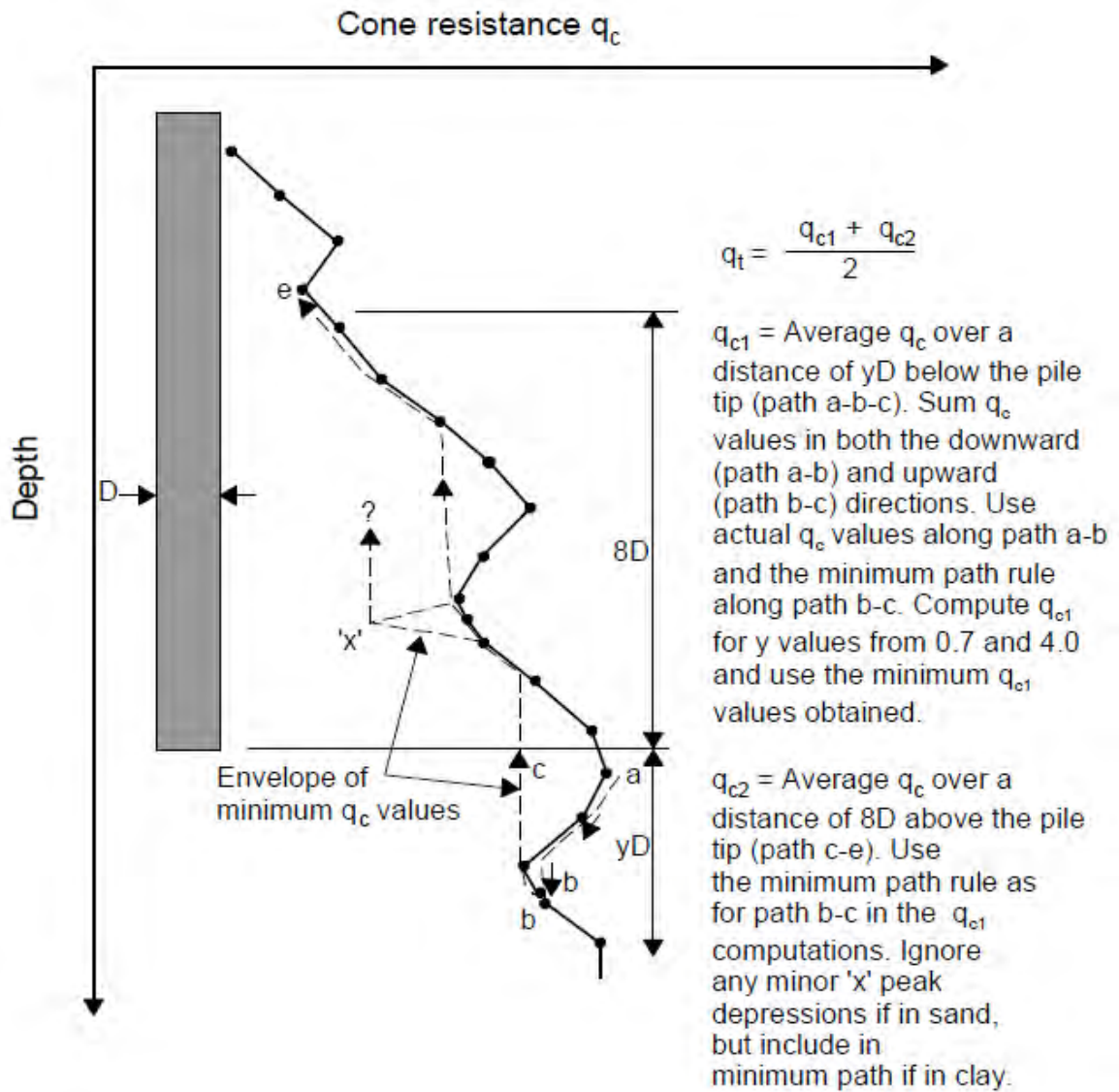


Figure 2.2 Calculation of the average cone tip resistance (after Schmertmann, 1978)



For piles in sand, the friction capacity ( $Q_s$ ) is obtained by:

$$Q_s = \alpha_s \left( \sum_{y=0}^{\delta D} \frac{y}{\delta D} f_s A_s + \sum_{y=\delta D}^L f_s A_s \right) \quad (2.5)$$

where  $\alpha_s$  is the correction factor for sand, which can be obtained from Figure 2.4,  $y$  is the depth at which side resistance is calculated, and  $L$  is the pile length.

Schmertmann (1978) suggested a limit of 1.2 TSF (120 kPa) on  $f$ .

### 2.3.2 de Ruiter and Beringen Method

This method is proposed by de Ruiter and Beringen (1979) and is based on the experience gained in the North Sea. This method is also known as the European method and uses different procedures for clay and sand. In clay, the undrained shear strength ( $S_u$ ) for each soil layer is first evaluated from the cone tip resistance ( $q_c$ ). Then, the unit tip bearing capacity and the unit skin friction are computed by applying suitable multiplying factors. The unit tip bearing capacity is given by:

$$\begin{aligned} q_t &= N_c S_u(\text{tip}) \\ S_u(\text{tip}) &= \frac{q_c(\text{tip})}{N_k} \end{aligned} \quad (2.6)$$

where  $N_c$  is the bearing capacity factor and  $N_c=9$  is considered by this method.  $N_k$  is the cone factor that ranges from 15 to 20, depending on the local experience.  $q_c(\text{tip})$  is the average of cone tip resistances around the pile tip computed similar to Schmertmann method (1978).

The unit skin friction is given by:

$$f = \beta S_u(\text{side}) \quad (2.7)$$

where  $\beta$  is the adhesion factor,  $\beta=1$  for normally consolidated (NC) clay, and  $\beta=0.5$  for

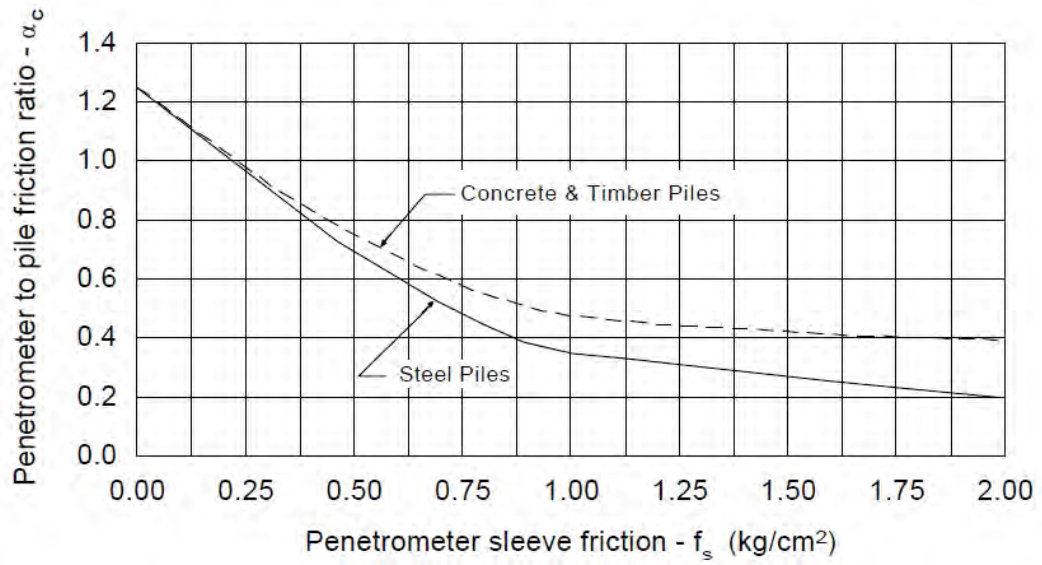


Figure 2.3 Penetration design curves for pile side friction in clay (after Schmertmann,1978)

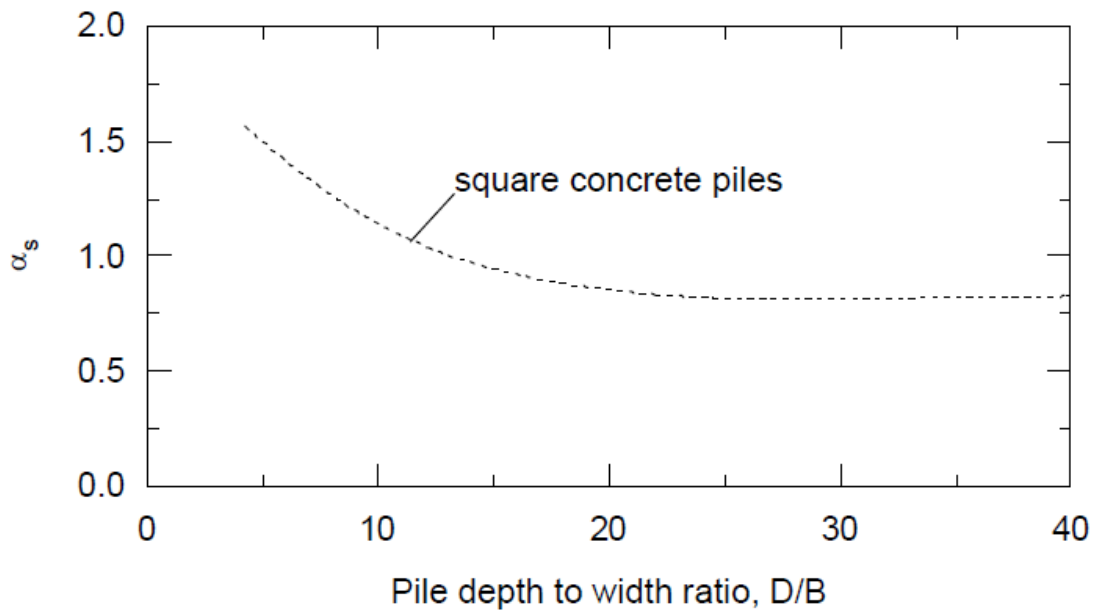


Figure 2.4 Penetrometer design curve for side pile friction in sand (after Schmertmann, 1978)

overconsolidated (OC) clay.  $S_u(side)$ , the undrained shear strength for each soil layer along the pile shaft, is determined by:

$$S_u(side) = \frac{q_c(side)}{N_k} \quad (2.8)$$

where  $q_c(side)$  is the average cone tip resistance along the soil layer.

In sand, the unit tip bearing capacity of the pile ( $q_t$ ) is calculated similar to Schmertmann method(1978). The unit skin friction ( $f$ ) for each soil layer along the pile shaft is given by:

$$f = \min \begin{cases} f_s \\ \frac{q_c(side)}{300} \text{ (compression)} \\ \frac{q_c(side)}{400} \text{ (tension)} \\ 1.2 \text{ TSF (120kPa)} \end{cases} \quad (2.9)$$

de Ruiter and Beringen(1979) imposed limits on  $q_t$  and  $f$  in which  $q_t = 150$  TSF (15 MPa) and  $f = 1.2$  TSF (120 kPa).

### 2.3.3 Bustamante and Gianceselli Method (LCPC/LCP Method)

Bustamante and Gianceselli (1982) proposed this method for the French Highway Department based on the analysis of 197 pile load tests with a variety of pile types and soil conditions . It is also known as the French method and the LCPC/LCP method. In this method, both the unit tip bearing capacity ( $q_t$ ) and the unit skin friction ( $f$ ) of the pile are obtained from the cone tip resistance ( $q_c$ ). The sleeve friction ( $f_s$ ) is not used. The unit tip bearing capacity of the pile ( $q_t$ ) is predicted from the following equation:

$$q_t = k_b q_{eq}(tip) \quad (2.10)$$

where  $k_b$  is an empirical bearing capacity factor that varies from 0.15 to 0.60 depending on the soil type and pile installation procedure (Table 2.1) and  $q_{eq}(tip)$  is the equivalent average cone tip resistance around the pile tip, which is obtained as follows:

1. calculate the average tip resistance ( $q_{ca}$ ) at the tip of the pile by averaging  $q_c$  values over a zone ranging from  $1.5D$  below the pile tip to  $1.5D$  above the pile tip ( $D$  is the pile diameter),
2. eliminate  $q_c$  values in the zone that are higher than  $1.3q_{ca}$  and those are lower than  $0.7q_{ca}$  as shown in **Figure 2.5**, and
3. calculate the equivalent average cone tip resistance ( $q_{eq}(tip)$ ) by averaging the remaining cone tip resistance ( $q_c$ ) values over the same zone (bordered by thick lines in **Figure 2.5**).

The pile unit skin friction ( $f$ ) in each soil layer is estimated from the equivalent cone tip resistance ( $q_{eq}(side)$ ) of the soil layer, soil type, pile type, and installation procedure. The following procedure explains how to determine the unit skin friction ( $f$ ):

- A. based on the pile type, select the pile category from **Table 2.2** (for example, pile category is 9 for square PPC piles),
- B. for each soil layer, select the appropriate curve number (**Tables 2.3 and 2.4**) based on soil type, equivalent cone tip resistance along the soil layer ( $q_{eq}(side)$ ), and pile category, use **Table 2.3** for clay and silt and **Table 2.4** for sand and gravel,
- C. from **Figure 2.6**, use the selected curve number and the equivalent cone tip resistance ( $q_{eq}(side)$ ) to obtain the maximum unit skin friction ( $f$ ), use **Figure 2.6a** for clay and silt and **Figure 2.6b** for sand and gravel.

Table 2.1 LCPC bearing capacity factor ( $k_b$ ) (after Bustamante and Gianceselli,1982)

Soil Type	Bored Piles	Driven Piles
Clay-Silt	0.375	0.60
Sand-Gravel	0.15	0.375
Chalk	0.20	0.40

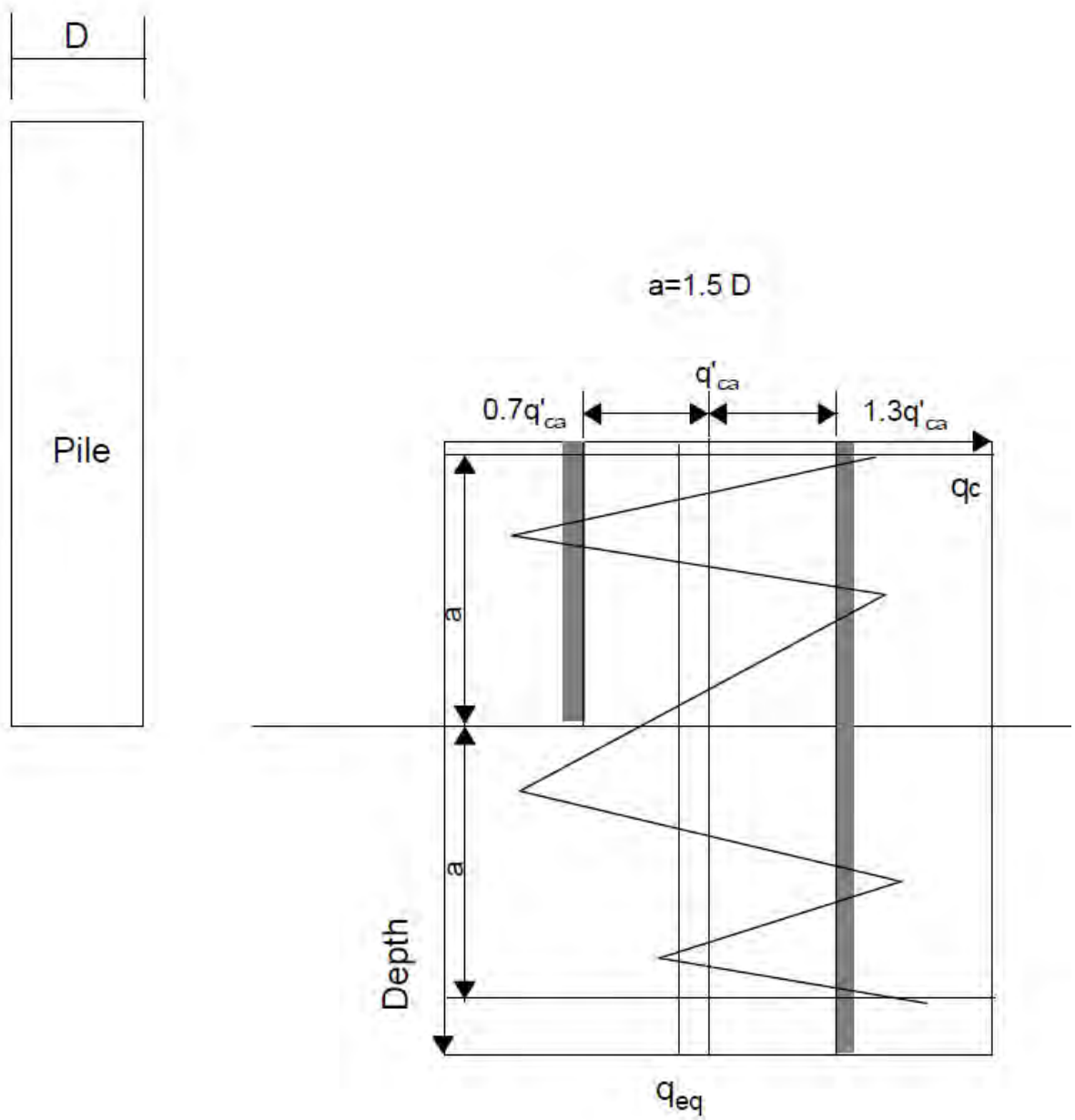


**Figure 2.5** Calculation of the equivalent average tip resistance for LCPC method (after Bustamante and Ganeselli, 1982)

**Table 2.2** Pile categories for the LCPC method (after Bustamante and Gianeselli, 1982)

1. FS Drilled shaft with no drilling mud	Installed without supporting the soil with drilling mud. Applicable only for cohesive soils above the water table.
2. FB Drilled shaft with drilling mud	Installed using mud to support the sides of the hole. Concrete is poured from the bottom up, displacing the mud.
3. FT Drilled shaft with casing (FTU)	Drilled within the confinement of a steel casing. As the casing is retrieved, concrete is poured in the hole.
4. FTC Drilled shaft, hollow auger (auger cast piles)	Installed using a hollow stem continuous auger having a length at least equal to the proposed pile length. The auger is extracted without turning while, simultaneously, concrete is injected through the auger stem.
5. FPU Pier	Hand excavated foundations. The drilling method requires the presence of workers at the bottom of the excavation. The sides are supported with retaining elements or casing.
6. FIG Micropile type I (BIG)	Drilled pile with casing. Diameter less than 250 mm (10 inch). After the casing has been filled with concrete, the top of the casing is plugged. Pressure is applied inside the casing between the concrete and the plug. The casing is recovered by maintaining the pressure against the concrete.
7. VMO Screwed-in piles	Not applicable for cohesionless or soils below water table. A screw type tool is placed in front of a corrugated pipe which is pushed and screwed in place. The rotation is reversed for pulling out the casing while concrete is poured.
8. BE Driven piles, concrete coated	<ul style="list-style-type: none"> <li>- pipe piles 150 mm (6 in.) To 500 mm (20 in.) External diameter</li> <li>- H piles</li> <li>- caissons made of 2, 3, or 4 sheet pile sections.</li> </ul> <p>The pile is driven with an oversized protecting shoe. As driving proceeds, concrete is injected through a hose near the oversized shoe producing a coating around the pile.</p>
9. BBA Driven prefabricated piles	Reinforced or prestressed concrete piles installed by driving or vibrodriving.
10. BM Steel driven piles	<p>Piles made of steel only and driven in place.</p> <ul style="list-style-type: none"> <li>- H piles</li> <li>- Pipe piles</li> <li>- any shape obtained by welding sheet-pile sections.</li> </ul>
11. BPR Prestressed tube pile	Made of hollow cylinder elements of lightly reinforced concrete assembled together by prestressing before driving. Each element is generally 1.5 to 3 m (4-9 ft) long and 0.7 to 0.9 m (2-3 ft) in diameter; the thickness is approximately 0.15 m (6 in.). The piles are driven open ended.
12. BFR Driven pile, bottom concrete plug	Driving is achieved through the bottom concrete plug. The casing is pulled out while low slump concrete is compacted in it.
13. BMO Driven pile, molded.	A plugged tube is driven until the final position is reached. The tube is filled with medium slump concrete to the top and the tube is extracted.
14. VBA Concrete piles, pushed-in.	Pile is made of cylindrical concrete elements prefabricated or cast-in-place, 0.5 to 2.5 m (1.5 to 8 ft) long and 30 to 60 cm (1 to 2 ft) in diameter. The elements are pushed in by a hydraulic jack.
15. VME Steel piles, pushed-in	Piles made of steel only are pushed in by a hydraulic jack..
16. FIP Micropile type II	Drilled pile < 250 mm ( 10 in.) In diameter. The reinforcing cage is placed in the hole and concrete placed from bottom up.
17. BIP High pressure injected pile, large diameter	Diameter > 250 mm (10 in.). The injection system should be able to produce high pressures.

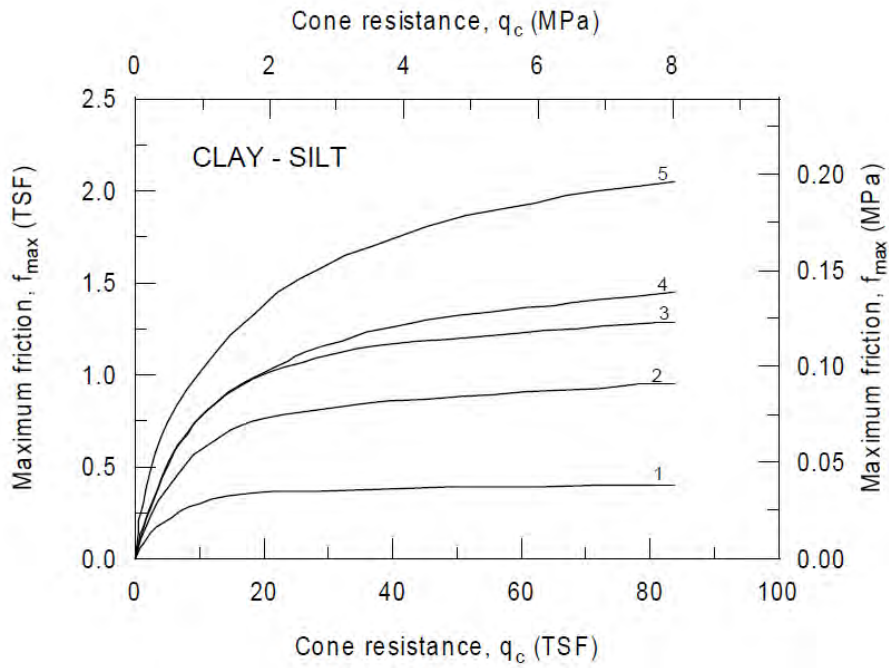
**Table 2.3** Input parameters for clay and silt for LCPC method (after Bustamante and Gianceselli, 1982)

CURVE #	$q_c$ (ksf)	PILE TYPE (see Table 2.2)	COMMENTS ON INSERTION PROCEDURE
1	< 14.6  > 14.6	1-17  1,2	- very probable values when using tools without teeth or with oversized blades and where a remoulded layer of material can be deposited along the sides of the drilled hole. Use these values also for deep holes below the water table where the hole must be cleaned several times. Use these values also for cases when the relaxation of the sides of the hole is allowed due to incidents slowing or stopping the pouring of concrete. For all the previous conditions, experience shows, however, that $q_s$ can be between curves 1 and 2; use an intermediate value of $q_s$ if such value is warranted by a load test.
2	> 25.1  > 25.1  > 25.1  > 25.1  > 25.1	4, 5, 8, 9, 10, 11, 13, 14, 15  7  6  1, 2  3	- for all steel piles, experience shows that, in plastic soils, $q_s$ is often as low as curve 1; therefore, use curve 1 when no previous load test is available. For all driven concrete piles use curve 3 in low plasticity soils with sand or sand and gravel layers or containing boulders and when $q_c > 52.2$ ksf.  - use these values for soils where $q_c < 52.2$ ksf and the rate of penetration is slow; otherwise use curve 1. Also for slow penetration, when $q_c > 93.9$ ksf, use curve 3.  - use curve 3 based on previous load test.  - use these values when careful method of drilling with an auger equipped with teeth and immediate concrete pouring is used. In the case of constant supervision with cleaning and grooving of the borehole walls followed by immediate concrete pouring, for soils of $q_c > 93.9$ ksf, curve 3 can be used.  - for dry holes. It is recommended to vibrate the concrete after taking out the casing. In the case of work below the water table, where pumping is required and frequent movement of the casing is necessary, use curve 1 unless load test results are available.
3	> 25.1 < 41.8	12	- usual conditions of execution as described in DTU 13.2
5	> 14.8	16, 17	- in the case of injection done selectively and repetitively at low flow rate it will be possible to use curve 5, if it is justified by previous load test.

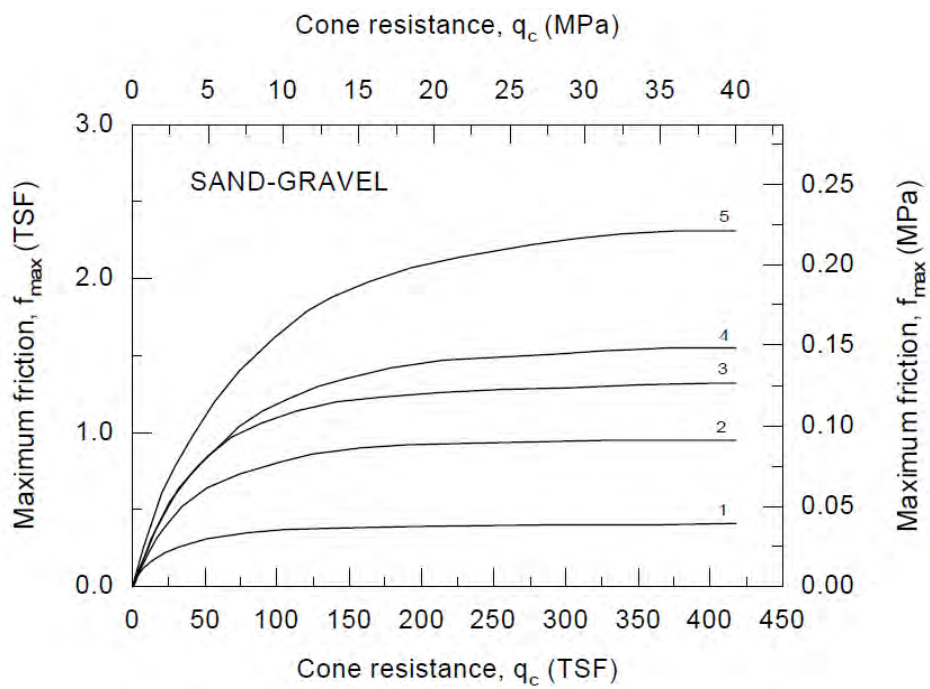
**Table 2.4** Input parameters for sand and gravel for LCPC method (after Bustamante and Gianceselli, 1982)

CURVE #	$q_c$ (ksf)	PILE TYPE (see Table 2.2)	COMMENTS ON INSERTION PROCEDURE
1	< 73.1	2, 3, 4, 6, 7, 8, 9, 10, 11, 12, 13, 14, 15	
2	> 73.1	6, 7, 9, 10, 11, 12, 13, 14, 15	- for fine sands. Since steel piles can lead to very small values of $q_s$ in such soils, use curve 1 unless higher values can be based on load test results. For concrete piles, use curve 2 for fine sands of $q_c > 156.6$ ksf.
	> 104.4	2, 3	- only for fine sands and bored piles which are less than 30 m (100 ft) long. For piles longer than 30 m (100 ft) in fine sand, $q_s$ may vary between curves 1 and 2. Where no load test data is available, use curve 1.
	> 104.4	4	- reserved for sands exhibiting some cohesion.
3	> 156.6	6, 7, 9, 10, 11, 13, 14, 15, 17	- for coarse gravelly sand or gravel only. For concrete piles, use curve 4 if it can be justified by a load test.
	> 156.6	2, 3	- for coarse gravelly sand or gravel and bored piles less than 30 m (100 ft) long. - for gravel where $q_c > 83.5$ ksf, use curve 4
4	> 156.6	8, 12	- for coarse gravelly sand and gravel only.
5	> 104.4	16, 17	- use of values higher than curve 5 is acceptable if based on load test.





(a) For clay and silt



(b) For sand and gravel

Figure 2.6 Maximum friction curves for LCPC method (after Briaud, 1986)

(a) for clay-silt and (b) for sand-gravel

### 2.3.4 Tumay and Fakhroo Method (Cone-m Method)

Tumay and Fakhroo (1982) proposed this method to predict the ultimate pile capacity of piles in clayey soils . The unit tip bearing capacity ( $q_t$ ) is estimated using a procedure similar to Schmertmann's method(1978) as follows:

$$q_t = \frac{q_{c1} + q_{c2}}{4} + \frac{q_a}{2} \quad (2.11)$$

where  $q_{c1}$  is the average of  $q_c$  values  $4D$  below the pile tip,  $q_{c2}$  is the average of the minimum  $q_c$  values  $4D$  below the pile tip, and  $q_a$  is the average of the minimum of  $q_c$  values  $8D$  above the pile tip. Tumay and Fakhroo suggested an upper limit of 150 TSF (15 MPa) for the unit pile tip bearing capacity ( $q_t$ ).

The unit skin friction ( $f$ ) is given by the following expression:

$$f = mf_{sa} \quad (2.12)$$

Tumay and Fakhroo(1982) suggested that  $f=0.72$  TSF (72 kPa). The adhesion factor ( $m$ ) is expressed as:

$$m = 0.5 + 9.5e^{-9f_{sa}} \quad (2.13)$$

where  $f_{sa}=F_t/L$  is the average local friction in TSF, and  $F_t$  is the total cone penetration friction determined for pile penetration length ( $L$ ).

### 2.3.5 Aoki and De Alencar Method

Aoki and De Alencar (1975) proposed the following method to estimate the ultimate load carrying capacity of the pile from CPT data .

The unit tip bearing capacity ( $q_t$ ) is obtained from:

$$q_t = \frac{q_{ca}(tip)}{F_b} \quad (2.14)$$

where  $q_{ca}(tip)$  is the average cone tip resistance around the pile tip, and  $F_b$  is an empirical factor that depends on the pile type. The unit skin friction of the pile ( $f$ ) is predicted by:

$$f = q_c(side) \frac{\alpha_s}{F_s} \quad (2.15)$$

where  $q_c(side)$  is the average cone tip resistance for each soil layer along the pile shaft,  $F_s$  is an empirical factor that depends on the pile type and  $\alpha_s$  is an empirical factor that depends on the soil type. Factors  $F_b$  and  $F_s$  are given in **Table 2.5**. The values of the empirical factor  $\alpha_s$  are presented in **Table 2.6**.

**Table 2.5** Empirical factors  $F_b$  and  $F_s$  (after Aoki and De Alencar ,1975)

Pile Type	$F_b$	$F_s$
Bored	3.5	7.0
Franki	2.5	5.0
Steel	1.75	3.5
Precast concrete	1.75	3.5

**Table 2.6** The empirical factor  $\alpha_s$  values for different soil type (after Aoki and De Alencar,1975)

Soil Type	$\alpha_s(\%)$	Soil Type	$\alpha_s(\%)$	Soil Type	$\alpha_s(\%)$
Sand	1.4	Sandy silt	2.2	Sandy clay	2.4
Silty sand	2.0	Sandy silt with clay	2.8	Sandy clay with silt	2.8
Silty sand with clay	2.4	Silt	3.0	Silt clay with sand	3.0
Clayey sand with silt	2.8	Clayey silt with sand	3.0	Silty clay	4.0
Clayey sand	3.0	Clayey silt	3.4	Clay	6.0

In the current study, the following were used as reference values: for sand  $\alpha_s = 1.4$  percent, for silt  $\alpha_s = 3.0$  percent, and for clay  $\alpha_s = 6.0$  percent. For soils consist of combination of sand, silt, and clay,  $\alpha_s$  values were interpolated based on the probability percentages of sand, silt, and clay in that soil. For example if the probabilistic region estimation (refer to section *Soil Classification by CPT in Background*) of a soil gives 50 percent clay, 20 percent silt, and 30 percent sand then  $\alpha_s = 0.50 \times \alpha_s(\text{clay}) + 0.20 \times \alpha_s(\text{silt}) + 0.30 \times \alpha_s(\text{sand}) = 0.5 \times 6 + 0.2 \times 3 + 0.3 \times 1.4 = 4.02$  percent.

Upper limits were imposed on  $q_t$  and  $f$  as follows:  $q_t = 150$  TSF (15 MPa) and  $f = 1.2$  TSF (120 kPa).

### 2.3.6 Price and Wardle Method

Price and Wardle (1982) proposed the following relationship to evaluate the unit tip bearing capacity ( $q_t$ ) of the pile from the cone tip resistance:

$$q_t = k_b q_c \quad (2.16)$$

where  $k_b$  is a factor depends on the pile type ( $k_b = 0.35$  for driven piles and 0.3 for jacked piles). The unit skin friction ( $f$ ) is obtained from:

$$f = k_s f_s \quad (2.17)$$

where  $k_s$  is a factor depends on the pile type ( $k_s=0.53$  for driven piles, 0.62 for jacked piles, and 0.49 for bored piles). Price and Wardle (1982) proposed the values for these factors based on analysis conducted on pile load tests in stiff clay (London clay).

Upper limits were imposed on  $q_t$  and  $f$  as follows:  $q_t=150$  TSF (15 MPa) and  $f=0.12$  TSF (120 kPa).

### 2.3.7 Philipponnat Method

Philipponnat(1980) proposed the following expression to estimate the unit tip bearing capacity of the pile ( $q_t$ ) from the cone tip resistance ( $q_c$ ):

$$q_t = k_b q_{ca} \quad (2.18)$$

where  $k_b$  is a factor that depends on the soil type as shown in [Table 2.7](#). The cone tip resistance ( $q_{ca}$ ) is averaged as follows:

$$q_{ca} = \frac{q_{ca(A)} + q_{cb(B)}}{2} \quad (2.19)$$

where  $q_{ca(A)}$  is the average cone tip resistance within  $3B$  ( $B$  is the pile width) above the pile tip and  $q_{cb(B)}$  is the average cone tip resistance within  $3B$  below the pile tip. Philipponnat (1980) recommended the removal of the extreme peaks (spikes) when the tip resistance profiles is irregular and imposed a condition in which  $q_{ca(A)} \cdot q_{cb(B)}$ .

The unit skin friction of the pile ( $f$ ) is determined by:

$$f = \frac{\alpha_s}{F_s} q_{cs} \quad (2.20)$$

where  $q_{cs}$  is the average cone tip resistance for each soil layer along the pile shaft,  $F_s$  is a factor depends on the soil type as presented in **Table 2.8**. The factor  $\alpha_s$  depends on the pile type where  $\alpha_s$  equals to 1.25 for precast concrete driven piles. Philipponnat (1980) suggested an upper limit for the skin friction ( $f_{lim}$ ), for precast concrete driven piles  $f_{lim} = 1.2 P_A$  ( $P_A$  is the atmospheric pressure).

**Table 2.7** Bearing capacity factor ( $k_b$ ) (after Philipponnat,1980)

Soil Type	$k_b$
Gravel	0.35
Sand	0.40
Silt	0.45
Clay	0.50

**Table 2.8** Empirical factor  $F_s$  (after Philipponnat,1980)

Soil Type	$F_s$
Clay and calcareous clay	50
Silt, sandy clay, and clayey sand	60
Loose sand	100
Medium dense sand	150
Dense sand and gravel	200

### 2.3.8 Penpile Method

The penpile method (1978) was proposed by Clisby et al. for the Mississippi Department of Transportation . The unit tip bearing capacity of the pile ( $q_t$ ) is determined from the following relationship:

$$q_t = \begin{cases} 0.25q_c & \text{for pile tip in clay} \\ 0.125q_c & \text{for pile tip in sand} \end{cases} \quad (2.21)$$

where  $q_c$  is the average of three cone tip resistances close to the pile tip.

The unit skin friction of the pile shaft ( $f$ ) is obtained from the following relationship:

$$f = \frac{f_s}{1.5 + 0.1f_s} \quad (2.22)$$

where  $f$  is expressed in psi (lb/in<sup>2</sup>) and  $f_s$  is the sleeve friction of the cone expressed in psi.

## 2.4 PREDICTION OF PILE CAPACITY BY SPT

The following soil characteristics and parameters are required to predict the pile capacity using this method: (a) soil profile and thickness of each soil layer, (b) the shear strength parameters: cohesion and angle of internal friction, and (c) unit weight. The angle of internal friction is obtained from the standard penetration test results or from laboratory tests.

For cohesive soil, the unit tip bearing capacity of the pile is evaluated from the following relationship:

$$q_t = cN_c \quad (2.23)$$

where  $c$  is the cohesion of the soil layer,  $N_c$  is the bearing capacity factor.

Figure 2.7 presents the variation of  $N_c$  with the ratio  $R$  ( $R=D/B$ , depth/pile diameter). The unit skin friction can be predicted by:

$$f = c_a \quad (2.24)$$

where  $c_a$  is the limiting pile/soil adhesion for cohesive soil. The variation of  $c_a$  with soil cohesion is shown in Figure 2.8.

For cohesionless soil, the unit tip bearing capacity of the pile is predicted by:

$$q_t = \alpha N_q \sigma'_v \quad (2.25)$$

where  $\alpha$  is an empirical factor depends on the angle of internal friction, pile width  $B$ , and pile depth  $D$  (Figure 2.9).  $N_q$  is the bearing capacity factor (Figure 2.10), and  $\sigma'_v$  is the effective vertical stress. For cohesionless soil,  $q_t$  calculated from equation 2.25 should be less or equal to the maximum unit tip bearing capacity evaluated from Figure 2.11.

The unit skin friction can be predicted by:



$$f = \sigma'_{avg} K \tan \phi \quad (2.26)$$

where  $\sigma'_{avg}$  is the average effective overburden pressure of the soil layer,  $K$  is the coefficient of lateral stress ( $K=1.3$  for PPC piles), and  $\phi$  is the angle of internal friction. The unit skin friction  $f$  evaluated from [equation 2.26](#) should be reduced based on soil type by the friction limit factors presented in [Table 2.9](#).

**Table 2.9** Friction limit factors for concrete piles (after Bowels, 1982)

Soil Type	Friction Limit for Concrete Piles
Clean sand	1.00
Silty sand	0.75
Clean silt	0.60
Sandy clay, clayey silt	0.40

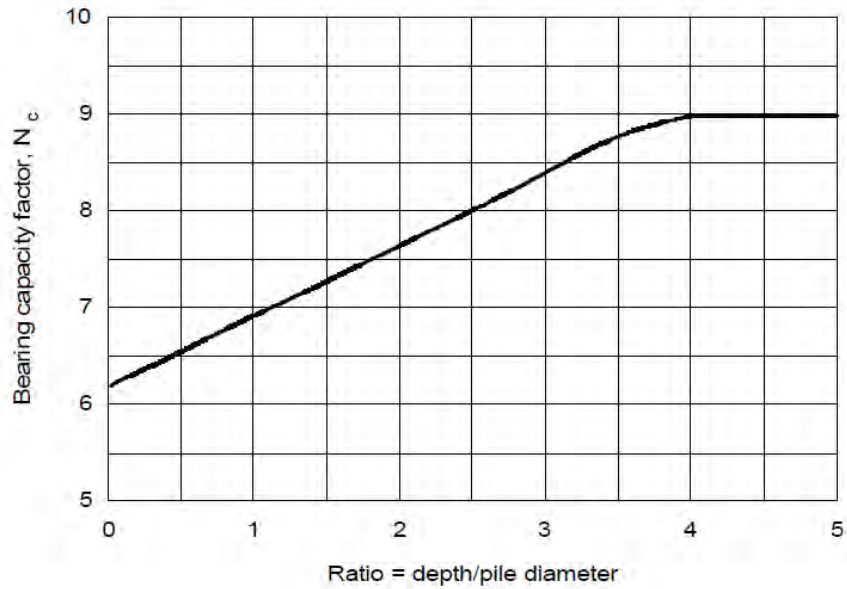


Figure 2.7 Bearing capacity factor  $N_c$  for foundations in clay (after Skempton,1951)

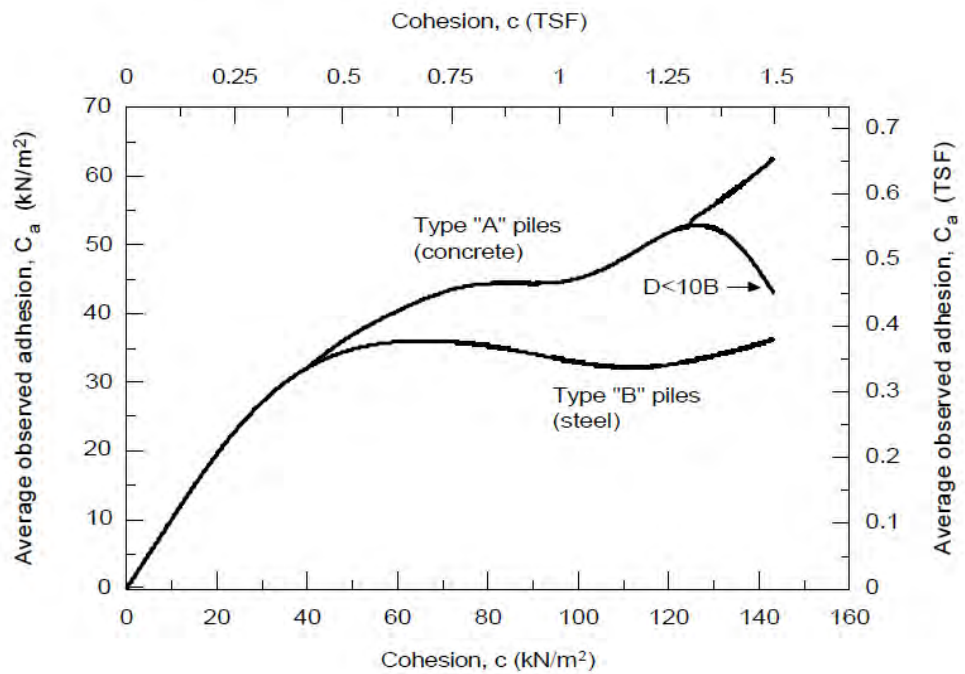
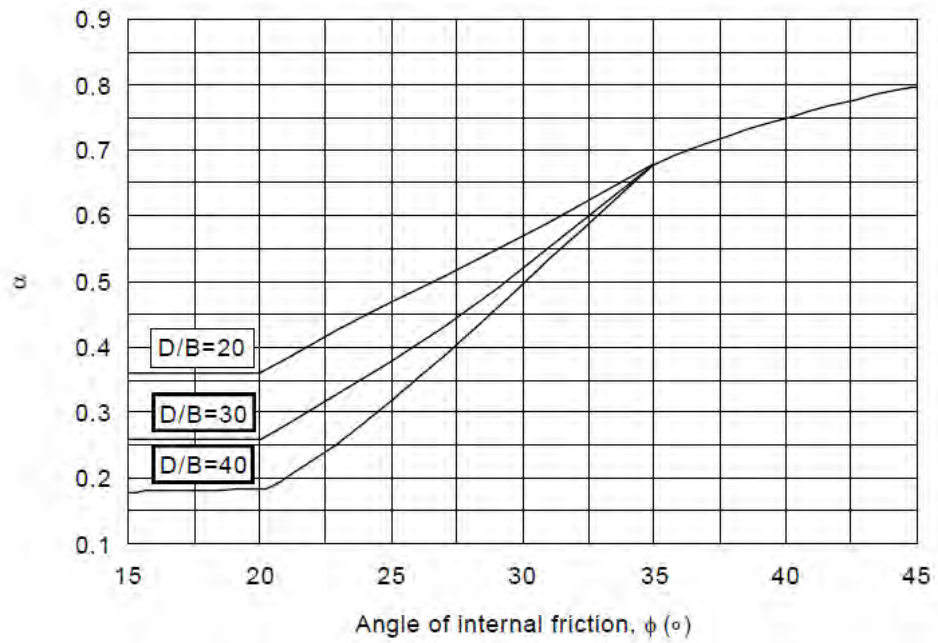
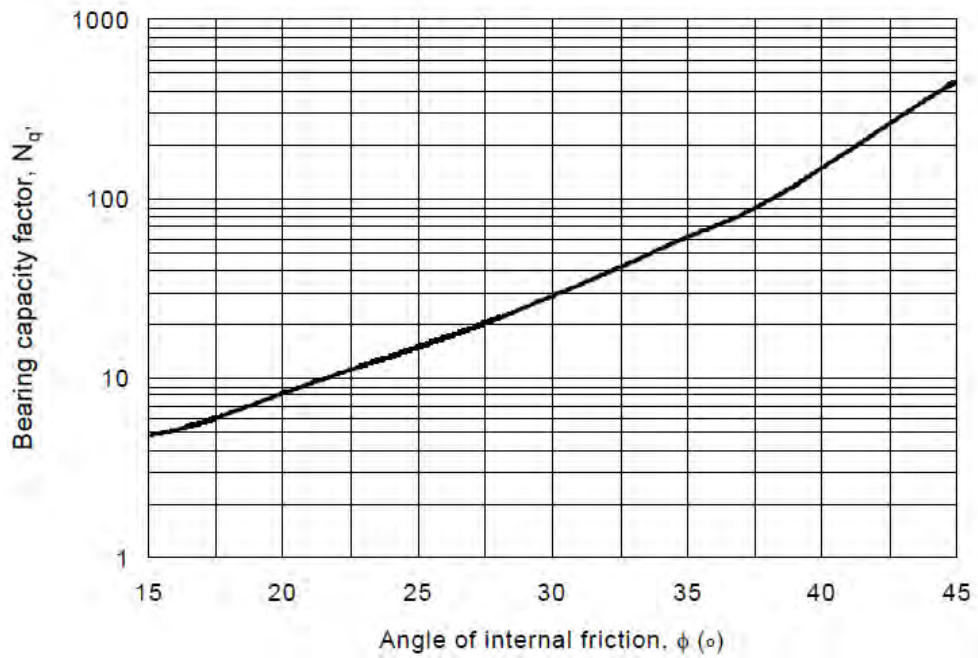


Figure 2.8 Limiting adhesion for piles in soft to stiff clays(after Tomlinson,1975)



**Figure 2.9** Relationship between  $\alpha$ -coefficient and angle of internal Friction for cohesionless soils (after Bowles, 1982)



**Figure 2.10** Estimating the bearing capacity factor  $N_{q'}$  (after Bowles, 1982)

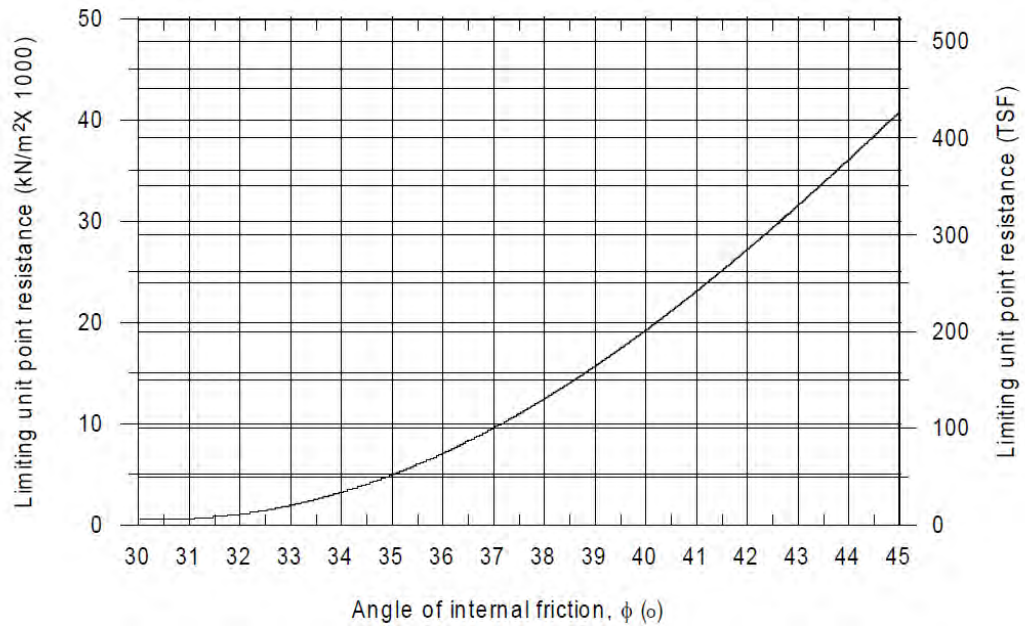
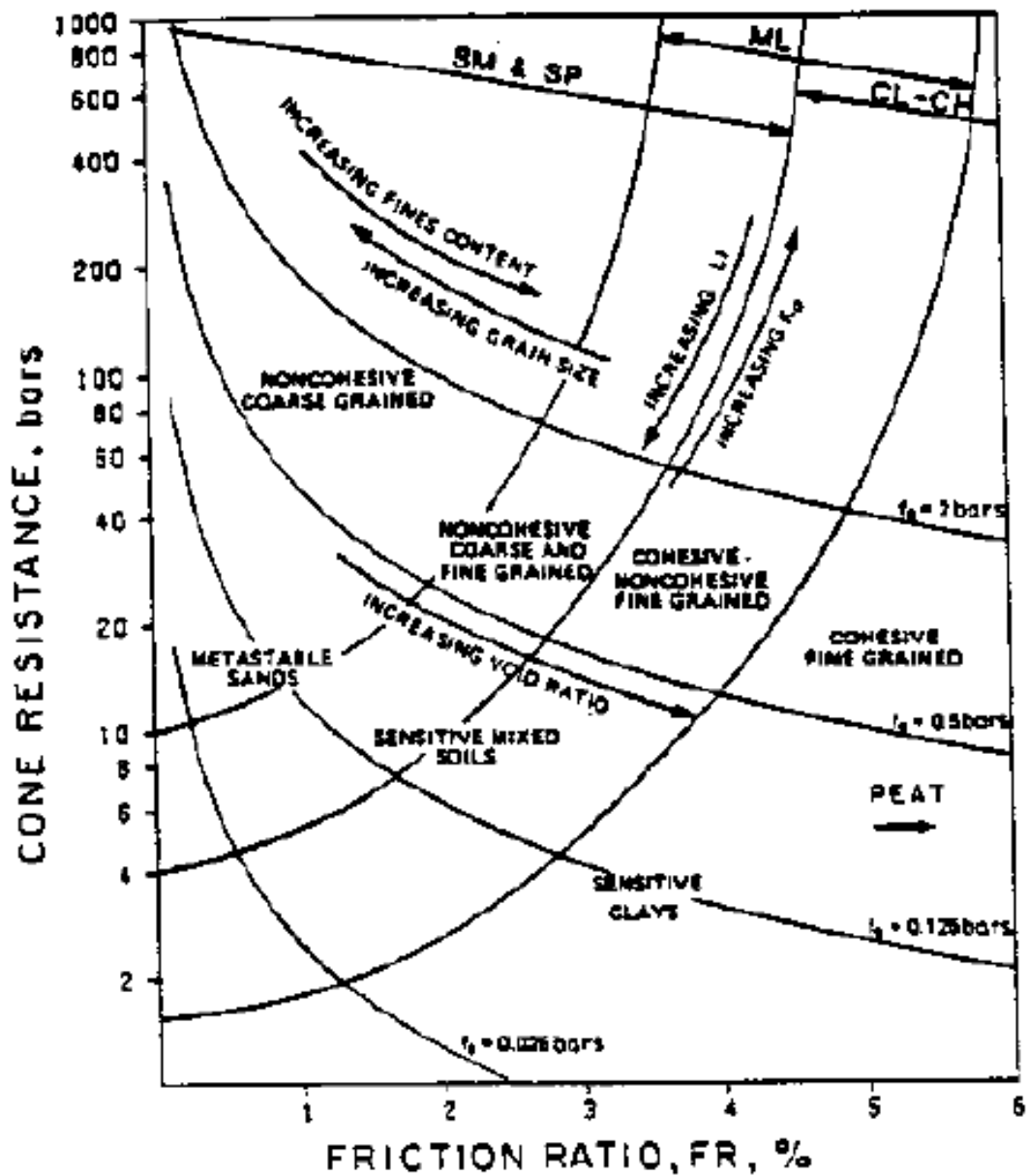


**Figure 2.11** Relationship between the maximum unit pile point resistance and friction angle for cohesionless soils (after Bowles, 1982)

## 2.5 SOIL CLASSIFICATION BY CPT

Cone penetration test is a popular tool for in situ site characterization. Soil classification and identification of soil stratigraphy can be achieved by analyzing the CPT data. Clayey soils usually show low cone tip resistance, high sleeve friction and therefore high friction ratio, while sandy soils show high cone tip resistance, low sleeve friction, and low friction ratio. Soil classification methods by CPT employ the CPT to identify soil from classification charts. Soil classification charts by Douglas and Olsen and Robertson and Campanella are shown in **Figures 2.12** and **2.14**. Zhang and Tumay proposed the probabilistic region estimation method for soil classification. This method is similar to the classical soil classification methods where it is based on soil composition. The method identifies three soil types: clayey, silty, and sandy soils. The probabilistic region estimation determines the probability of each soil constituent (clay, silt, and sand) at certain depth. Typical soil profile obtained by the probabilistic region estimation is shown in **Figure 2.13**.



$$1 \text{ bar} = 100 \text{ kPa} \approx 1 \text{ kg/cm}^2$$

Figure 2.12 Soil classification chart for standard electric friction cone (after Douglas and Olsen, 1981)

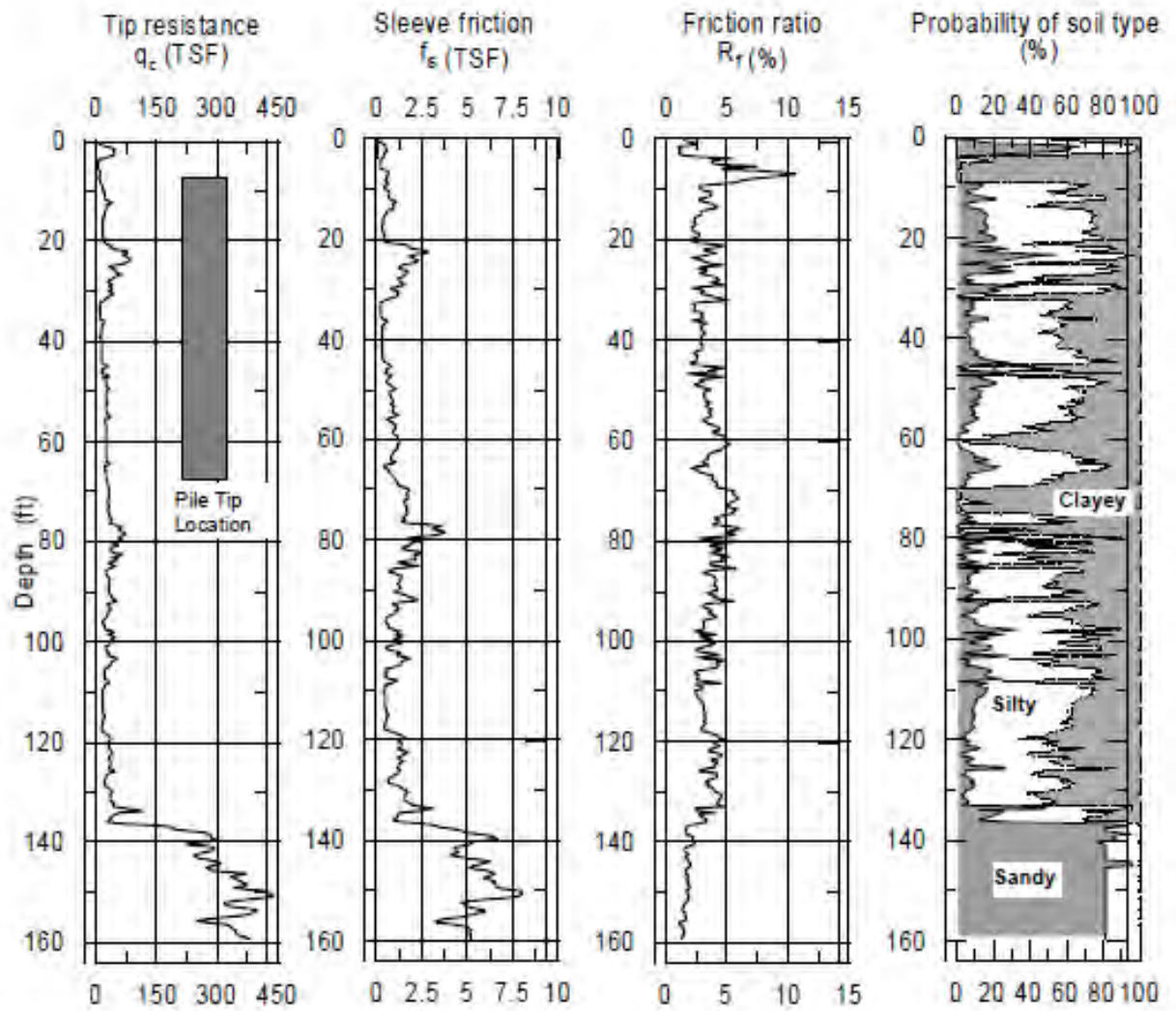


**Figure 2.13** Soil classification using the probabilistic region method (after Zhang and Tumay, 1999)

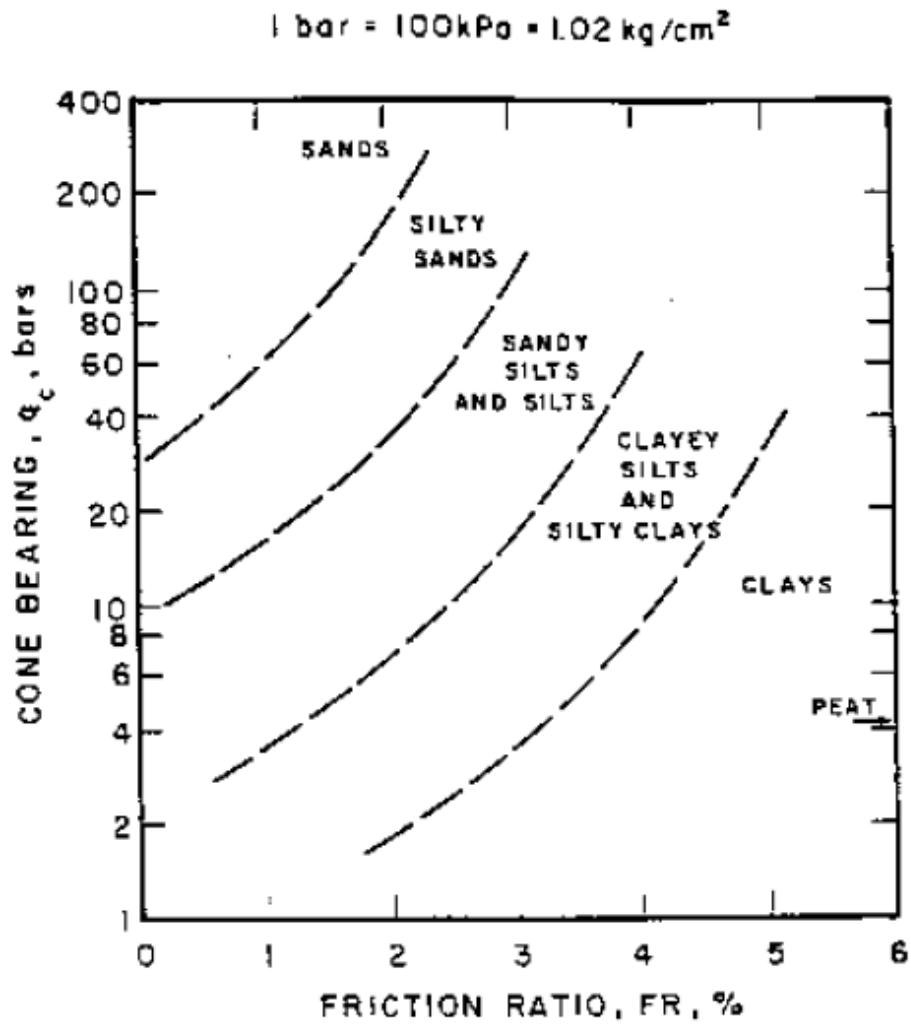


Figure 2.14 Simplified classification chart for standard electric friction cone (after Robertson and Campanella, 1984)

## 2.6 CONCLUDING REMARKS

In this chapter various methods for estimating pile capacity using CPT and SPT have been discussed. The ultimate axial load carrying capacity of the pile ( $Q_u$ ) consists of the end-bearing capacity of the pile ( $Q_t$ ) and the shaft friction capacity ( $Q_s$ ). Classifying piles as end-bearing piles and friction piles is very important based on the nature of support provided by the surrounding soil in the case of pile design and analysis. In the case of the cone penetration test two forces are measured during penetration: the total tip resistance ( $q_c$ ) and the sleeve friction ( $f_s$ ). The friction ratio ( $R_f$ ) is defined as the ratio between the sleeve friction and tip resistance and is expressed in percent. Eight methods of predicting the pile capacity utilizing the CPT data are described in detail. These methods are Schmertmann(1978), de Ruiter and Beringen(1979), Bustamante and Gianselli (LCPC/LPC)(1982), Tumay and Fakhroo (cone-m)(1982), Aoki and De Alencar(1975), Price and Wardle(1982), Philipponnat(1980), and the Penpile (1978) method. The direct CPT methods evaluate the unit tip bearing capacity of the pile ( $q_t$ ) from the measured cone tip resistance ( $q_c$ ) by averaging the cone tip resistance over an assumed influence zone. The unit shaft resistance ( $f$ ) is either evaluated from the measured sleeve friction ( $f_s$ ) in some methods or from the measured cone tip resistance ( $q_c$ ) in others. The following soil characteristics and parameters are required to predict the pile capacity using the method based on SPT: (a) soil profile and thickness of each soil layer, (b) the shear strength parameters: cohesion and angle of internal friction, and (c) unit weight. The angle of internal friction is obtained from the standard penetration test results or from laboratory tests.



## **CHAPTER THREE**

### **DATA COLLECTION AND ANALYSIS**

#### **3.1 GENERAL**

The study location is at a site in Siddhirganj. In this site seven CPT and twelve SPT have been carried out. In this chapter pile capacity has been estimated from CPT and SPT methods discussed in chapter 2.

#### **3.2 GEOLOGY OF THE PROJECT**

According to geological map of Bangladesh published in 1990 geological characteristics of Siddhirganj is described. Geology of this location is alluvial silt – light to medium grey, fine sandy to clayey silt. Commonly poorly stratified; average grain size decreases away from main channels. Chiefly deposited in flood basins and interstream areas. Unit includes small backswamp deposits and varying amounts of thin, interstratified sand, deposited during episodic or unusually large floods. Illite is the most abundant clay mineral. Most areas are flooded annually. Included in this unit are thin veneers of sand spread by episodic large floods over flood-plain silts. Historic pottery, artefacts, and charcoal ( radiocarbon dated 500-6000 yrs. B.P.) found in upper 4 m.

#### **3.3 SUBSOIL INVESTIGATION BASED ON SPT**

**Figure 3.1** represents the site plan showing the five sections of soil profiles, location of twelve bore holes for SPT values and location of seven CPT points. **Figures 3.2-3.6** describe the five soil profile sections having twelve bore holes which exhibit SPT values with depth, visual soil classification and thickness of soil layers. RL of the site is not the same. RL is 5.7m for bore hole no. 02, 03,04, 05, 06, 07, 08, 09, 10, 11 and RL is 4.0m and 5.3m for bore hole no. 12 and 01 respectively.

The soil of the site is very erratic in nature. The predominant soil of the whole site is clay and the thickness of the clay layers varies drastically among the bore holes. The maximum and minimum thickness of clay layers is 26m and 12m respectively when total depth of all bore holes is 26m. For bore hole no. 05 and 06, soil of 26m depth is clay; for bore hole no. 3, 8, 9, 11 and 12 the maximum 6m top soil is either fine sand or nonplastic silt when the soil of the remaining depth is clay; for bore hole no. 1, 7 and 10 the maximum 16m top soil is clay when the soil of the remaining depth is nonplastic silt and clay; for bore hole no. 4, the 8m top soil is fine sand, clay and nonplastic silt when the soil of the remaining depth is clay; for bore hole no. 2, the 2m top soil is nonplastic silt, then 18m depth is clay, then 2m depth is nonplastic silt and the remaining depth is clay.

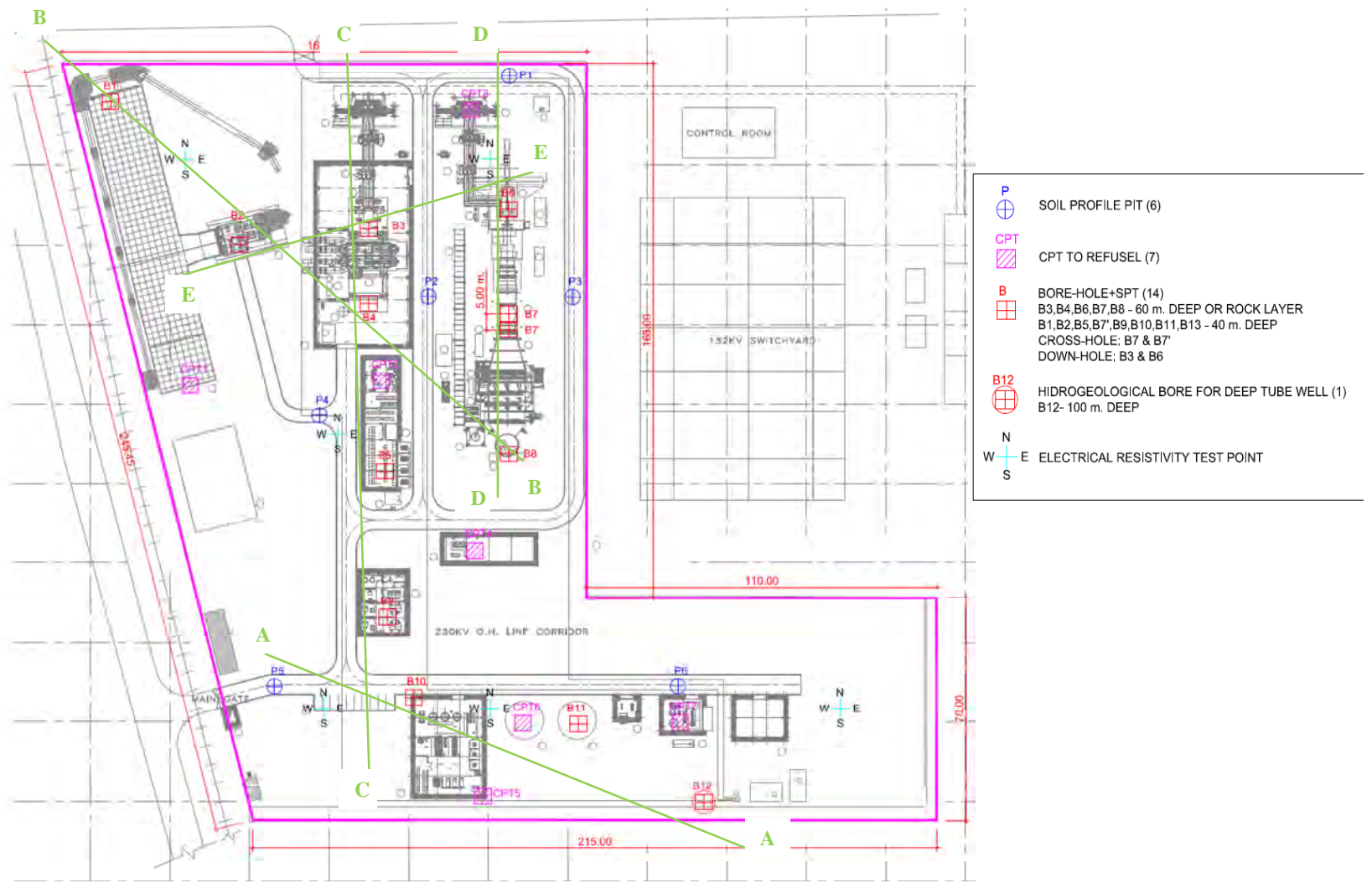


Figure 3.1 Layout of bore holes and sections

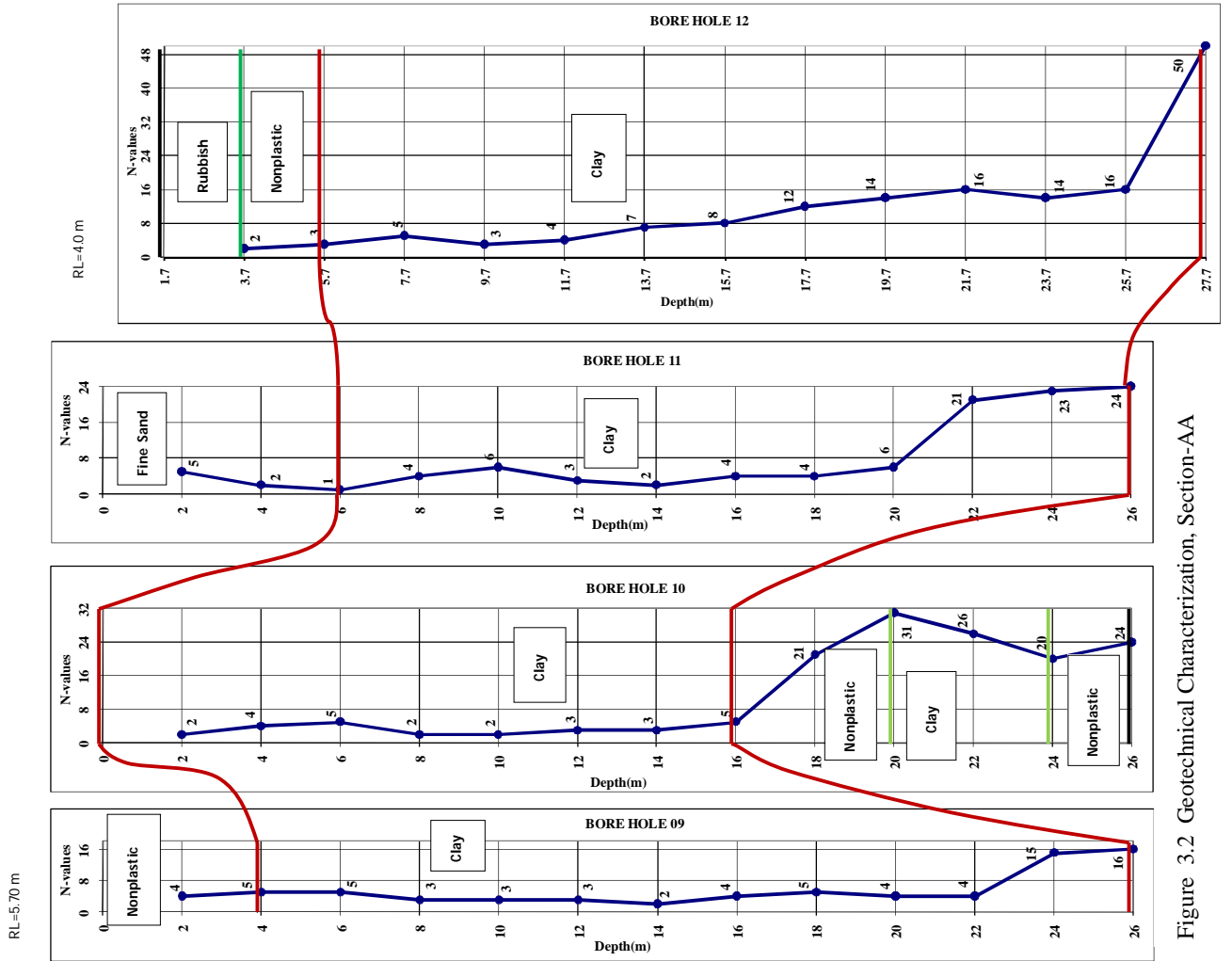


Figure 3.2 Geotechnical Characterization, Section-AA

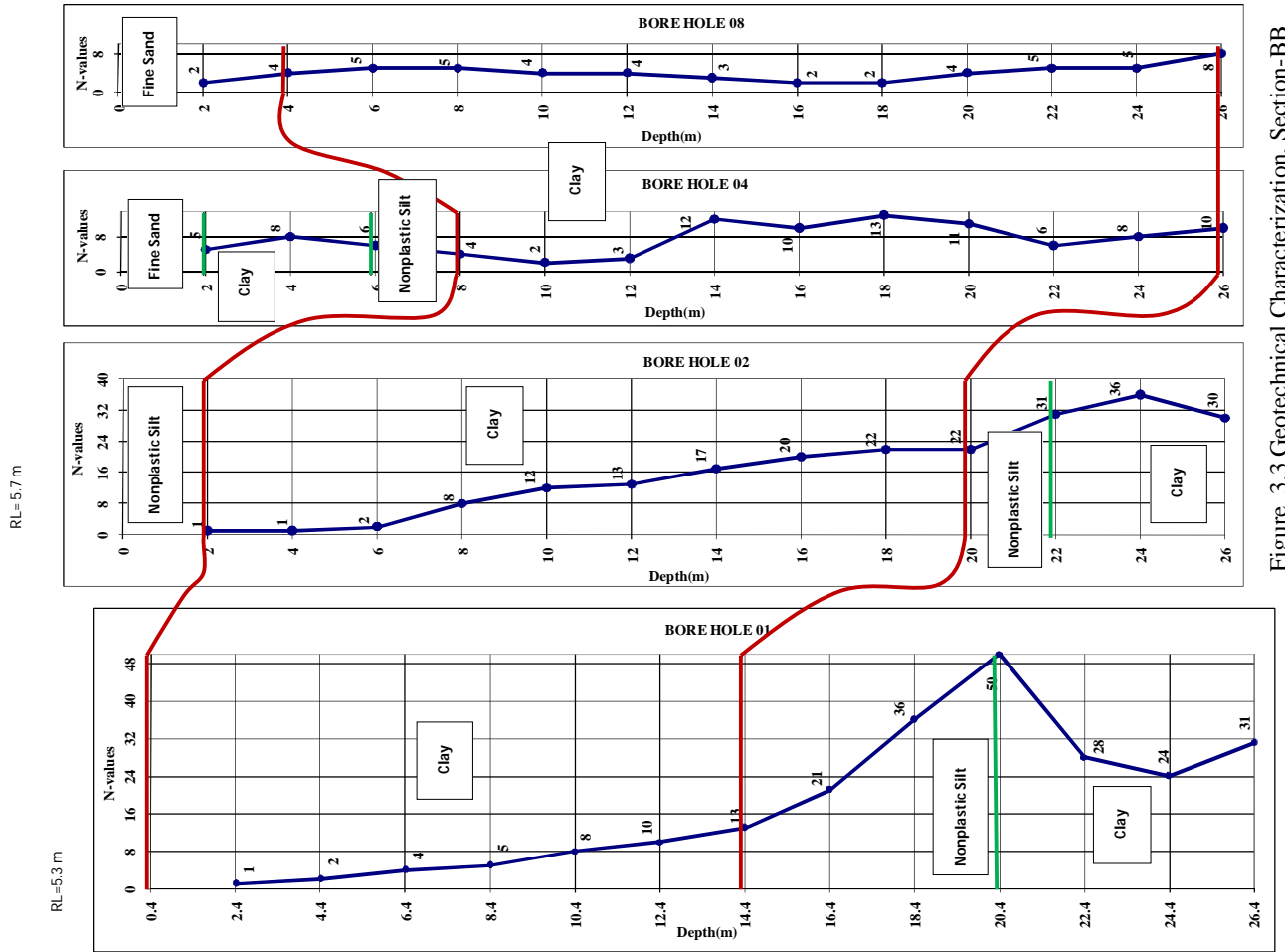


Figure 3.3 Geotechnical Characterization, Section-BB

RL=5.70 m

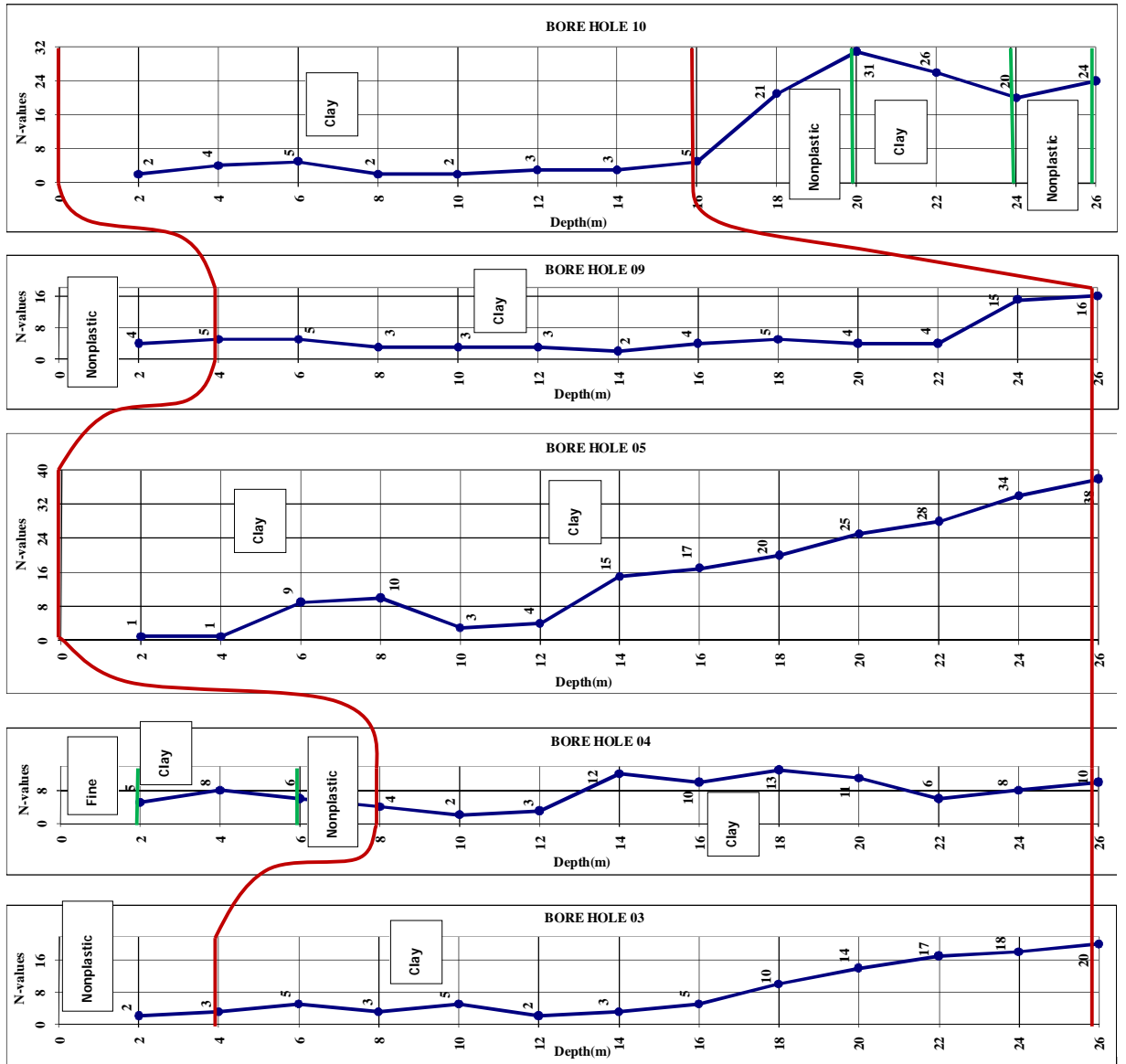


Figure 3.4 Geotechnical Characterization, Section-CC

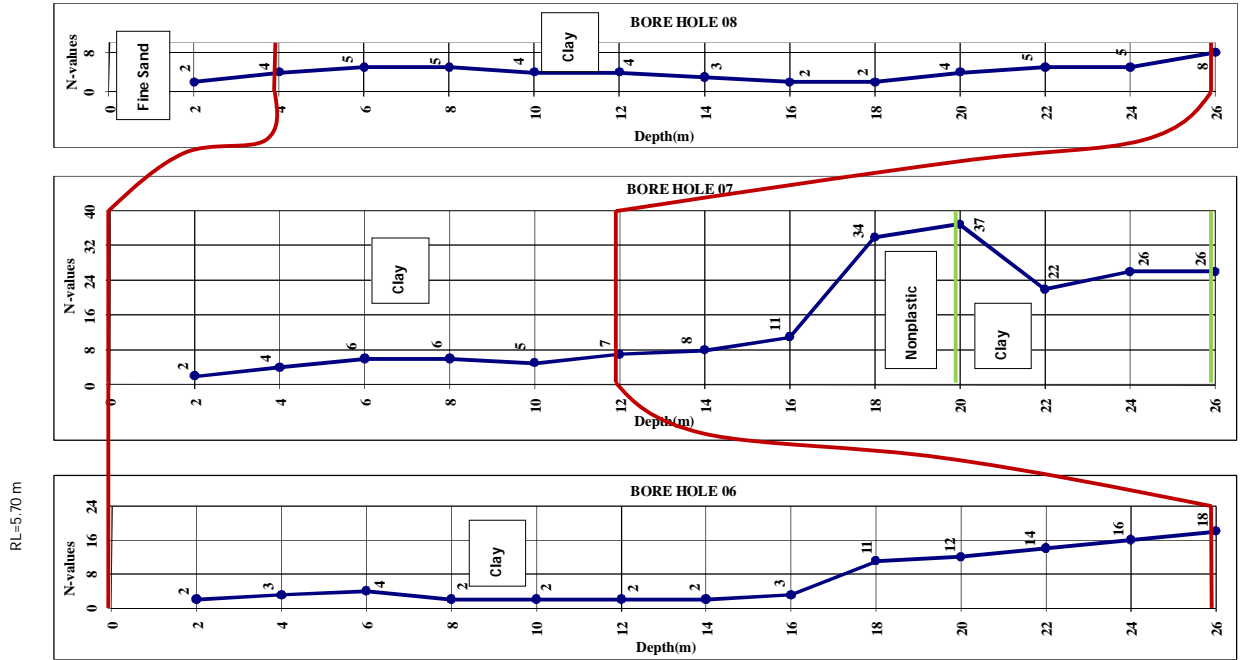


Figure 3.5 Geotechnical Characterization, Section-DD

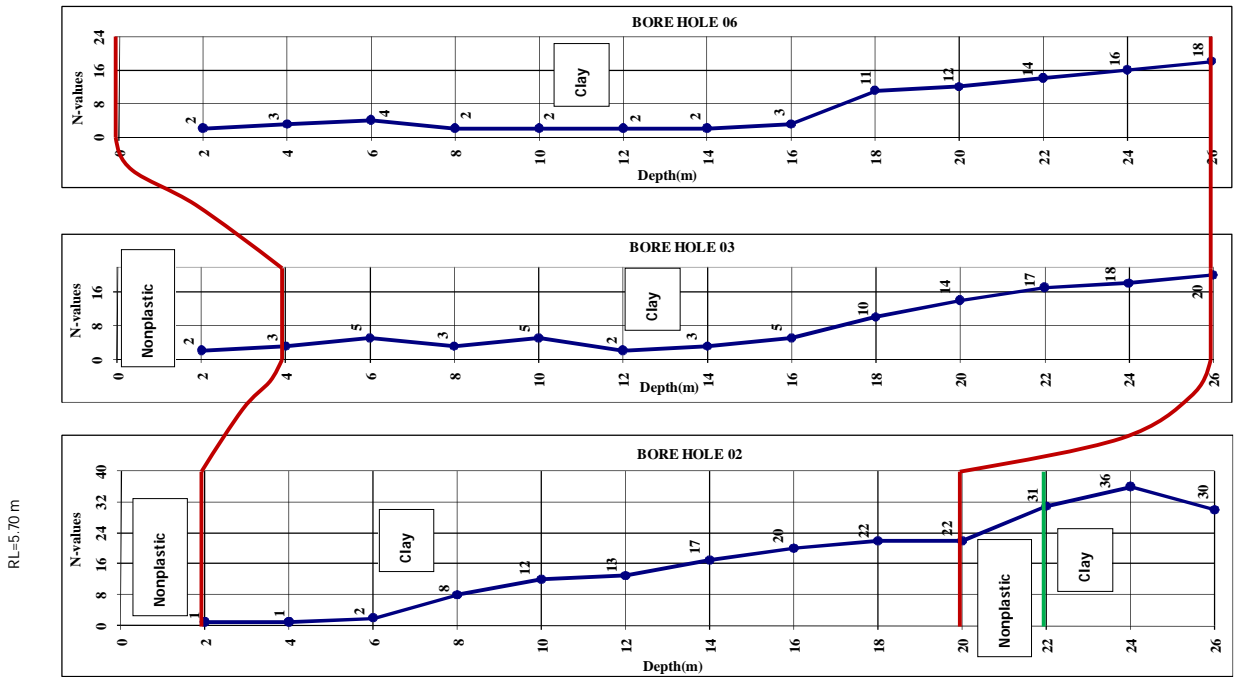


Figure 3.6 Geotechnical Characterization, Section-EE

### **3.4 SUBSOIL INVESTIGATION BASED ON CPT**

Figure 3.7-3.13 presents cone tip resistance, shaft friction, friction ratio and soil classification for seven different locations. The total depth of the soil profile tested for CPT data is variable and the maximum total depth is 22m. From seven CPT points it is seen that the soil of the whole site is erratic and the predominant soil of the site is cohesive soil. For soil profiles as shown in Figures 3.7, 3.10 and 3.12, the plus and minus 18m top soil is cohesive soil (clay, silty clay) and the remaining soil of the profiles is cohesionless soil ( nonplastic silt, silty sand). For soil profiles as shown in Figures 3.8, 3.9 and 3.13, the 2m top soil is fine sand and the remaining soil of the profiles is cohesive soil ( clay, silty clay) except 1m nonplastic silt existing in the soil profile as shown in Figure 3.13. For soil profile as shown in Figure 3.11, the 2m top soil is fine sand, the bottom soil below 19.5m depth is nonplastic silt and the remaining 17.5m middle soil of the profile is cohesive soil ( clay, silty clay).

### **3.5 INTERPRETATION OF SOIL PROFILE FROM CPT**

In this report, soil classification chart by Robertson and Campanella as presented in Article 2.5 is used to identify the soil layers. This method is selected since it is simple and provides output that can be easily understood. Douglas and Olsen chart shows the soil classification change (diagonally) from SP to SM to ML to CL to CH as the cone tip resistance decreases and friction ratio increases. Douglas and Olsen (1981) method demonstrates that the CPT classification charts cannot provide an accurate prediction of soil type based on soil composition, but rather serve as a guide to soil behavior type. Figures 3.7-3.13 present CPT as well as soil classification after Robertson and Campanella.

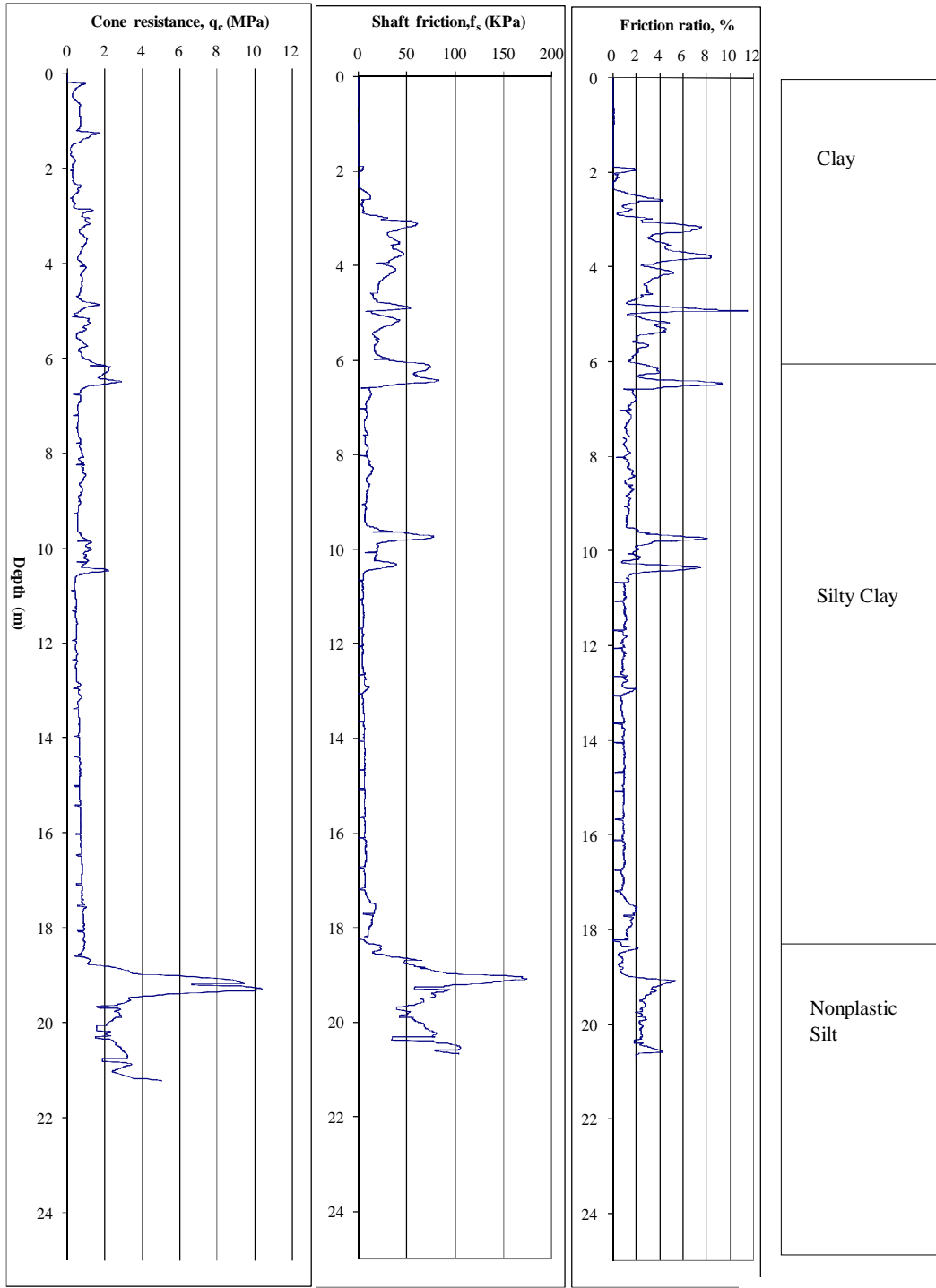


Figure 3.7 Cone Tip Resistance, Shaft Friction and Friction Ratio with Depth

Soil Classification based on CPT (after Robertson and Campanella)



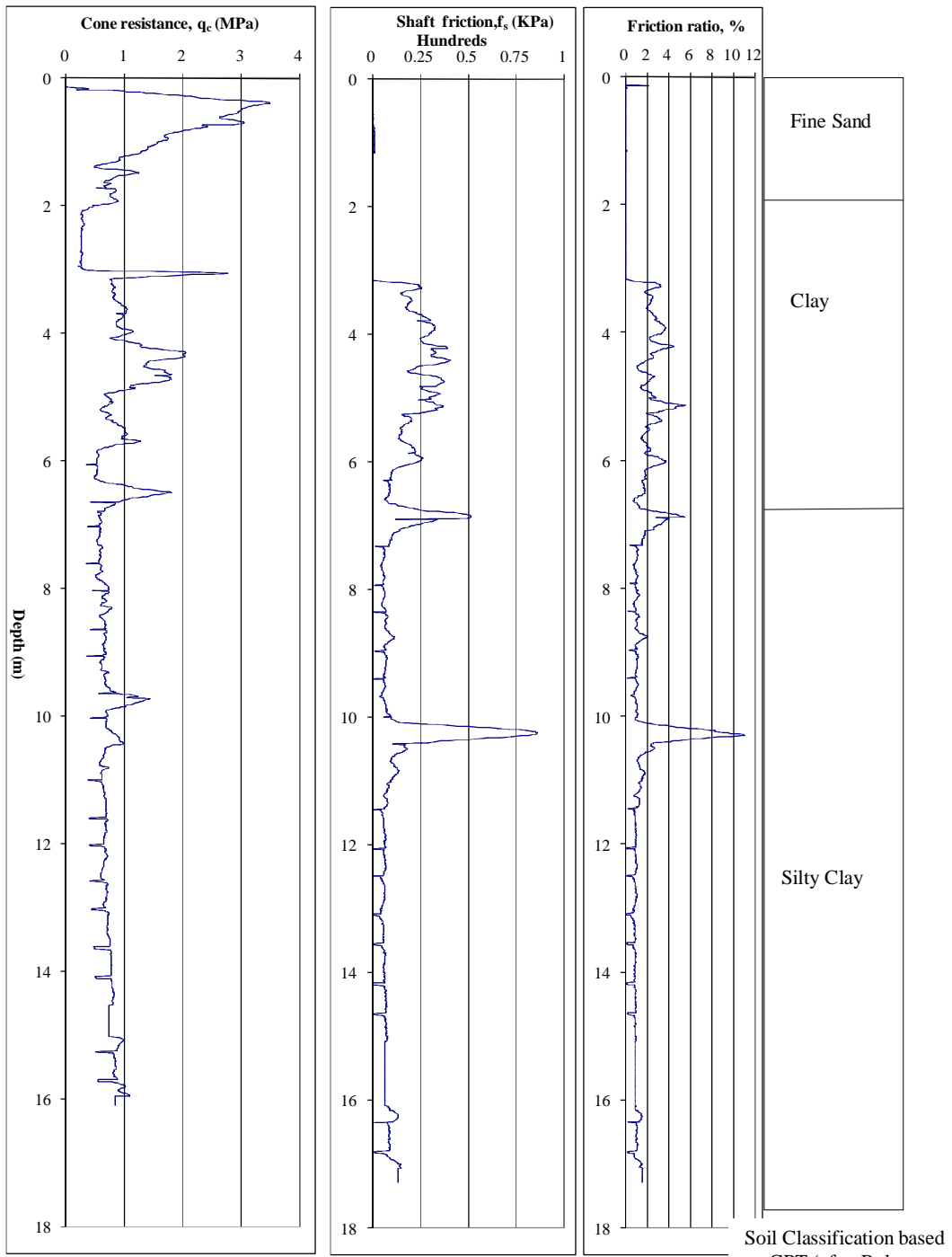


Figure 3.8 Cone Tip Resistance, Shaft Friction and Friction Ratio with Depth

Soil Classification based on CPT (after Robertson and Campanella)

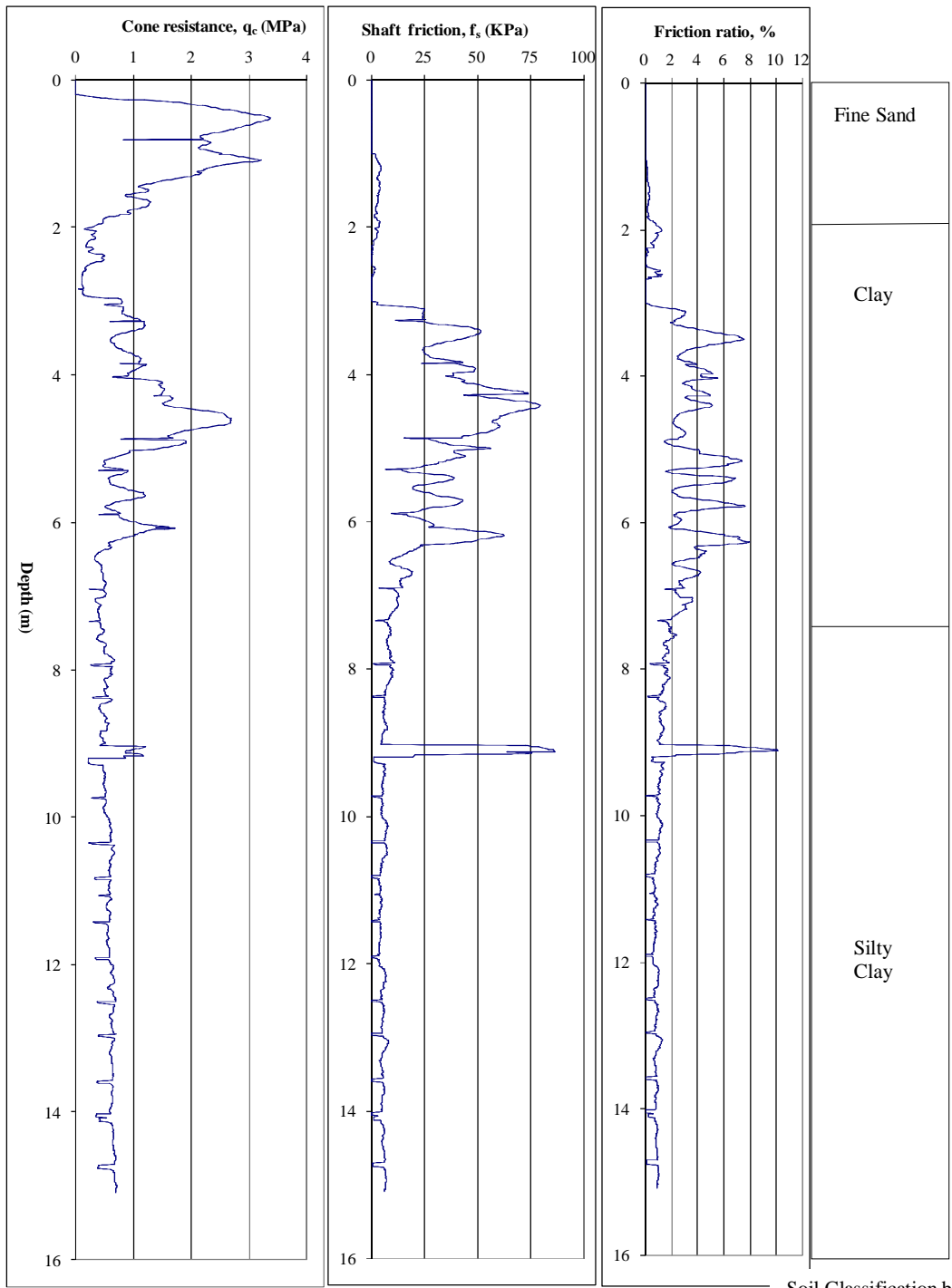


Figure 3.9 Cone Tip Resistance, Shaft Friction and Friction Ratio with Depth

Soil Classification based on CPT (after Robertson and Campanella)

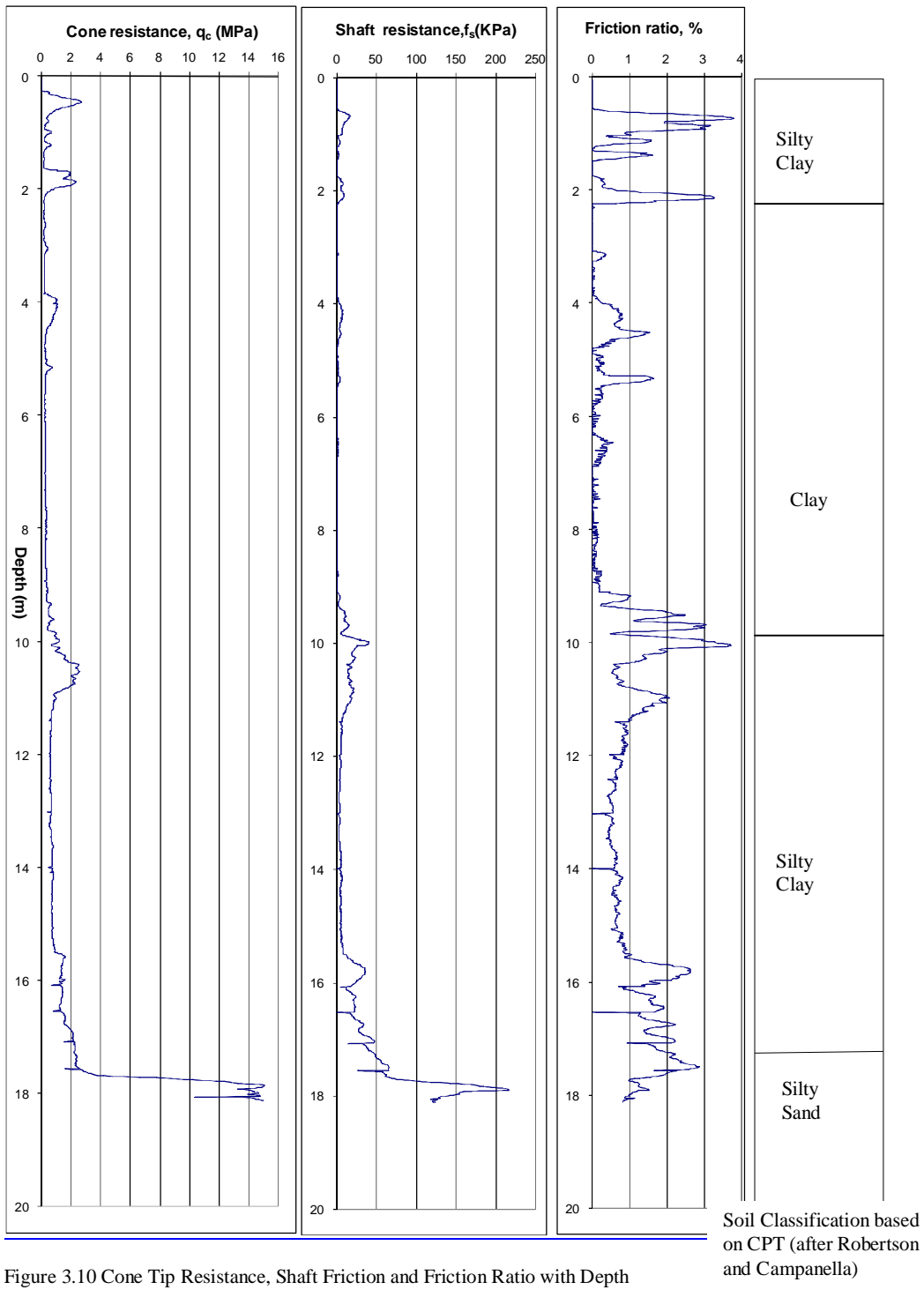


Figure 3.10 Cone Tip Resistance, Shaft Friction and Friction Ratio with Depth

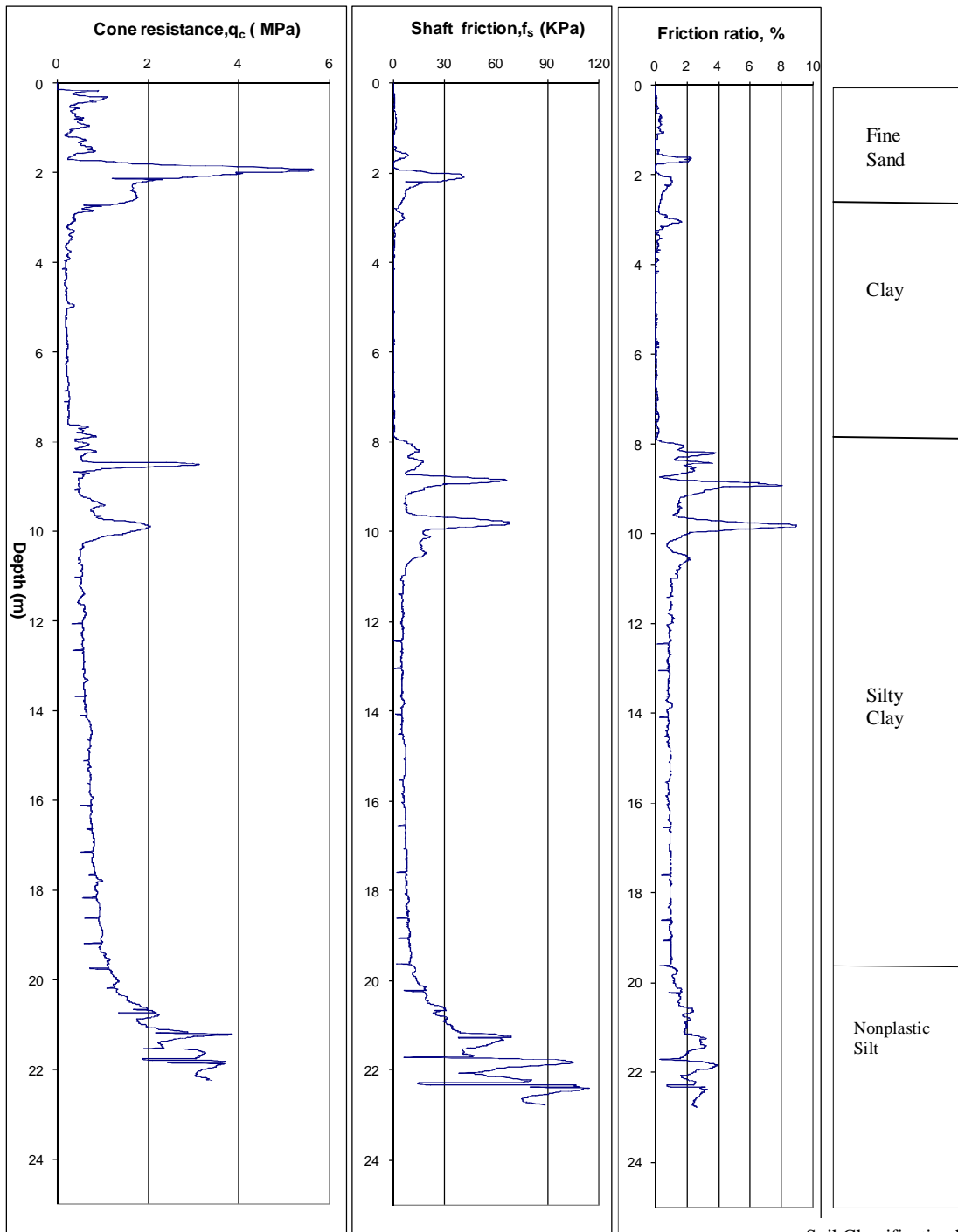


Figure 3.11 Cone Tip Resistance, Shaft Friction and Friction Ratio with Depth

Soil Classification based on CPT (after Robertson and Campanella)

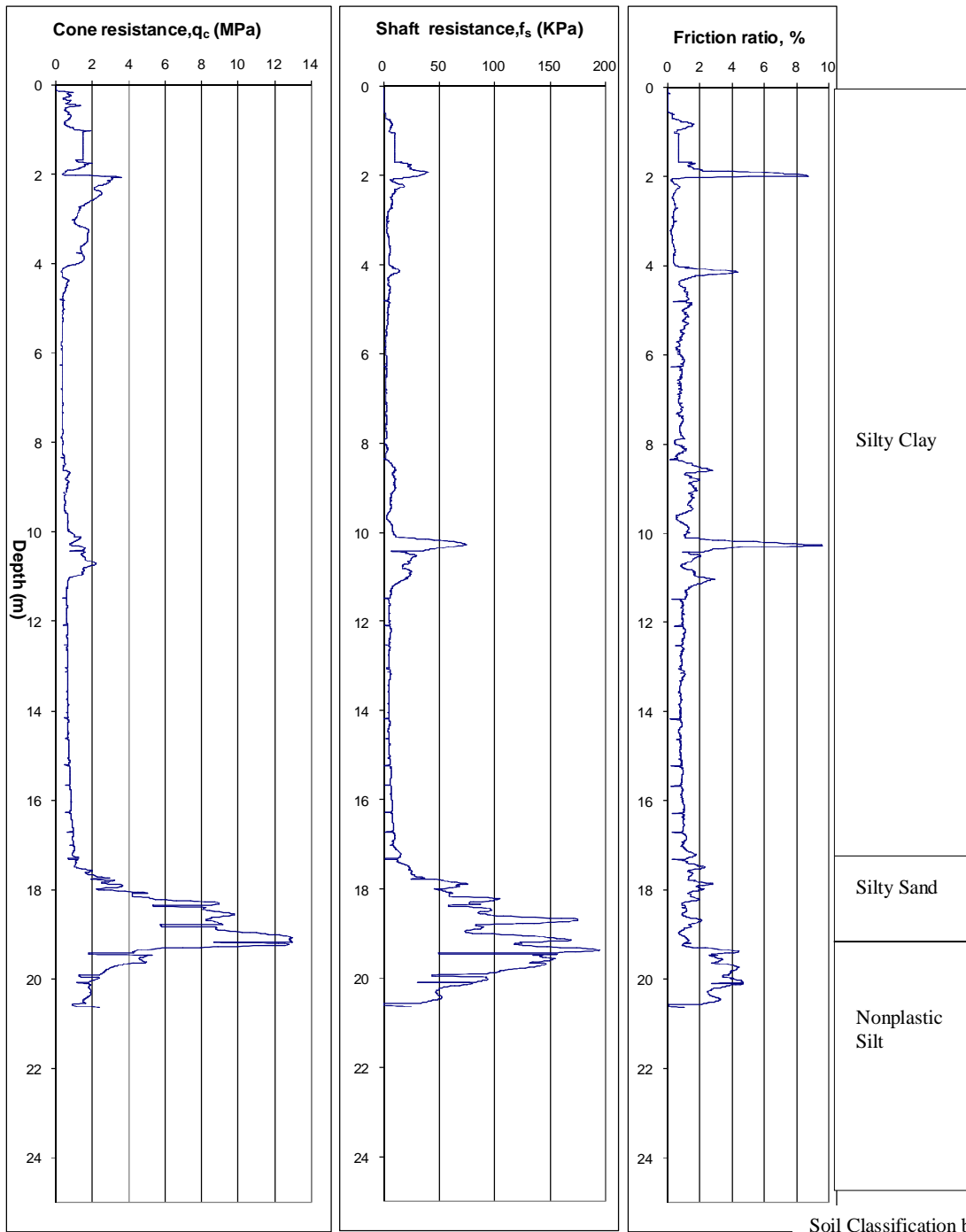
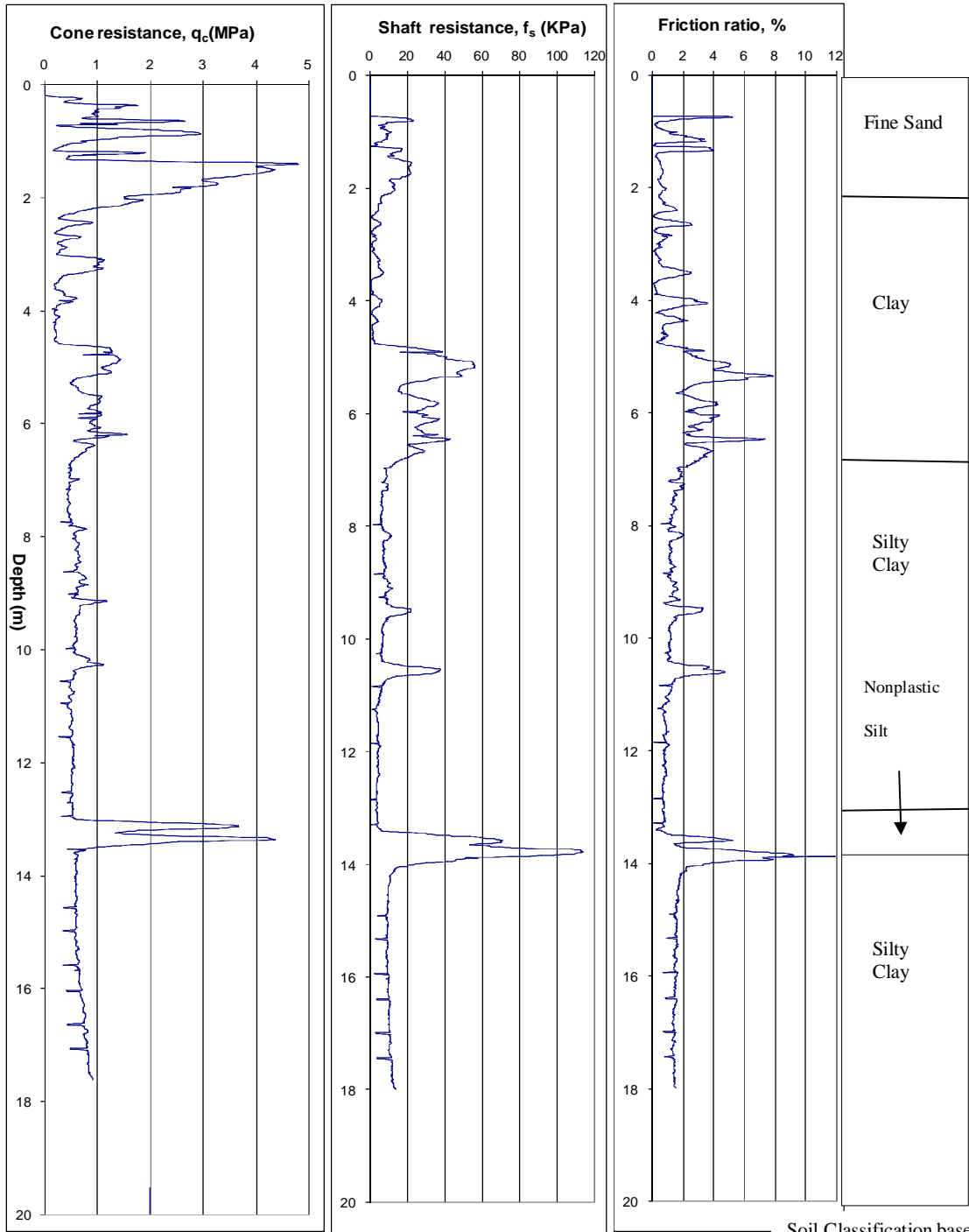


Figure 3.12 Cone Tip Resistance, Shaft Friction and Friction Ratio with Depth

Soil Classification based on CPT (after Robertson and Campanella)



Soil Classification based on CPT (after Robertson and Campanella)

Figure 3.13 Cone Tip Resistance, Shaft Friction and Friction Ratio with Depth

### 3.6 CHARACTERIZATION OF THE INVESTIGATED PILES

Seven square precast RC concrete piles depending on depth and soil characteristics are considered in the current study. A summary of the characteristics of the investigated piles is presented in [Table 3.1](#). The piles are categorized based on the predominant soil type, pile type and pile splicing. [Appendix A](#) shows the square precast RC concrete piles (spliced) before driving and during driving.

**Table 3.1:** Seven precast piles investigated based on pile type, soil type, and pile splicing

355mm Square Precast Pile Length	Pile Type		Predominant Soil Type			Splicing of Pile	
	Friction	End-bearing	Cohesive	Cohesionless	Both	Yes	No
21m	1	1	1	0	0	1	0
15m	1	0	1	0	0	0	1
14m	1	0	1	0	0	0	1
20.5m	0	1	0	0	1	1	0
22m	1	0	1	0	0	1	0
20m	1	0	1	0	0	1	0
17m	1	0	1	0	0	0	1

Note: 1 = Yes, 0=No

### 3.7 PREDICTED PILE CAPACITY USING SPT AND CPT DATA

Only seven piles depending on depth and soil characteristics are used in the analyses and most of the piles are identified as friction piles. To predict the ultimate axial load capacity of the piles, the methods used are the Schmertmann, de Ruiter and Beringen, Bustamante and Gianceselli, Tumay and Fakhroo, Aoki and De Alencar, Price and Wardle, Philipponnat, and Penpile method. The ultimate load capacity for each pile is also predicted from the soil properties (soil boring close to the pile) using the SPT data. The ultimate load carrying capacity predicted by these methods ( $Q_p$ ) using the CPT data is compared to the pile capacity ( $Q_m$ ) obtained from the SPT data. **Table 3.2** summarizes the results of the analyses conducted on the investigated piles. Among the data presented in **Table 3.2** are: the pile size, type, length, the predicted ultimate load carrying capacity from CPT, the predicted ultimate load carrying capacity from SPT, average ultimate pile capacity for each pile and standard deviation for each pile. Appendix B presents an illustration of predicting the pile capacity by different CPT methods and the SPT method.

The predicted ultimate load carrying capacity ( $Q_p$ ) consists of pile tip capacity ( $Q_t$ ) and pile shaft resistance ( $Q_s$ ). Comparison between the pile capacities  $Q_t$ ,  $Q_s$ , and  $Q_p$  predicted by the CPT methods and the pile capacities  $Q_t$ ,  $Q_s$ , and  $Q_m$  predicted by the SPT method are shown in **Figures 3.14-3.21**. The results of five friction piles, one friction and end-bearing pile and one end-bearing pile are shown in these figures. Inspection of these figures shows that the ratio  $Q_t/Q_p$  for the 5 piles is relatively small, which is consistent with the previous classification of these piles as friction piles (pile capacity is derived mainly from the shaft resistance). On the other hand, the ratio  $Q_t/Q_p$  for 1 pile is relatively large and hence this pile is considered as end bearing pile (pile capacity is derived mainly from the pile tip capacity). The ratio  $Q_t/Q_p$  for 1 pile is almost one and hence this pile is considered as friction and end bearing pile (pile capacity is derived mainly from the shaft resistance and pile tip capacity). These figures also find out the method giving the maximum/minimum ultimate end bearing capacity, the maximum/minimum ultimate shaft friction capacity, the maximum /minimum total ultimate pile capacity for seven piles.



Table 3.2: Results of the analyses conducted on square reinforced concrete piles at a site in Siddhirganj.

Pile and Soil Identification	Pile ID	TP1, 355mm Square Precast RC Concrete Pile (Spliced)			TP2, 355mm Square Precast RC Concrete Pile			Increase or decrease of pile capacity compared with arithmetic mean (in %)	
	Pile Length(m)	21			15				
	Embedded Length(m)	21			15				
	Pile Classification	Friction and end bearing			Friction				
	Predominant Soil	Cohesive			Cohesive				
Methods of Predicting Pile Capacity by Cone Penetration Test (CPT)	Predicted Ultimate Load (KN)	$Q_s$	$Q_t$	$Q_u$	$Q_s$	$Q_t$	$Q_u$	TP1	TP2
	Schmertmann	453	450	<b>903</b>	240	94	<b>334</b>	2	-25
	de Ruiter & Beringen	478	450	<b>928</b>	394	56	<b>450</b>	5	1
	LCPC	905	221	<b>1126</b>	673	62	<b>735</b>	28	64
	Tumay & Fakhroo	1028	417	<b>1445</b>	722	93	<b>815</b>	64	82
	Aoki & De Alencar	257	303	<b>560</b>	261	54	<b>315</b>	-37	-30
	Price & Wardle	263	157	<b>420</b>	129	33	<b>162</b>	-52	-64
	Philipponnat	528	210	<b>738</b>	397	50	<b>447</b>	-16	0
Penpile	280	56	<b>336</b>	142	23	<b>165</b>	-62	-63	
Pile Capacity by SPT		847	630	<b>1477</b>	540	61	<b>601</b>	67	34
Arithmetic Mean		<b>881</b>			<b>447</b>				
Standard Deviation		<b>390</b>			<b>219</b>				

$Q_s$ : Pile shaft capacity (friction),  $Q_t$ : Pile tip capacity (end-bearing),  $Q_u$ : Total ultimate capacity( $Q_s+Q_t$ )

Table 3.2: Results of the analyses conducted on square reinforced concrete piles at a site in Siddhirganj, continued

Pile and Soil Identification	Pile ID	TP3, 355mm Square Precast RC Concrete Pile (Spliced)			TP4, 355mm Square Precast RC Concrete Pile (Spliced)			Increase or decrease of pile capacity compared with arithmetic mean (in %)	
	Pile Length(m)	14			20.5				
	Embedded Length(m)	14			20.5				
	Pile Classification	Friction			End bearing				
	Predominant Soil	Cohesive			Cohesive & Cohesionless				
Methods of Predicting Pile Capacity by Cone Penetration Test (CPT)	Predicted Ultimate Load (KN)	$Q_s$	$Q_t$	$Q_u$	$Q_s$	$Q_t$	$Q_u$	TP3	TP4
	Schmertmann	239	78	<b>317</b>	537	1628	<b>2165</b>	<b>-18</b>	<b>36</b>
	de Ruiter & Beringen	398	47	<b>445</b>	698	1628	<b>2326</b>	14	46
	LCPC	560	48	<b>608</b>	1244	699	<b>1943</b>	56	22
	Tumay & Fakhroo	647	75	<b>722</b>	480	1628	<b>2108</b>	86	32
	Aoki & De Alencar	188	45	<b>233</b>	615	930	<b>1545</b>	-40	-3
	Price & Wardle	137	27	<b>164</b>	335	570	<b>905</b>	-58	-43
	Philipponnat	338	40	<b>378</b>	771	746	<b>1517</b>	-3	-5
Penpile	149	19	<b>168</b>	307	203	<b>510</b>	-57	-68	
Pile Capacity by SPT		437	20	<b>457</b>	819	516	<b>1335</b>	18	-16
Arithmetic Mean		<b>388</b>			<b>1595</b>				
Standard Deviation		<b>181</b>			<b>575</b>				

$Q_s$ : Pile shaft capacity (friction),  $Q_t$ : Pile tip capacity (end-bearing),  $Q_u$ : Total ultimate capacity( $Q_s+Q_t$ )

Table 3.2: Results of the analyses conducted on square reinforced concrete piles at a site in Siddhirganj, continued

Pile and Soil Identification	Pile ID	TP5, 355mm Square Precast RC Concrete Pile			TP6, 355mm Square Precast RC Concrete Pile			TP7, 355mm Square Precast RC Concrete Pile			Increase or decrease of pile capacity compared with arithmetic mean (in %)		
	Pile Length(m)	22			20			17					
	Embedded Length(m)	22			20			17					
	Pile Classification	Friction			Friction			Friction					
	Predominant Soil	Cohesive			Cohesive			Cohesive					
Methods of Predicting Pile Capacity by Cone Penetration Test (CPT)	Predicted Ultimate Load (KN)	Q <sub>s</sub>	Q <sub>t</sub>	Q <sub>u</sub>	Q <sub>s</sub>	Q <sub>t</sub>	Q <sub>u</sub>	Q <sub>s</sub>	Q <sub>t</sub>	Q <sub>u</sub>	TP5	TP6	TP7
	Schmertmann	333	321	<b>654</b>	497	434	<b>931</b>	318	98	<b>416</b>	-10	-5	-15
	de Ruitter & Beringen	435	321	<b>756</b>	663	434	<b>1097</b>	508	59	<b>567</b>	5	12	15
	LCPC	738	164	<b>902</b>	1239	272	<b>1511</b>	667	42	<b>709</b>	25	55	44
	Tumay & Fakhroo	909	310	<b>1219</b>	1045	406	<b>1451</b>	1036	90	<b>1126</b>	69	49	129
	Aoki & De Alencar	316	183	<b>499</b>	381	248	<b>629</b>	260	56	<b>316</b>	-31	-36	-36
	Price & Wardle	189	112	<b>301</b>	389	152	<b>541</b>	142	34	<b>176</b>	-58	-45	-64
	Philipponnat	470	148	<b>618</b>	673	278	<b>951</b>	380	44	<b>424</b>	-15	-3	-14
	Penpile	206	40	<b>246</b>	387	108	<b>495</b>	175	24	<b>199</b>	-66	-49	-59
Pile Capacity by SPT		749	554	<b>1303</b>	697	479	<b>1176</b>	461	20	<b>481</b>	80	20	-2
Arithmetic Mean		<b>722</b>			<b>976</b>			<b>490</b>					
Standard Deviation		<b>347</b>			<b>351</b>			<b>275</b>					

Q<sub>s</sub>: Pile shaft capacity (friction), Q<sub>t</sub>: Pile tip capacity (end-bearing), Q<sub>u</sub>: Total ultimate capacity(Q<sub>s</sub>+Q<sub>t</sub>)

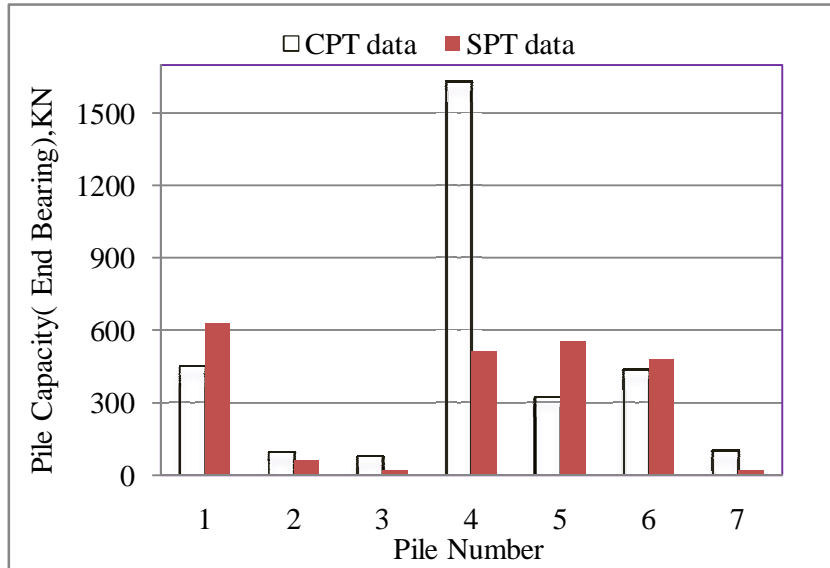


**Figure 3.14a** Comparison of ultimate end bearing capacity of pile predicted by Schmertmann method(1978) with the one predicted by SPT data

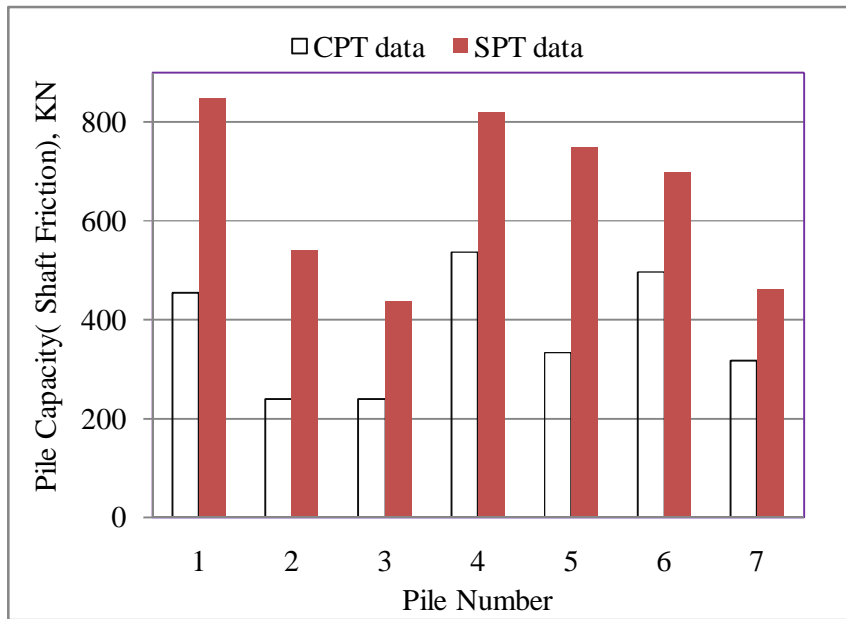


**Figure 3.14b** Comparison of ultimate shaft friction capacity of pile predicted by Schmertmann method(1978) with the one predicted by SPT data

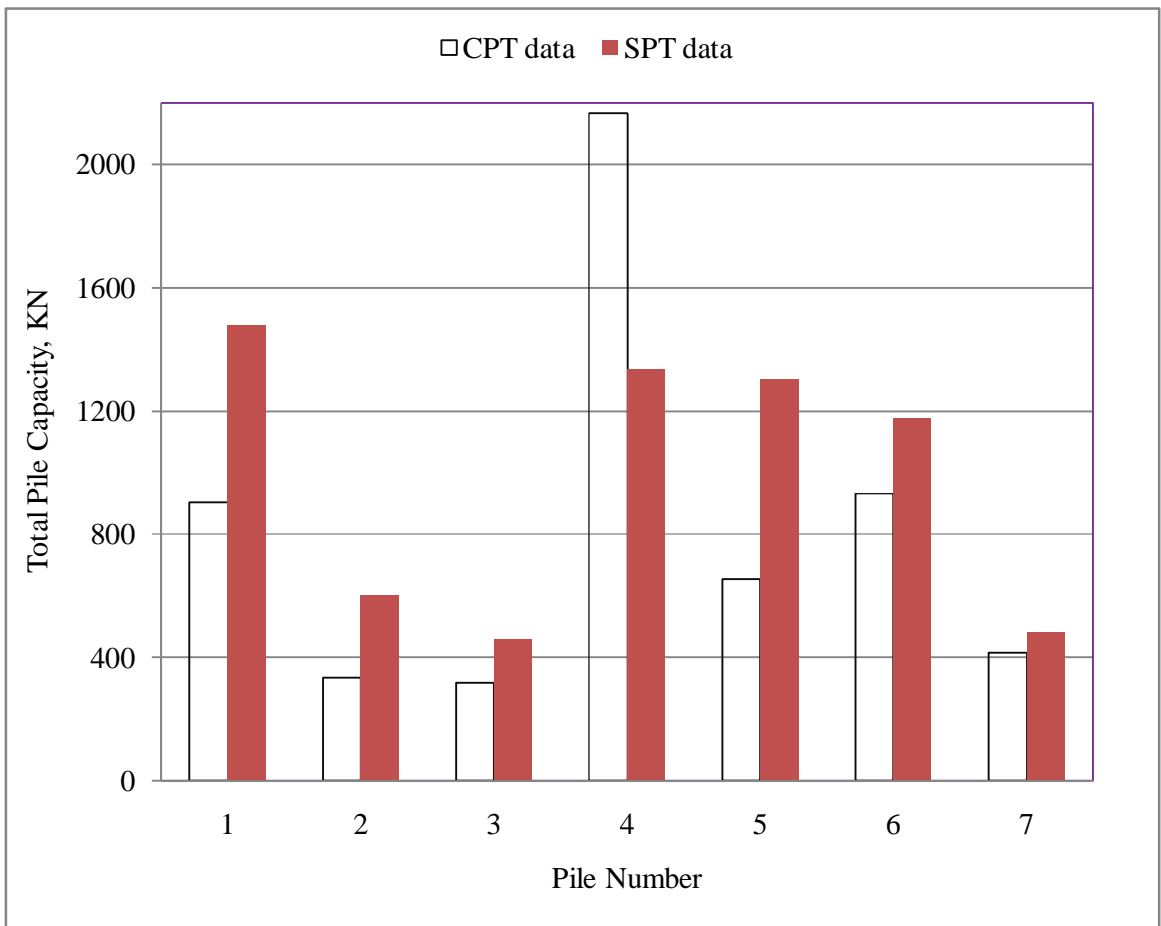


**Figure 3.14c** Comparison of ultimate pile capacity predicted by Schmertmann method(1978) with the one predicted by SPT data

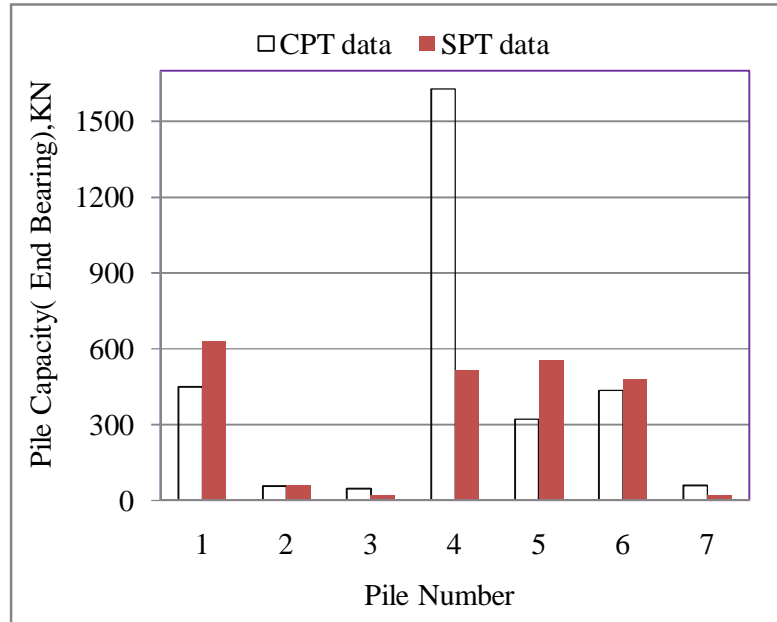


Figure 3.15a Comparison of ultimate end bearing capacity of pile predicted by de Ruiter and Beringen method (1979) with the one predicted by SPT data

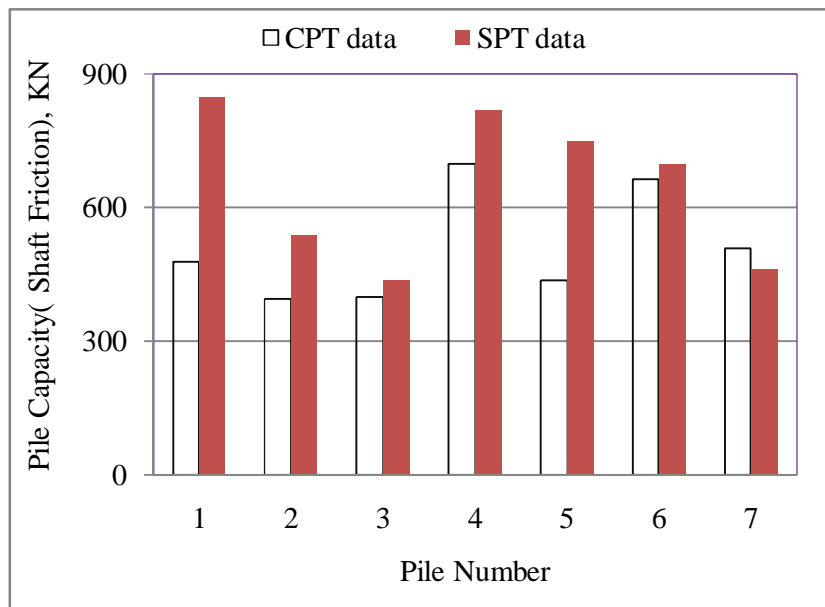
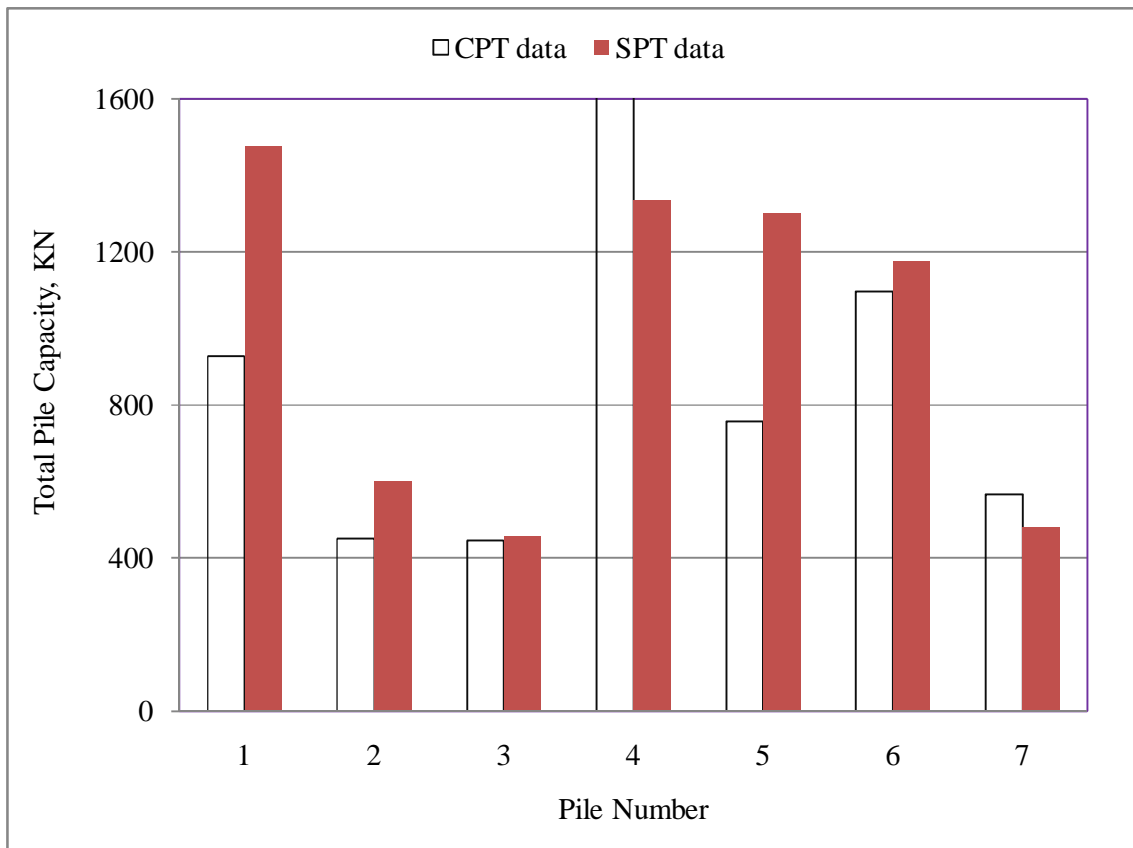
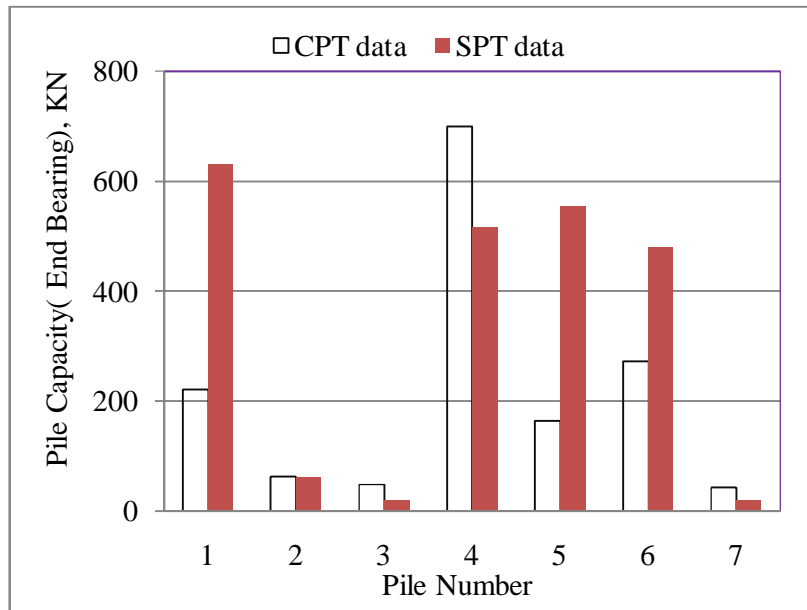


Figure 3.15b Comparison of ultimate shaft friction capacity of pile predicted by de Ruiter and Beringen method (1979) with the one predicted by SPT data



**Figure 3.15c** Comparison of ultimate pile capacity predicted by de Ruiter and Beringen method(1979) with the one predicted by SPT data



**Figure 3.16a** Comparison of ultimate end bearing capacity of pile predicted by LCPC method (1982) with the one predicted by SPT data

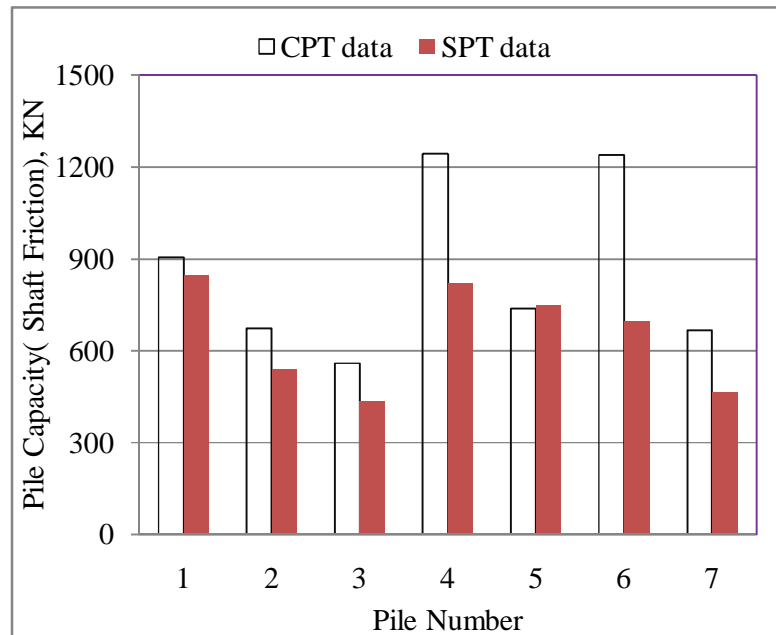


**Figure 3.16b** Comparison of ultimate shaft friction capacity of pile predicted by LCPC method (1982) with the one predicted by SPT data



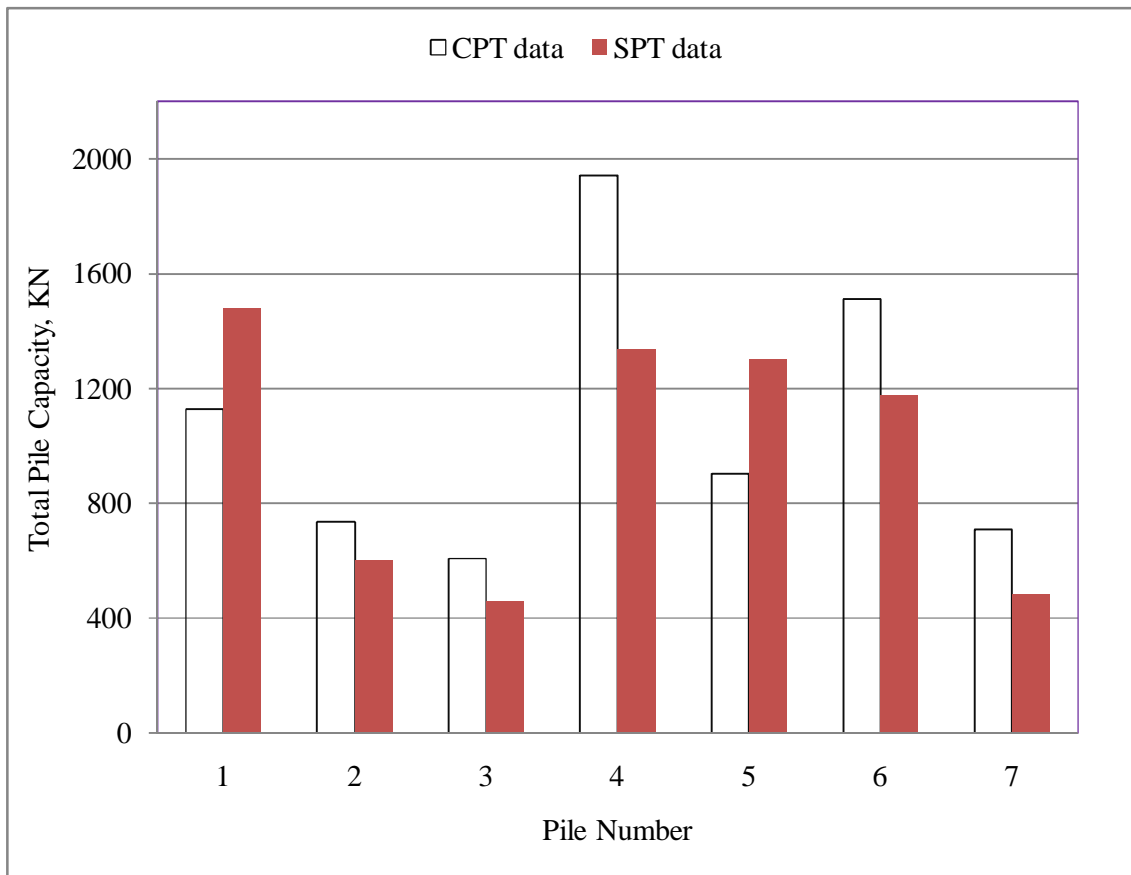


**Figure 3.16c** Comparison of ultimate pile capacity predicted by LCPC method (1982) with the one predicted by SPT data

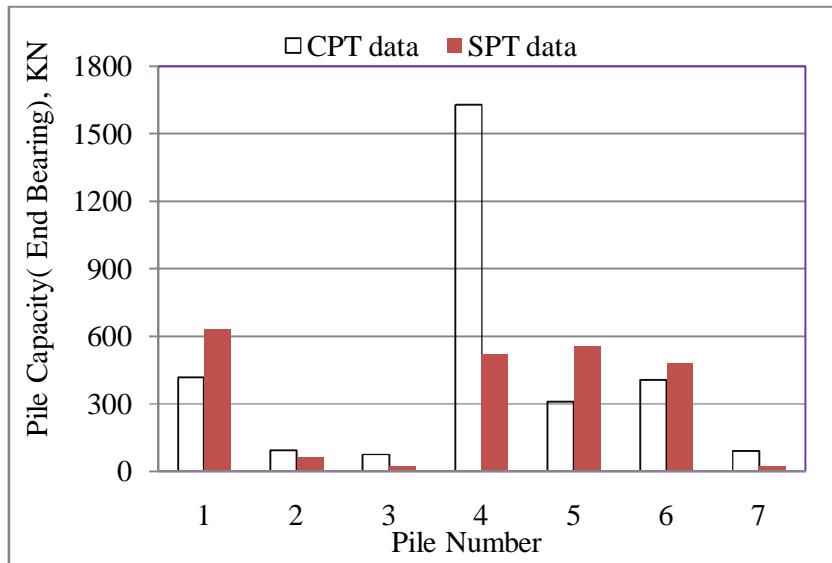


**Figure 3.17a** Comparison of ultimate end bearing capacity of pile predicted by Tumay and Fakhroo method (1982) with the one predicted by SPT data

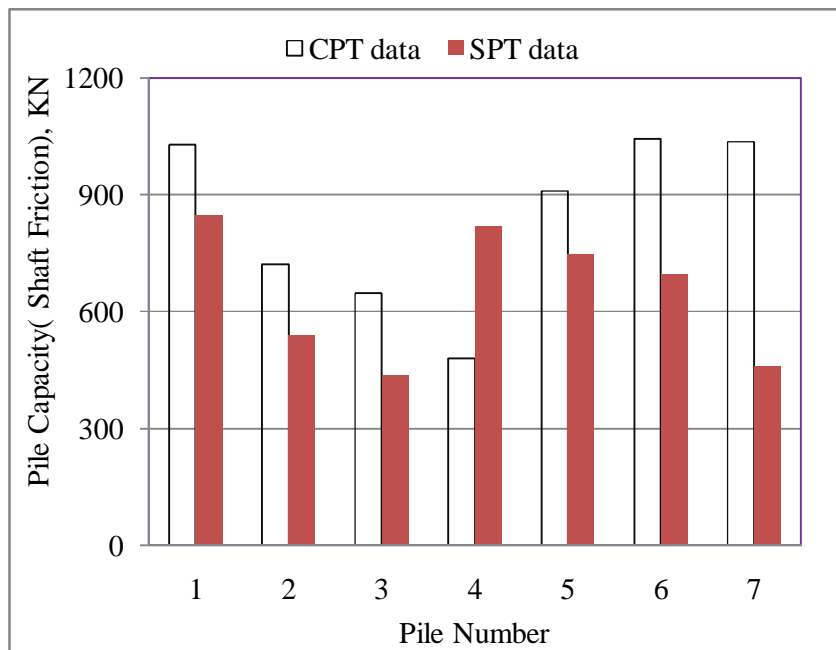


**Figure 3.17b** Comparison of ultimate shaft friction capacity of pile predicted by Tumay and Fakhroo method (1982) with the one predicted by SPT data

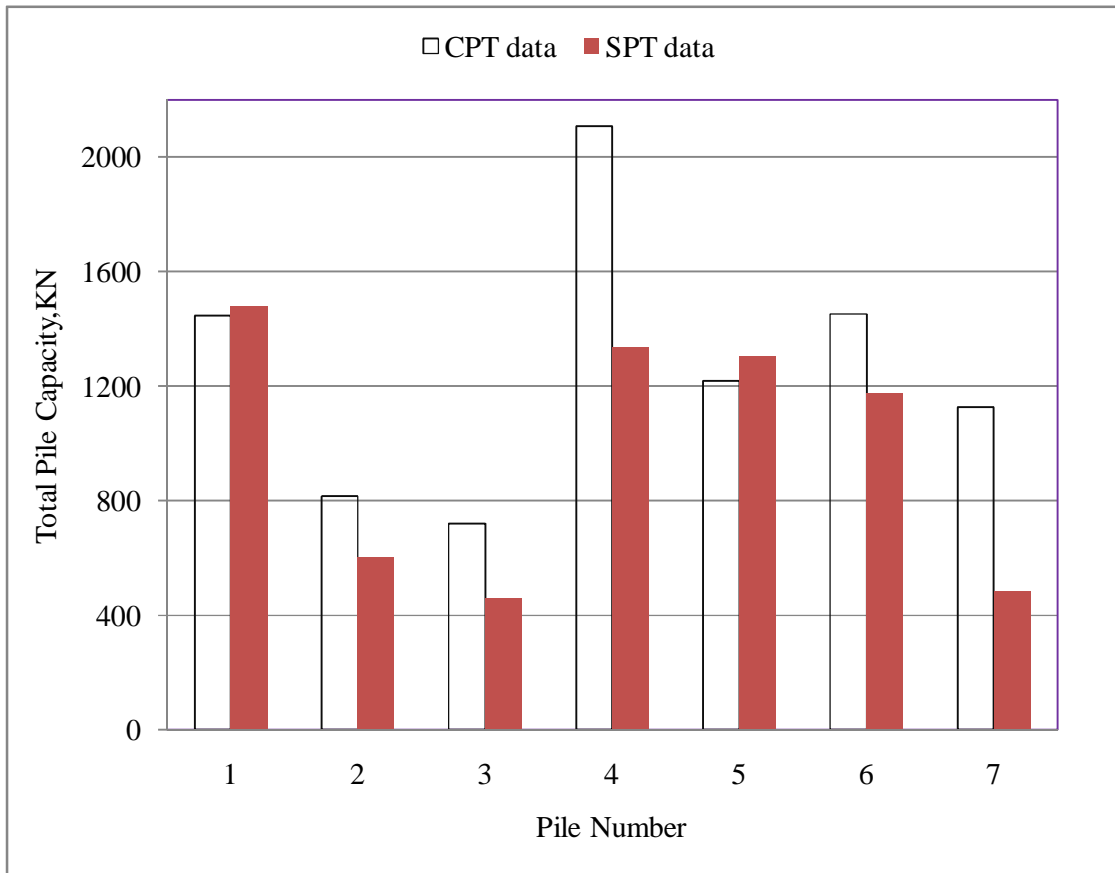


**Figure 3.17c** Comparison of ultimate pile capacity predicted by Tumay and Fakhroo method (1982) with the one predicted by SPT data

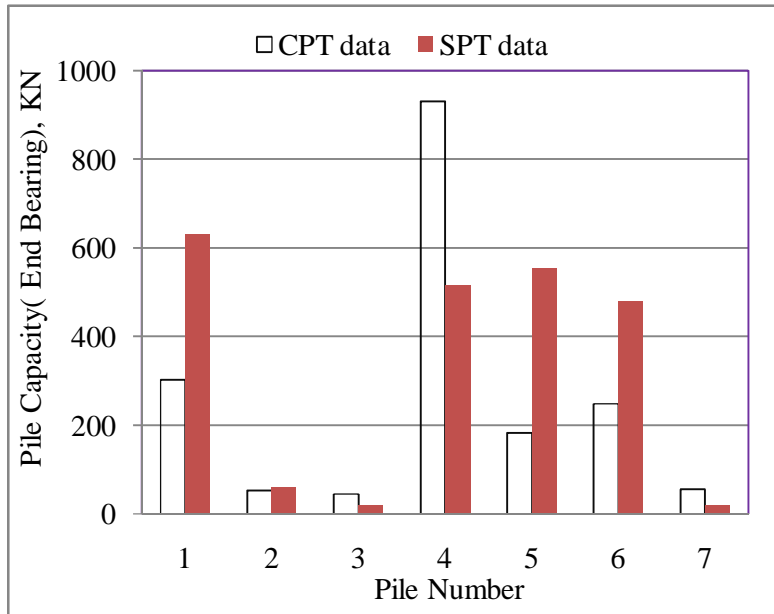


**Figure 3.18a** Comparison of ultimate end bearing capacity of pile predicted by Aoki and De Alencar method (1975) with the one predicted by SPT data

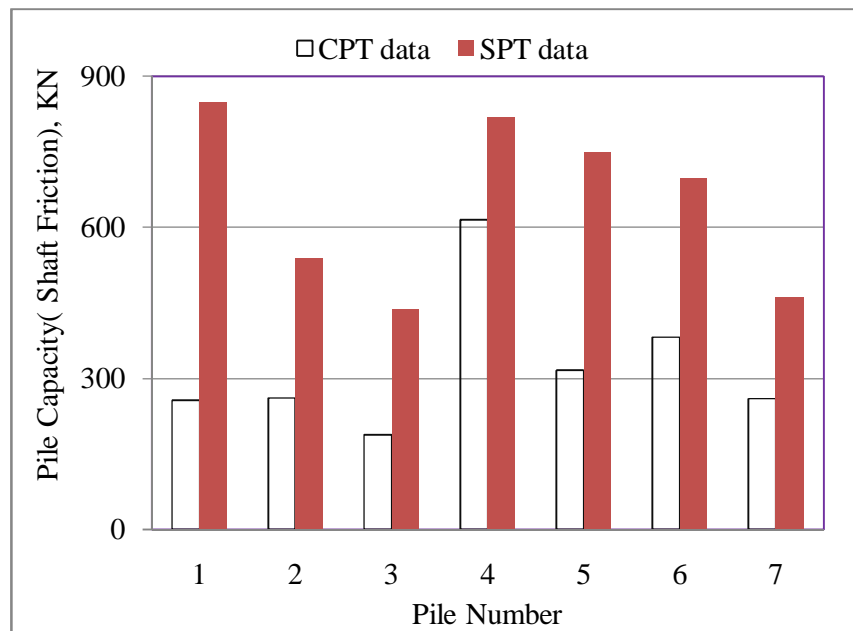


**Figure 3.18b** Comparison of ultimate shaft friction capacity of pile predicted by Aoki and De Alencar method (1975) with the one predicted by SPT data

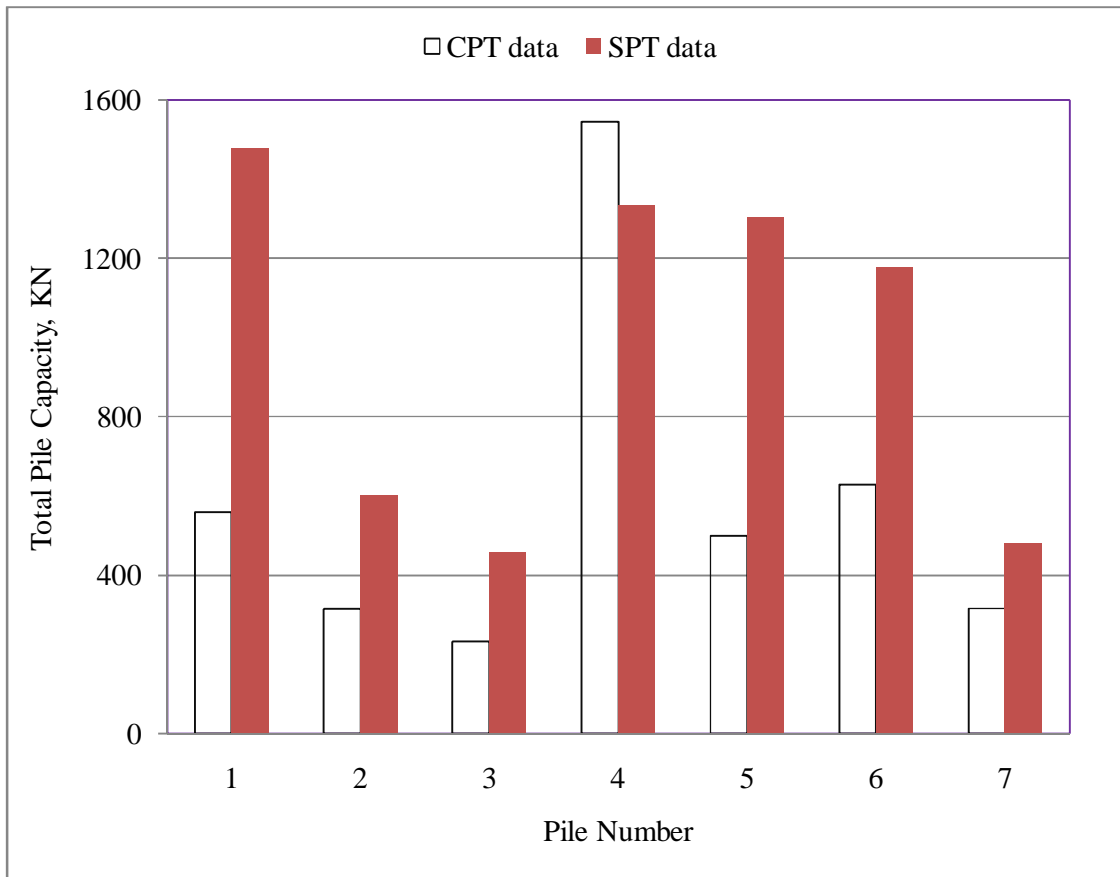
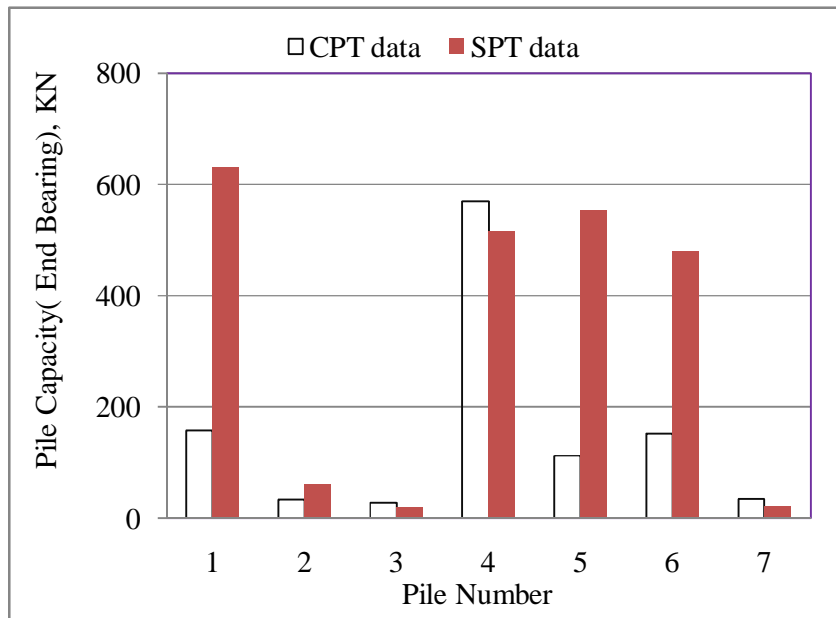
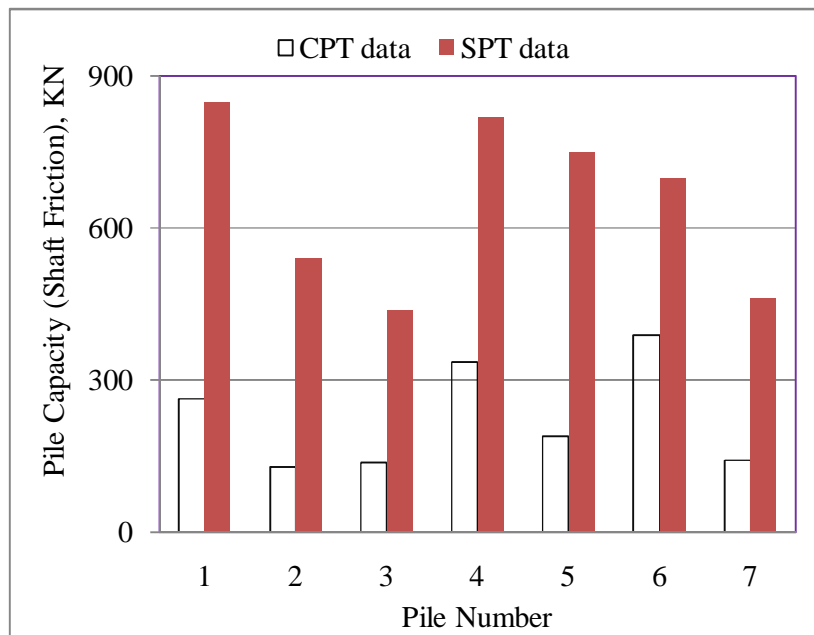


Figure 3.18c Comparison of ultimate pile capacity predicted by Aoki and De Alencar method (1975) with the one predicted by SPT data



**Figure 3.19a** Comparison of ultimate end bearing capacity of pile predicted by Price and Wardle method (1982) with the one predicted by SPT data



**Figure 3.19b** Comparison of ultimate shaft friction capacity of pile predicted by Price and Wardle method (1982) with the one predicted by SPT data

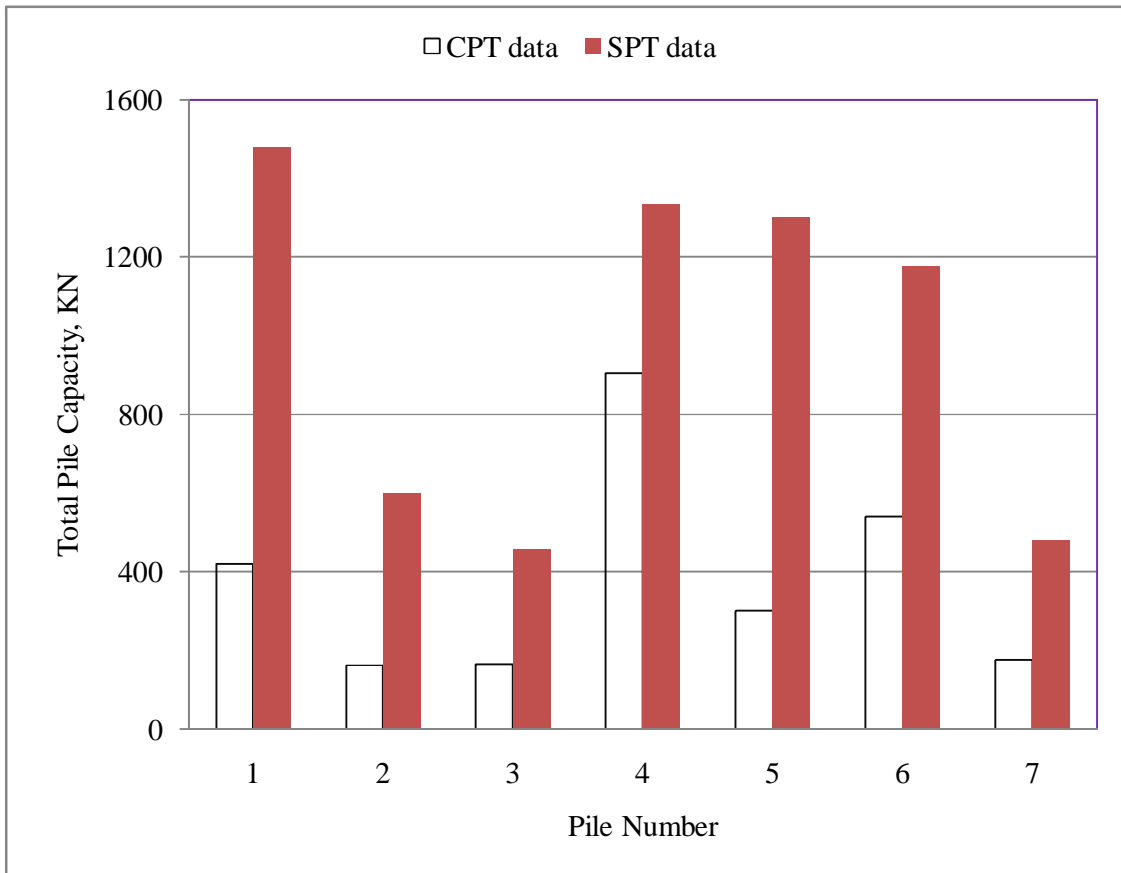


Figure 3.19c Comparison of ultimate pile capacity predicted by Price and Wardle method (1982) with the one predicted by SPT data

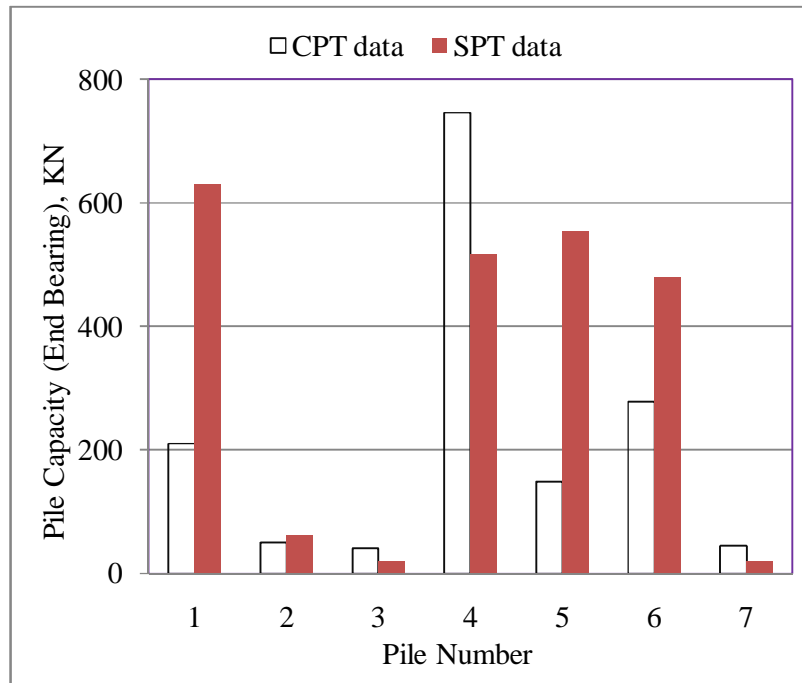


Figure 3.20a Comparison of ultimate end bearing capacity of pile predicted by Philipponnat method (1980) with the one predicted by SPT data

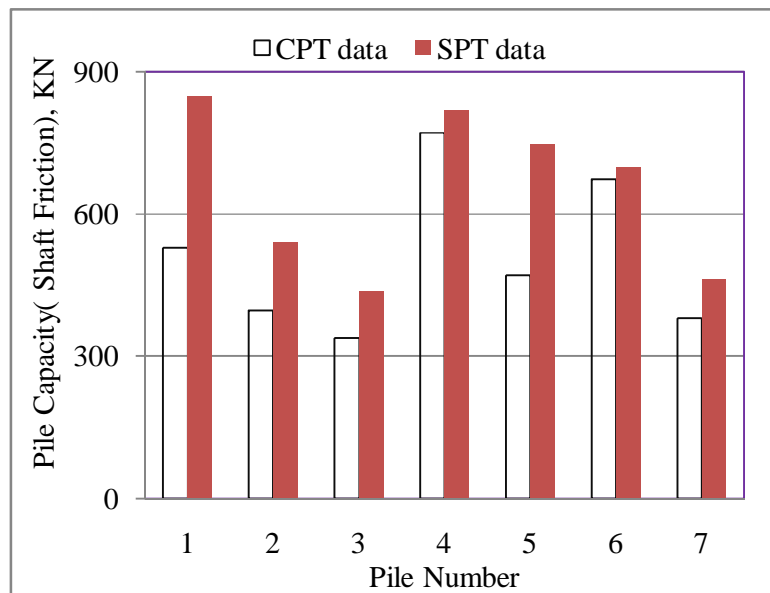


Figure 3.20b Comparison of ultimate shaft friction capacity of pile predicted by Philipponnat method (1980) with the one predicted by SPT data



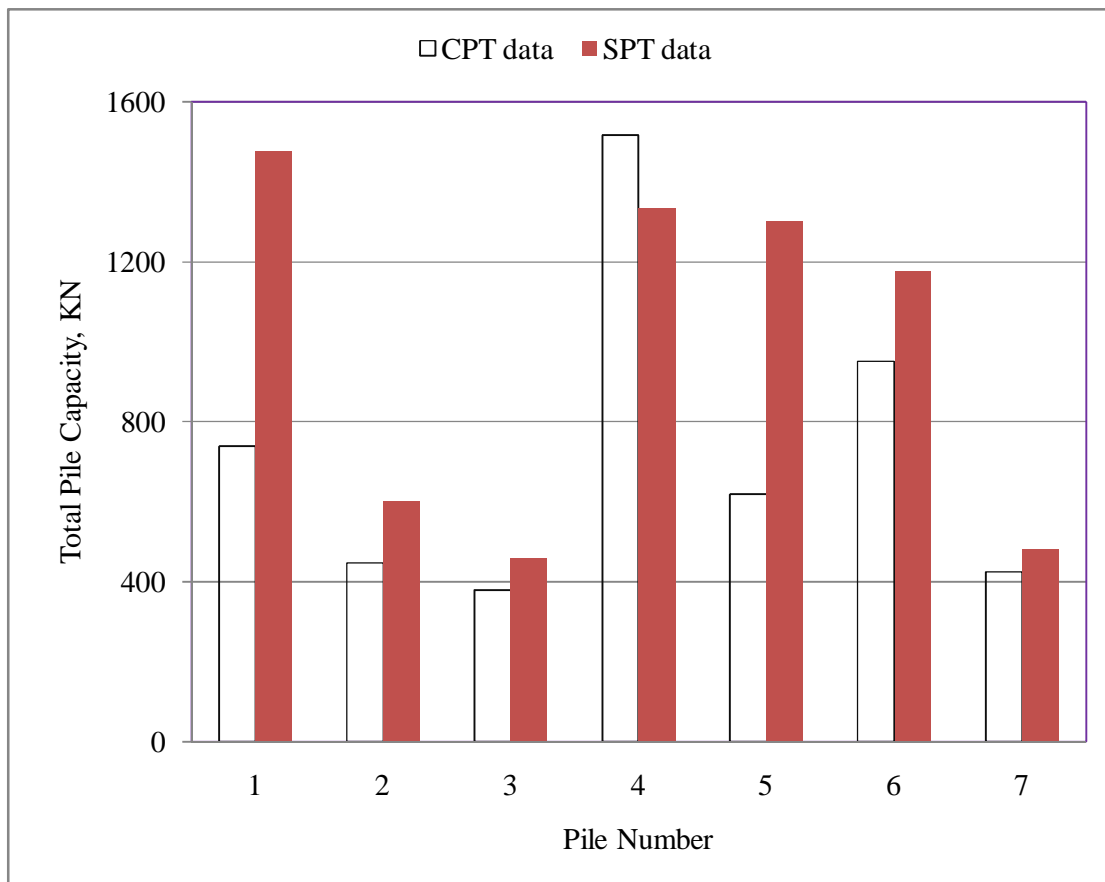
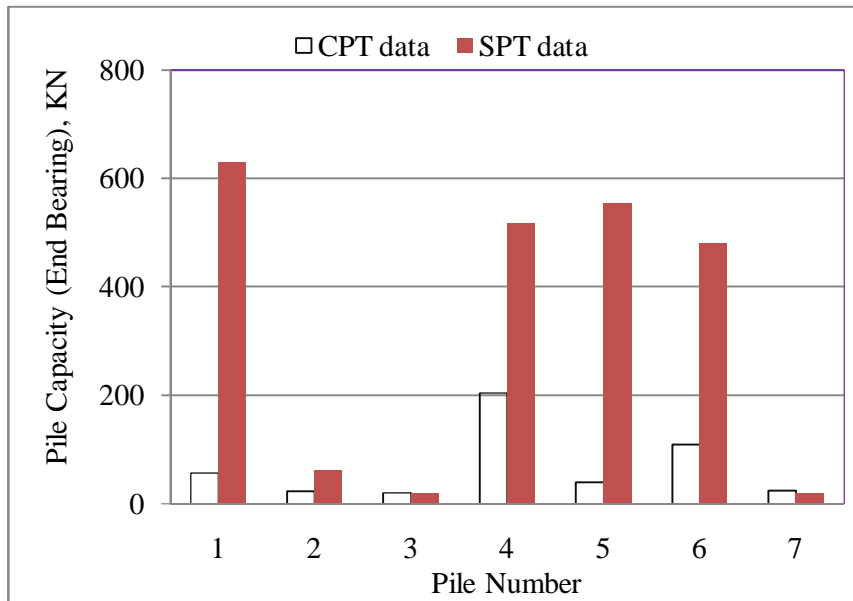
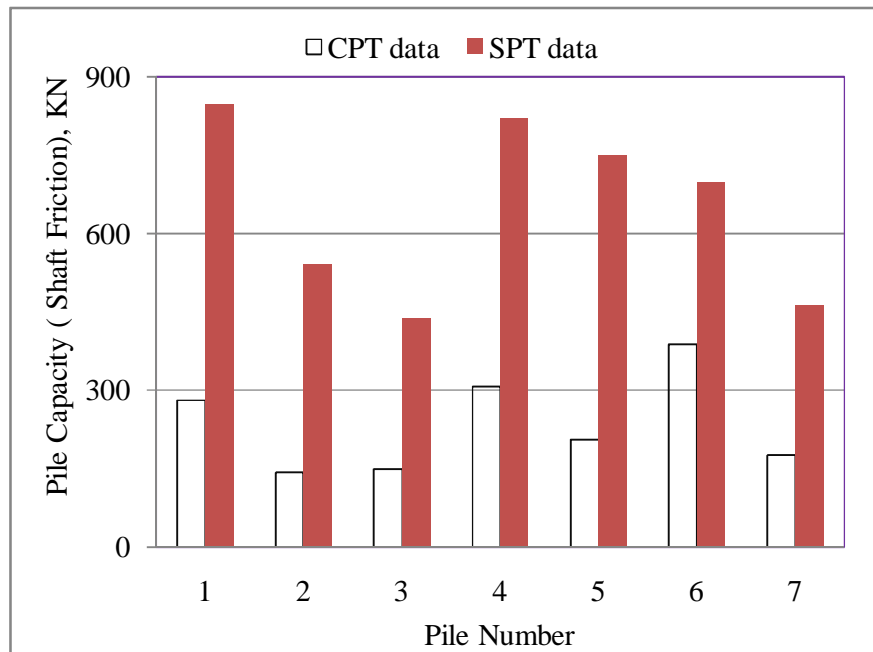


Figure 3.20c Comparison of ultimate pile capacity predicted by Philipponnat method (1980) with the one predicted by SPT data



**Figure 3.21a** Comparison of ultimate end bearing capacity of pile predicted by Penpile method (1978) with the one predicted by SPT data



**Figure 3.21b** Comparison of ultimate shaft friction capacity of pile predicted by Penpile method (1978) with the one predicted by SPT data

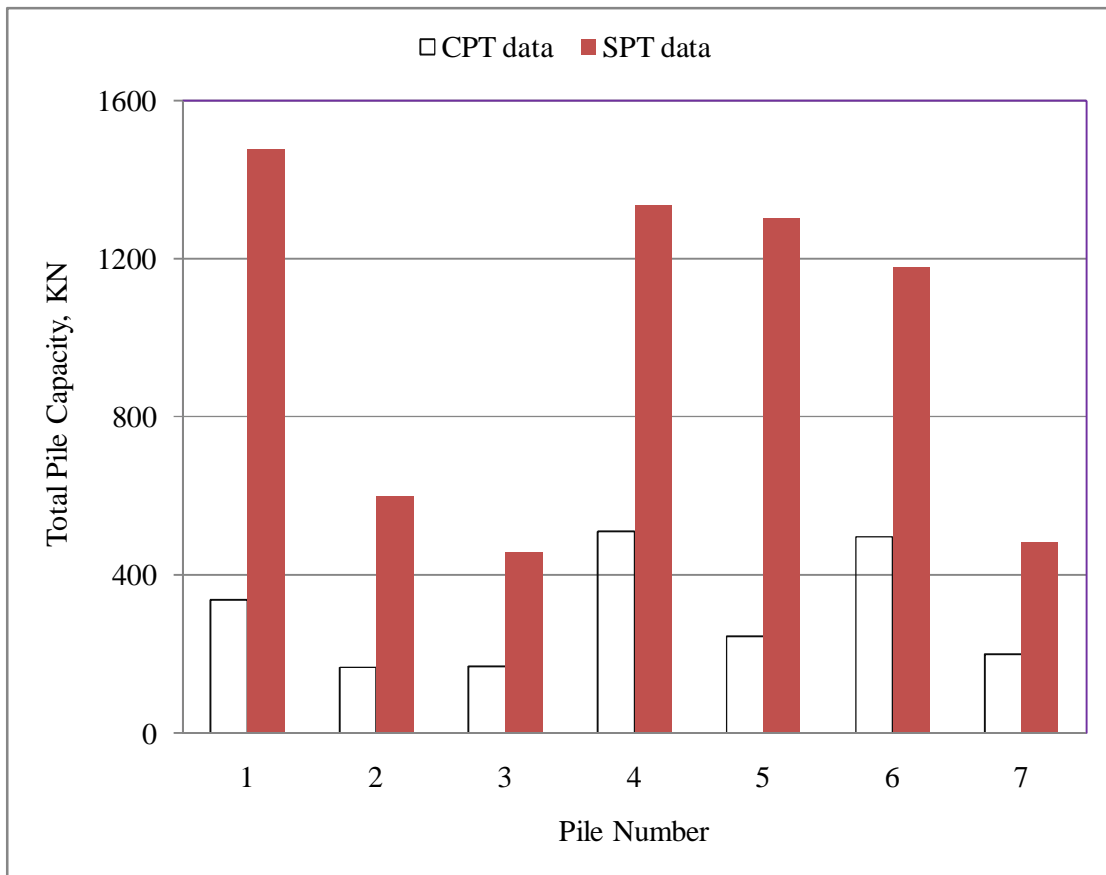


Figure 3.21c Comparison of ultimate pile capacity predicted by Penpile method (1978) with the one predicted by SPT data

### **3.8 APPLICABILITY OF THE VARIOUS METHODS USED FOR PREDICTING PILE CAPACITY**

Evaluating the performance of different pile capacity prediction methods is not an easy task. In this study, an evaluation scheme using only analytical criteria is considered in order to observe the performance of different CPT methods for predicting the ultimate axial capacity of piles. The arithmetic mean and standard deviation of piles at seven locations( such as TP1, TP2, TP3, TP4, TP5, TP6 and TP7) for each method are calculated. The best applied method among nine methods is the one which is closer to the mean of nine methods.

Ultimate pile capacities of piles at six locations calculated by Schmertmann method and de Ruiter and Beringen method are closer to mean of nine methods than any other methods except Philipponnat method. All the values at six locations determined by these two methods are lying within plus and minus of one standard deviation.

Ultimate pile capacities for piles at five locations calculated by Schmertmann method tend to underpredict the ultimate pile capacity by not more than 25% in comparison with the mean of nine methods. This method uses sleeve friction,  $f_s$  to calculate ultimate friction capacity of pile and sleeve friction is lower in clayey soil which is predominant as shown in Figure 3.8. Ultimate pile capacities for piles at two locations calculated by this method tend to overpredict the ultimate pile capacity. According to CPT values as shown in Figure 3.10, this method exhibits 35% higher pile capacity than the mean of nine methods. In Figure 3.10 the bearing stratum of the pile is dense silty sand where high cone tip resistance exists. The ultimate end bearing capacity estimated by this method shows the largest value because of not applying any reduction factor to cone tip resistance like only Tumay and Fakhroo method. Besides this, ultimate shaft friction capacity by this method is lower, because cone shaft friction exhibits lower value in predominant clayey soil. Philipponnat method estimates better results for piles at all locations of this site fortunately, though it does not consider the consistency of cohesive soil (soft or hard) to determine the ultimate shaft friction capacity,  $Q_s$  of pile and assumes the same empirical factor for all types of clay.

de Ruiter and Beringen method also exhibits relatively better performance. Ultimate pile capacities of piles at six locations calculated by this method are closer to mean of nine methods. Ultimate pile capacity at CPT4 location is 46% higher than the mean of nine methods. In this method no reduction factor is imposed in sandy soil to calculate ultimate end-bearing capacity like Schmertmann method. This method assumes the larger empirical factor for soft clay and the lower empirical factor for stiff clay to calculate the ultimate shaft capacity of pile. Ultimate pile capacities for piles at seven locations calculated by de Ruiter

and Beringen method tend to overpredict the pile capacity. The maximum value has been observed at CPT4 location as shown in Figure 3.10.

The performance of Bustamante and Gianeselli method (LCPC/LCP method) is not satisfactory at this study. This method overpredicts the pile capacity by 24%-64% and the values at three locations are lying beyond one standard deviation. This method for the French Highway Department is based on the analysis of 197 pile load tests with a variety of pile types and soil conditions. It utilizes cone tip resistance,  $q_c$  instead of shaft friction,  $f_s$  to determine the ultimate shaft friction capacity,  $Q_s$ . To calculate shaft friction capacity it shows much larger value in clayey soil which is predominant at all seven CPT locations.

Tumay and Fakhroo method overpredicts the pile capacity excessively and pile capacities for piles at six locations are beyond one standard deviation. In this method no reduction factor is assumed for cone tip resistance,  $q_c$  to calculate the ultimate end bearing capacity. Same adhesion factor is used both for cohesive and cohesionless soil to calculate the ultimate shaft friction capacity of pile and this factor becomes very high when sleeve friction is very low.

Aoki and De Alencar method underpredicts the pile capacity and the results show the moderate performance. This method assumes the identical empirical factor for both clayey and sandy soil to find out the ultimate end bearing capacity of pile. It does not consider the consistency of cohesive soil (soft or hard) to determine the ultimate shaft friction capacity,  $Q_s$  of pile and assumes the same empirical factor for all types of clay.

Both Price and Wardle method and Penpile method tend to underpredict the pile capacity seriously and show the values beyond one standard deviation. Those are very conservative to calculate the pile capacity. Penpile method uses empirical factor 0.25 for clay and 0.125 for sand to calculate the end bearing capacity of pile when Price and Wardle method utilizes 0.35 for both types of soil. Both method uses sleeve friction,  $f_s$  to determine the shaft friction capacity.

The results of pile capacity have been estimated for different depths at seven locations using SPT values. Arithmetic mean and standard deviation at different depths for those seven locations have also been estimated. Ultimate pile capacities based on SPT values show the wide variation. Pile capacities at five locations overpredict or underpredict the pile capacity satisfactorily. The rest of the piles at two locations overpredict the pile capacity beyond one standard deviation. The soil of this site is very erratic and the thickness of soil layers varies drastically throughout the soil layer. SPT is not reliable for cohesive soil which is predominant for the whole site.

### **3.9 CONCLUDING REMARKS**

In this chapter five soil profile sections having twelve bore holes describe SPT values with depth, visual soil classification and thickness of soil layers. Cone tip resistance, sleeve friction, friction ratio and soil classification at seven different locations are presented graphically. The results of the analyses based on SPT and CPT data are conducted on square reinforced concrete piles at a site in Siddhirganj. Applicability of eight CPT methods are focused to predict the ultimate axial compression load carrying capacity of piles. The static analysis using the SPT method is applied to evaluate the load carrying capacity for seven locations of the site. Ultimate pile capacity predicted by various methods of CPT are compared graphically with the one predicted by SPT data. The pile size, type, length, the predicted ultimate load carrying capacity from CPT, the predicted ultimate load carrying capacity from SPT, average ultimate pile capacity, and standard deviation are presented in tabular form. The arithmetic mean and standard deviation are calculated in order to observe the performance of different CPT methods for predicting the ultimate axial capacity of piles. The four CPT methods, which are de Ruiter and Beringen method, Philipponnat method, Schmertmann method and Aoki and De Alencar method show better performance than the currently used method based on SPT.

## **CHAPTER FOUR**

### **CONCLUSIONS AND RECOMMENDATIONS**

#### **4.1 CONCLUSIONS**

This study presents an evaluation of the performance of eight CPT methods in predicting the ultimate load carrying capacity of square precast RC concrete piles at a site in Sidhirganj. The following CPT methods are used to predict the load carrying capacity of the piles using the CPT data: Schmertmann, Bustamante and Gianceselli (LCPC/LCP), de Ruiter and Beringen, Tumay and Fakhroo, Price and Wardle, Philipponnat, Aoki and De Alencar, and the Penpile method. The ultimate load carrying capacity for each pile is also predicted using the traditional method based on SPT, which is used by engineers for pile design and analysis. An evaluation scheme is executed to evaluate the CPT methods based on their ability to predict the ultimate pile capacity. The arithmetic mean and standard deviation of the piles are calculated for evaluation of different methods. Based on the results, the followings are the major finding of this study:

- Schmertmann method, de Ruiter and Beringen method and Philipponnat method show the best capability in predicting the load carrying capacity of square RC piles at a site in Siddhirganj. But Philipponnat method does not consider the consistency of cohesive soil (soft or hard) to determine the ultimate shaft friction capacity,  $Q_s$  of pile and assumes the same empirical factor for all types of clay.
- Aoki and De Alencar method shows moderate performance and Bustamante and Gianceselli (LCPC/LCP) method exhibits unsatisfactory performance to estimate the pile capacity for piles at this site.
- The worst methods of prediction are Penpile method and Price and Wardle method which are very conservative (underpredict the pile capacities) and the Tumay and Fakhroo method which overpredicts the pile capacities excessively.
- The four CPT methods, which are de Ruiter and Beringen method, Philipponnat method, Schmertmann method and Aoki and De Alencar method show better performance than the currently used method based on SPT. The soil of this site is very erratic and the thickness of soil layers varies drastically throughout the soil layer. SPT is not reliable for cohesive soil which is predominant for the whole site.

## 4.2 RECOMMENDATIONS FOR FURTHER STUDY

The results of this study demonstrates the capability of CPT methods in predicting the ultimate load carrying capacity of square RC piles at a site in Siddhirganj. Schmertmann method, de Ruiter and Beringen method and Philipponnat method show the best performance in predicting the ultimate load carrying capacity of square RC piles. But Philipponnat method does not consider the consistency of cohesive soil (soft or hard) to determine the ultimate shaft friction capacity,  $Q_s$  of pile and applies the same empirical factor to all types of clay. It is recommended to implement these three methods in design and analysis of square RC concrete piles.

In fact, implementation of the CPT technology in pile design will reduce the level of uncertainties associated with traditional design methods. Based on the results of the analyses, it is recommended to implement the cone penetration technology in different geotechnical applications. Regarding design and analysis of driven piles, the followings are recommended:

- Confidence of the design engineers in the CPT technology by adding the CPT to the list of the primary variables in subsurface exploration should be achieved and for soil identification and classification, and site stratigraphy it should be used. Different soil classification methods can be used such as Zhang and Tumay, Robertson and Campanella, and Olsen and Mitchell.
- The test results from the traditional subsurface exploration methods and the results interpreted from the CPT methods should be compared. With time and experience, the dependency level on the traditional subsurface exploration methods will be reduced and dependency level on the CPT technology will be increased.
- The CPT pile design methods in conjunction with the pile load tests and the method based on SPT to predict the load carrying capacity of the square RC concrete piles should be used. The following CPT methods are recommended: de Ruiter and Beringen method, Schmertmann method and Philipponnat method. If a pile load test is conducted for the site, the results of the CPT methods with the measured ultimate pile load capacity will be compared. If the measured and predicted capacities are different, then a correction to the predicted capacity in the amount of the difference between the measured and predicted capacity will be made. This correction for the design of other piles at this site should be applied.
- The role of the CPT design method will be increased and the dependency on the method based on SPT will be decreased.



## REFERENCES

Abedin, M. Z. et al. ( 1998). “ Ultimate Capacity of a Low Cost Pile Foundation in Soft Ground” , Proceedings of Conference on Low and Low Medium Cost Housing Development, 9-10 July, 1998, Kuching, Sarawak, Malaysia.

Ansary, M. A. et al. ( 1999). “ Status of Static Pile Load Tests in Bangladesh” , Proceedings of the Eleventh Asian Regional Conference on Soil Mechanics and Geotechnical Engineering, Seoul, Korea.

Aoki, N. and de Alencar, D.(1975). “An Approximate Method to Estimate the Bearing Capacity of Piles”, *Proceedings of the 5th Pan-American Conference of Soil Mechanics and Foundation Engineering*, Buenos Aires, Vl. 1, pp. 367-376.

Bandini, P. and Salgado, R. (1998). "Methods of Pile Design Based on CPT and SPT results", Proceedings of 1<sup>st</sup> International Conference on Site Characterization (P. Robertson and P. Mayne ed.), Balkema, Rotterdam, pp. 967 - 976.

Bowles, J.E.(1982). “Foundation Analysis and Design”, McGraw-Hill, Inc., New York, p.816.

**Briaud**, J-L and, Tucker, L.M.(1988). “Measured and Predicted Axial Response of 98 Piles”, Journal of Geotechnical Engineering, ASCE, Vol. 114, No. 8, pp. 984-1001.

**Briaud**, J-L et al. (1986). “H.M. Development of An improved Design Procedure for Single Piles in Clays and Sands”, Report No. MSHDRD-86-050-1, Mississippi State Highway Department, Jackson, MS, p. 192.

Bullock, P.J. et al.(2005). Side shear set-up I; Test piles driven in Florida. *ASCE Journal of Geotechnical and Environmental Engineering*. 131 (3) 292-300

Bustamante, M., and L. Gianeeselli(1982). "Pile Bearing Capacity Predictions by Means of Static Penetrometer CPT", *Proceedings of the 2nd European Symposium on Penetration Testing*, ESOPT-II, Amsterdam, Vol. 2, pp. 493-500.

Clisby, M.B. et al.(1978). "An Evaluation of Pile Bearing Capacities", Volume I, Final Report, Mississippi State Highway Department. Campanella, R.G., et al. (1989). "Use of In Situ Tests in Pile Design", *Proceedings of International Conference on Soil Mechanics and Foundation Engineering*, pp. 199 - 203.

de Ruiter, J., and F.L. Beringen.(1979). "Pile Foundations for Large North Sea Structures", *Marine Geotechnology*, Vol. 3, No. 3, pp. 267-314.

Douglas, J.B. and Olsen, R.S.(1981). "Soil Classification Using Electric Cone Penetrometer, Symposium on Cone Penetration Testing and Experience", *Geotechnical Engineering Division, ASCE, St. Louis*, pp. 209-227.

El-Sakhawy N.R. et al. (2008), "Prediction of the Axial Bearing Capacity of Piles by Five - Cone Penetration Test Based Design Methods" ,(IAMAG),India.

Eslami, A., and Fellenius, B.H.(1997). "Pile Capacity by Direct CPT and CPTU Methods Applied to 102 Case Histories", *Canadian Geotechnical Journal*, Vol. 34, pp. 886-904.

FDOT. (2010). *Standard specifications for road and bridge construction 2010. Section 455-2.2.1. Florida Department of Transportation, Tallahassee, Florida.*

Fellenius, B. H., and Eslami, A. (2002). "Soil Profile Interpreted from CPT Data", *Geotechnical Engineering Conference. Asian Institute of Technology. Bangkok. Thailand.* 18 p.

Fellenius, B. H., (1991). Summary of pile capacity predictions and comparison with observed behavior. *American Society of Civil Engineers, ASCE, Journal of Geotechnical Engineering*, Vol. 117, No. 1, pp. 192 - 195.

Fellenius B.H. (2008). Effective Stress Analysis and Set-up Capacity of Piles in clay. *Geotechnical Special Publication No. 180*.ASCE

Hu, Z. (2007). Updating Florida Department of Transportation's (FDOT) pile/shaft design procedures based on CPT & DTP data. Ph.D. dissertation, University of Florida, Gainesville, Florida.

Lambe, W.T. and Whitman, R.V. (1986). Soil Mechanics, SI Version, John Wiley and Sons, Korea.

Lehane, B.M. et al.( 2005). CPT based design of driven piles in sand for offshore structures. UWA Report, GEO: 05345.

**Long, J.H.** and Wysockey, M.H.(1999). "Accuracy of Methods for Predicting Axial Capacity of Deep Foundations", ASCE Geotechnical Special Publication GSP 88, OTRC '99 Conference, Analysis, Design, Construction, and Testing of Deep Foundations, Austin, TX, pp. 180-195.

**Lunne, T.** et al. (1997). "Cone Penetration Testing in Geotechnical Practice", Blackie Academic and Professional, London.

**Meyerhof, G. G.** (1956). "Penetration Tests and Bearing Capacity of Cohesionless Soils", Journal of Geotechnical Engineering, ASCE, 82(1), 1- 19.

Paikowsky, G.S. (2004). Load and resistance factor design (LRFD) for deep foundations. NCHRP Report 507.

Philipponnat, G.(1980). "Methode Pratique de Calcul d'un Pieu Isole a l'aide du Penetrometre Statique", *Revue Francaise de Geotechnique*, 10, pp. 55-64.

Price, G. and Wardle, I.F.(1982). “A Comparison Between Cone Penetration Test Results and the Performance of Small Diameter Instrumented Piles in Stiff Clay”, *Proceedings of the 2nd European Symposium on Penetration Testing*, Amsterdam, Vol. 2, pp. 775-780.

Robertson, P.K. and Campanella, R.G.(1984). “Guidelines for Use and Interpretation of the Electric Cone Penetration Test”, Hogentogler & Company, Inc., Gaithersburg, MD, Second Edition, p. 175.

Robertson, P.K. (1990). Soil classification using the cone penetration test. *Canadian Geotechnical Journal* 27(1): 151-158.

Robertson, P. K., and Campanella, R. G., (1989). Guidelines for use, interpretation, and application of CPT and CPTU. *Soil Mechanics Series*, No. 105, UBC, Dept. of Civil Engineering.

Schmertmann, J.H.(1978). “Guidelines for Cone Penetration Test, Performance and Design”, U.S. Department of Transportation, Report No. FHWA-TS-78-209, Washington, D.C., p.145.

Skempton, A.W.(1951). “The Bearing Capacity of Clays”, *Proceedings Building Research Congress*, Vol. 1, pp. 180-189.

Sumanta H. and Sivakumar B.(2008),”Reliability measures for pile foundations based on CPT test data”,NRC Canada.

Terzaghi, K. and Peck, R. B. (1948). *Soil Mechanics in Engineering Practice*, John Wiley and Sons Inc., New York, N.Y.

Terzaghi, K. and Peck, R. B. (1967). *Soil Mechanics in Engineering Practice*, 2nd Edition, John Wiley and Sons Inc., New York, N.Y.

Togliani G.( 2008). “Pile Capacity Prediction for in Situ Tests”, *Proceedings ISC-3. Taiwan*, 1187-1192. Taylor & Francis Group, London, UK.

Tomlinson, M. J. (1971). Some effects of pile driving on skin friction, Proceedings of the Conference on the Behavior of Piles, Institution of Civil Engineers, London, 107-14.

Tomlinson, M. J. (2001). *Foundation Design and Construction*. 7th ed., Pearson Education Ltd, Essex, 99 - 154.

Tumay, M.T.(1994). “Implementation of Louisiana Electric Cone Penetrometer System (LECOPS) for Design of Transportation Facilities”, Executive Summary, Report No. FHWA/LA-94/280 A&B. LTRC, Baton Rouge, LA.

Tumay, M.T., and Fakhroo, M.(1982). “Friction Pile Capacity Prediction in Cohesive Soils Using Electric Quasi-Static Penetration Tests”, Interim Research Report No. 1, Louisiana Department of Transportation and Development, Research and Development Section, Baton Rouge, LA, 275 p.

**Zhang, Z. and M.T. Tumay** (2003). “Nontraditional Approaches in Soil Classification Derived from the Cone Penetration Test,” ASCE Special Publication No. 121 on Probabilistic Site Characterization at the National Geotechnical Experimentation Sites, ISBN 0-7844-06693, pp. 101-149.

Zhou, J. et al. (1982). " Prediction of Limit Load of Driven Pile by CPT,” Penetration Testing, Proc. 2nd European Symp. Penetration Testing, *ESOPT II*, Amsterdam, Vol. 2, pp. 957-961.

**APPENDIX-A**  
**SPLICED PRECAST R.C. CONCRETE PILES**



Figure A1 Spliced Precast RC Concrete Piles before driving  
(Source: PWD)



Figure A2 Spliced Precast RC Concrete Piles before casting and during driving  
(Source: PWD)

**APPENDIX B**  
**SAMPLE CALCULATION**

$$Q_u = Q_s + Q_t$$

Where  $Q_u$  = total ultimate pile capacity

$Q_s$  = ultimate shaft friction capacity

$Q_t$  = ultimate end bearing capacity

Ultimate pile capacity of 355mm×355mm×21m spliced precast RC concrete pile is calculated from figure 3.7 as shown in chapter 3 using 8 different CPT methods.

**1. Schmertmann method**

$$q_t = \frac{q_{c1} + q_{c2}}{2}$$

$$q_{c1} = 5030 \text{ KPa}$$

$$q_{c2} = \frac{\left( \frac{4.3+2.73}{2} \right) \times 1.3 + 2.73 \times 0.82 + \left( \frac{2.73+1.24}{2} \right) \times 0.18 + 0.77 \times 1.72}{4.02} \times 1000$$

$$= 2110 \text{ KPa}$$

$$\text{Unit tip resistance, } q_t = \frac{5030 + 2110}{2}$$

$$= 3570 \text{ KPa}$$

Ultimate end bearing capacity,  $Q_t = 3570 \times 0.355 \times 0.355$

$$= 450 \text{ KN}$$



Shaft friction is used to calculate ultimate friction capacity.

$$f_s = 0.8 \times \frac{100+67.4}{2} \times 1.27 + 0.8 \times 67.4 \times 0.63 + 0.8 \times \frac{67.4+6}{2} \times 0.7 +$$

$$1.16 \times 5 \times 7.9 + 1.05 \times 18.2 \times 0.88 + 1.14 \times 8 \times 2.99 + 0.78 \times 46.3 \times 0.6 + 1 \times 21.1 \times 3.23$$

$$= 319.4 \text{ KN/m}$$

Ultimate shaft friction capacity,  $Q_s = 319.4 \times 4 \times 0.355 = 453.5 \text{ KN}$

Ultimate pile capacity,  $Q_u = 453.5 + 450$   
 $= 903.5 \text{ KN}$

## 2. de Ruiter and Beringen method

$$q_{c1} = 5030 \text{ KPa}$$

$$q_{c2} = 2110 \text{ KPa}$$

$$q_t = \frac{5030 + 2110}{2} = 3570 \text{ KPa}$$

Ultimate end bearing capacity,  $Q_t = 3570 \times 0.355 \times 0.355$   
 $= 450 \text{ KN}$

Cone tip resistance,  $q_c$  is used to calculate ultimate friction capacity.

$$f_s = 11.72 \times 1.3 + 9.1 \times 0.82 + 6.62 \times 0.18 + (770 \times 1.72 \times 0.5)/20 + (650 \times 6.3)/20 + (0.5 \times 900 \times 0.9)/20$$

$$+ (600 \times 3.0)/20 + (0.5 \times 770 \times 5.8)/20$$

$$= 483.8 \text{ KN/m}$$

Ultimate shaft friction capacity,  $Q_s = 483.8 \times 4 \times 0.355 = 687 \text{ KN}$

Ultimate pile capacity,  $Q_u = 687 + 450$   
 $= 1137 \text{ KN}$

## 2. Bustamante and Gianeselli method ( LCPC method)

$$q_{ca} = \frac{q_{c1} + q_{c2}}{2}$$
$$= \frac{5030 + 3305}{2}$$
$$= 4170 \text{ KPa}$$

$$q_{eq} = 3900 \text{ KPa}$$

Unit tip resistance,  $q_t = k_b q_{eq}(\text{tip})$

$$= 0.45 \times 3900$$
$$= 1755 \text{ KPa}$$

Ultimate end bearing capacity,  $Q_t = 1755 \times 0.355 \times 0.355$

$$= 221.2 \text{ KN}$$

Cone tip resistance,  $q_c$  is used to calculate ultimate friction capacity.

Curve no. 1 or 2 based on pile category no. 9 and the value of  $q_c$  are used to obtain friction capacity.

$$f_s = 30 \times 1.3 + 28 \times 0.82 + 21 \times 0.18 + 40 \times 1.72 + 25 \times 6.3 + 40 \times 0.9 + 24 \times 3 + 40 \times 5.8$$
$$= 632 \text{ KN/m}$$

Ultimate shaft friction capacity,  $Q_s = 632 \times 4 \times 0.355 = 897.5 \text{ KN}$

Ultimate pile capacity,  $Q_u = 897.5 + 221.2$

$$= 1118.7 \text{ KN}$$

#### 4. Tumay and Fakhroo method( Cone-m method)

$$q_t = \frac{5030+4000}{4} + \frac{2110}{2}$$
$$= 3310 \text{ KPa}$$

Ultimate end bearing capacity,  $Q_t = 3310 \times 0.355 \times 0.355$   
 $= 417.5 \text{ KN}$

Shaft friction is used to calculate ultimate friction capacity.

$$f_{sa} = \frac{F_t}{L}$$
$$= \frac{106.3+42.5+25.7+39.5+16+23.92+27.8+68.2}{18.2}$$
$$= 19.23 \text{ KPa}$$
$$= 0.2 \text{ tsf}$$

$$m = 0.5 + 9.5e^{-9f_{sa}}$$
$$= 2.07$$

Ultimate shaft friction capacity,  $Q_s = 2.07 \times 19.23 \times (4 \times 0.355 \times 18.2) = 1029 \text{ KN}$

Ultimate pile capacity,  $Q_u = 1029 + 417.5$   
 $= 1446.5 \text{ KN}$

#### 5. Aoki and De Alencar method

$$q_{ca} = 3570 \text{ KPa}$$

$$q_t = \frac{q_{ca}(\text{tip})}{F_b}$$

$$q_t = \frac{3570}{1.75} = 2040 \text{ KPa}$$

Ultimate end bearing capacity,  $Q_t = 2040 \times 0.355 \times 0.355$   
 $= 257.1 \text{ KN}$

Cone tip resistance,  $q_c$  is used to calculate ultimate friction capacity.

$$f_s = \frac{0.022}{3.5} \times (3.52 \times 1.3 + 2.73 \times 0.82 + 2 \times 0.18) \times 1000 + (0.04 \times 770 \times 1.72) / 3.5 + \frac{0.04}{3.5} \times$$

$$(650 \times 6.3 + 900 \times 0.9 + 600 \times 3) + (770 \times 5.8 \times 0.06) / 3.5$$

$$= 213.4 \text{ KN/m}$$

Ultimate shaft friction capacity,  $Q_s = 213.4 \times 4 \times 0.355 = 303.1 \text{ KN}$

Ultimate pile capacity,  $Q_u = 303.1 + 257.1$   
 $= 560.2 \text{ KN}$

## 6. Price and Wardle method

$$q_t = k_b q_c$$

$$= 0.35 \times 3570$$

$$= 1249.5 \text{ KPa}$$

Ultimate end bearing capacity,  $Q_t = 1249.5 \times 0.355 \times 0.355$   
 $= 157.5 \text{ KN}$

Shaft friction is used to calculate ultimate friction capacity.

$$f_s = 0.53 \times (106.3 + 42.5 + 25.7 + 39.5 + 16 + 23.92 + 27.8 + 68.2)$$

$$= 185.5 \text{ KN/m}$$

Ultimate shaft friction capacity,  $Q_s = 185.5 \times 4 \times 0.355 = 263.35$  KN

Ultimate pile capacity,  $Q_u = 263.35 + 157.7$   
 $= 421.05$  KN

## 7. Philipponnat method

$$q_{ca} = \frac{5030 + 3305}{2}$$

$$= 4170 \text{ KPa}$$

$$q_t = k_b q_{ca}$$

$$= 0.42 \times 4170$$

$$= 1715.4 \text{ KPa}$$

Ultimate end bearing capacity,  $Q_t = 1715.4 \times 0.355 \times 0.355$   
 $= 220.7$  KN

Cone tip resistance,  $q_c$  is used to calculate ultimate friction capacity.

$$f_s = \frac{1.25}{60} \times (3.52 \times 1.3 + 2.73 \times 0.82 + 2 \times 0.18) \times 1000 + \frac{1.25}{50} \times (0.77 \times 1.72 + 0.65 \times 6.3$$
  
 $+ 0.9 \times 0.9 + 0.6 \times 3 + 0.77 \times 5.8) \times 1000$   
 $= 461.86 \text{ KN/m}$

Ultimate shaft friction capacity,  $Q_s = 461.86 \times 4 \times 0.355 = 655.8$  KN

Ultimate pile capacity,  $Q_u = 655.8 + 262.8$   
 $= 876.5$  KN

## 8. Penpile method

$$q_t = 0.125 \times 3570$$

$$= 446.3 \text{ KPa}$$

$$\text{Ultimate end bearing capacity, } Q_t = 446.3 \times 0.355 \times 0.355$$

$$= 56.2 \text{ KN}$$

$$q_s = \frac{f_s}{1.5 + 0.1f_s}$$

$$f_s = \frac{106.3 + 42.5 + 25.7 + 39.5 + 16 + 23.92 + 27.8 + 68.2}{18.2}$$

$$= 19.23 \text{ KPa}$$

$$= 2.79 \text{ psi}$$

$$q_s = 1.57 \text{ psi}$$

$$\text{Ultimate shaft friction capacity, } Q_s = (1.57 \times 14 \times 4 \times 716.54) / 1000 = 63 \text{ K} = 280.23 \text{ KN}$$

$$\text{Ultimate pile capacity, } Q_u = 280.23 + 56.2$$

$$= 336.4 \text{ KN}$$

### ULTIMATE PILE CAPACITY BASED ON SPT

For cohesionless soil,  $q_t = \alpha N_q \sigma_v'$

$$N_{\text{avg}} = \frac{32 + 26}{2} = 29$$

For  $N=29$ ,  $\phi=34^\circ$

$$\sigma_v' = (18-9.8) \times 21 = 172.2 \text{ KPa}$$

$$\begin{aligned} \text{Unit tip resistance, } q_t &= 0.62 \times 50 \times 172.2 \\ &= 5338 \text{ KPa} \leq 5000 \text{ KPa} \end{aligned}$$

$$\begin{aligned} \text{Ultimate end bearing capacity, } Q_t &= 5000 \times 0.355 \times 0.355 \\ &= 630 \text{ KN} \end{aligned}$$

$$q_{s1} = \sigma'_{\text{avg}} K \tan \phi$$

For  $N_{\text{avg}}=28$ ,  $\phi=34^\circ$

$$\begin{aligned} q_{s1} &= 86 \times 1.3 \tan 34 \\ &= 75.5 \text{ KPa} \end{aligned}$$

$$q_{s2} = c_a l$$

For  $N_{\text{avg}}=8$ ,  $c=0.5 \text{ tsf}$

$$q_{s2} = 35 \times 8 = 280 \text{ KN/m}$$

$$\text{Ultimate shaft friction capacity, } Q_s = (75.5 \times 7 \times 0.6 + 280) \times 4 \times 0.355 = 847.7 \text{ KN}$$

$$\text{Ultimate pile capacity, } Q_u = 847.7 + 630 = 1477.7 \text{ KN}$$

## APPENDIX-C

### CPT EQUIPMENT

The components of CPT equipment are as follows:

- CPT Machine
- Hydraulic pump
- CPT cone
- CPT rods
- Soil anchors
- Reaction beams
- PC Interface monitor



Figure C1 Hydraulic Pump





Figure C2 CPT Machine



Figure C3 Short beams inside the machine



Figure C4 Long beams on top of the short ones

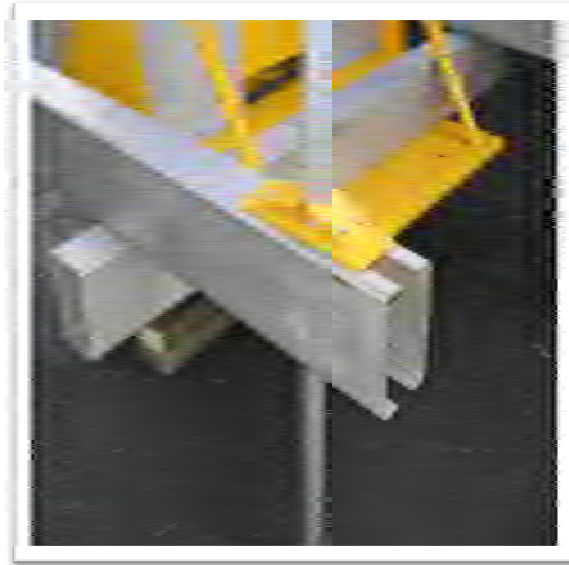


Figure C5 Automatic locks on the auger rods.

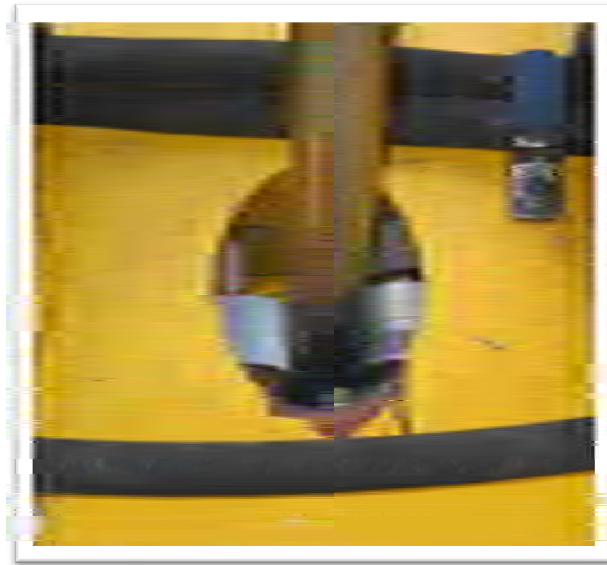
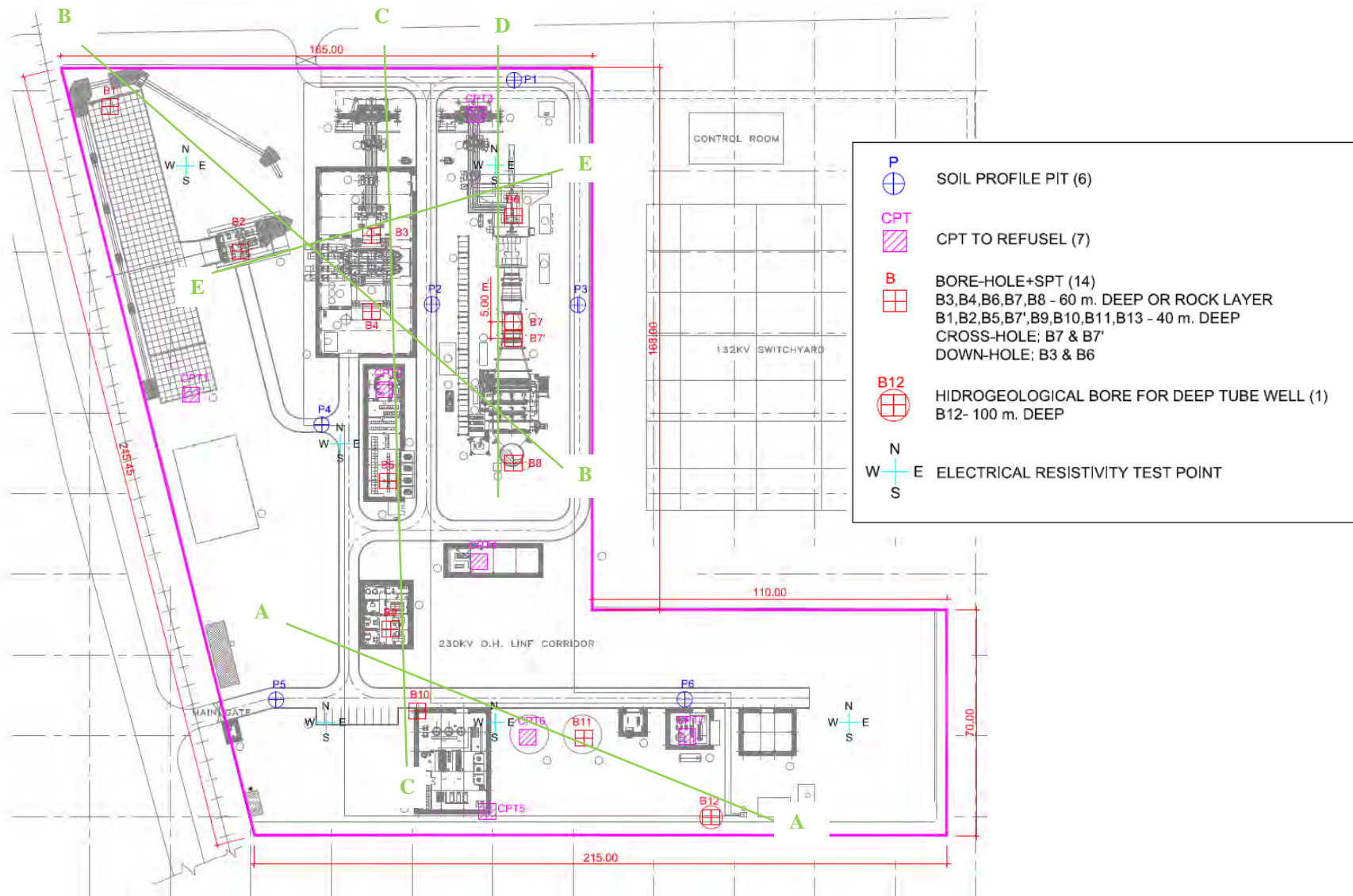


Figure C6 Depth Sensor Wheel



**Figure A1: Layout of bore holes and sections**

RL=570 m

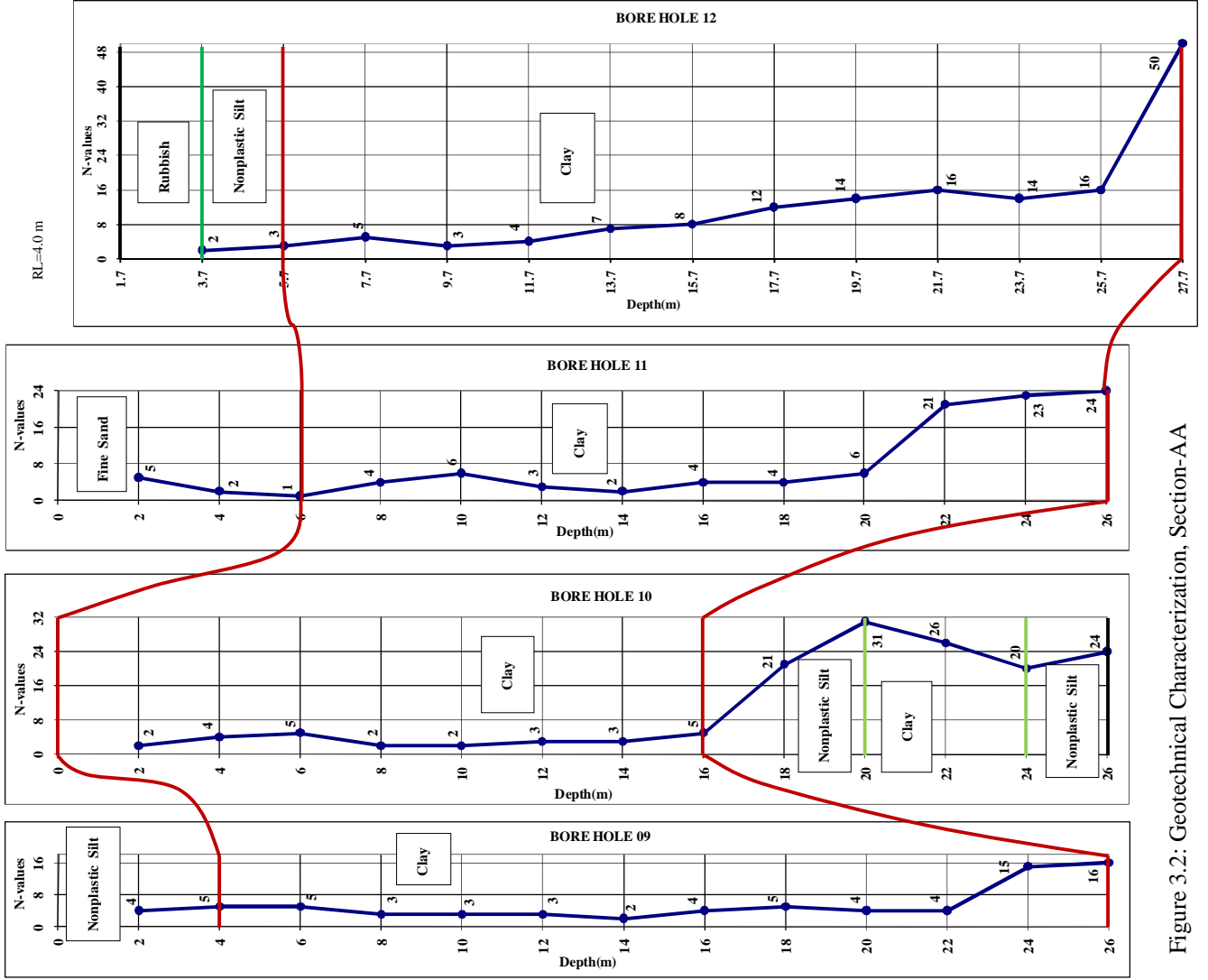


Figure 3.2: Geotechnical Characterization, Section-AA

RL=5.7 m

RL=5.3 m

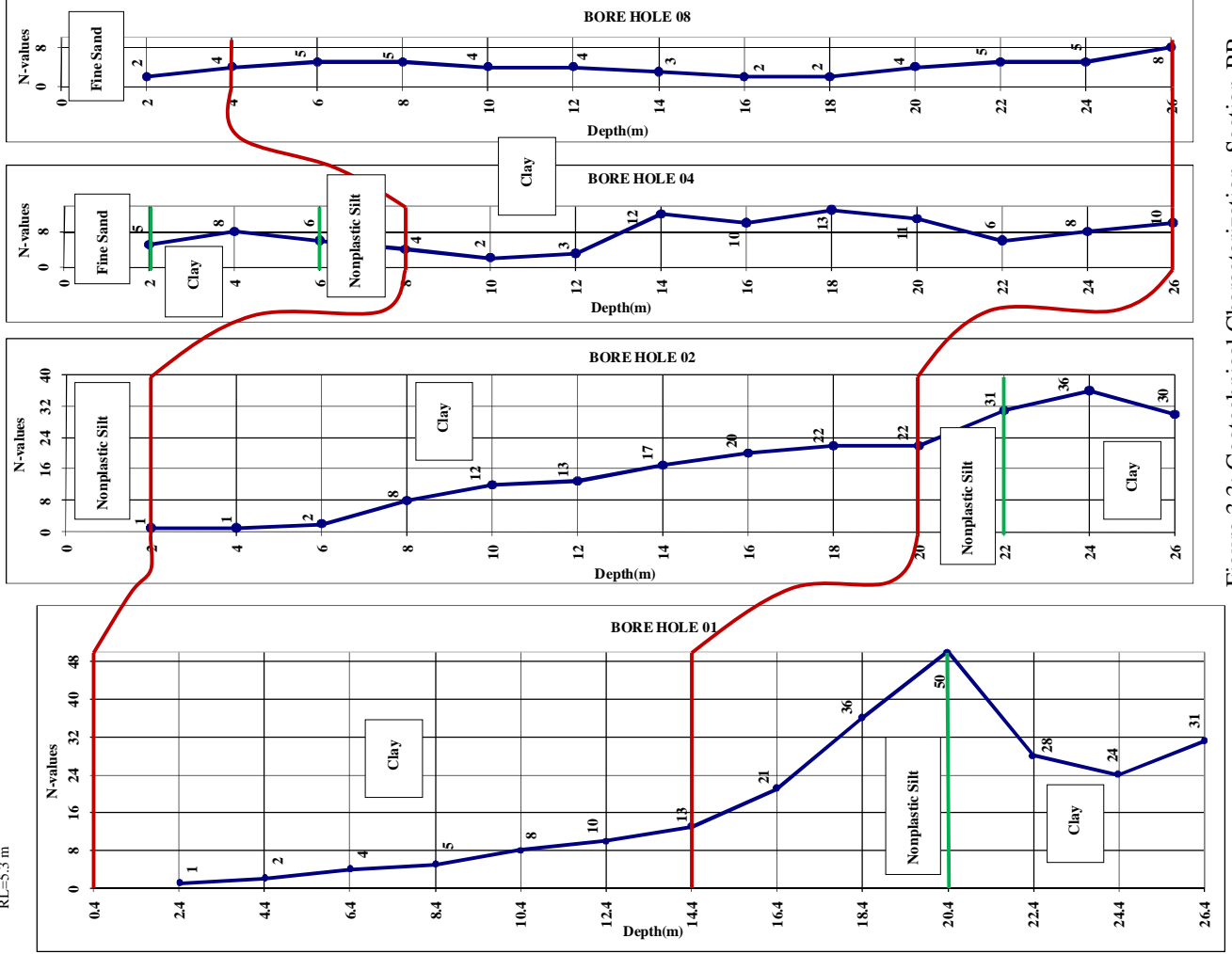


Figure 3.3: Geotechnical Characterization, Section-BB

RL=5.70 m

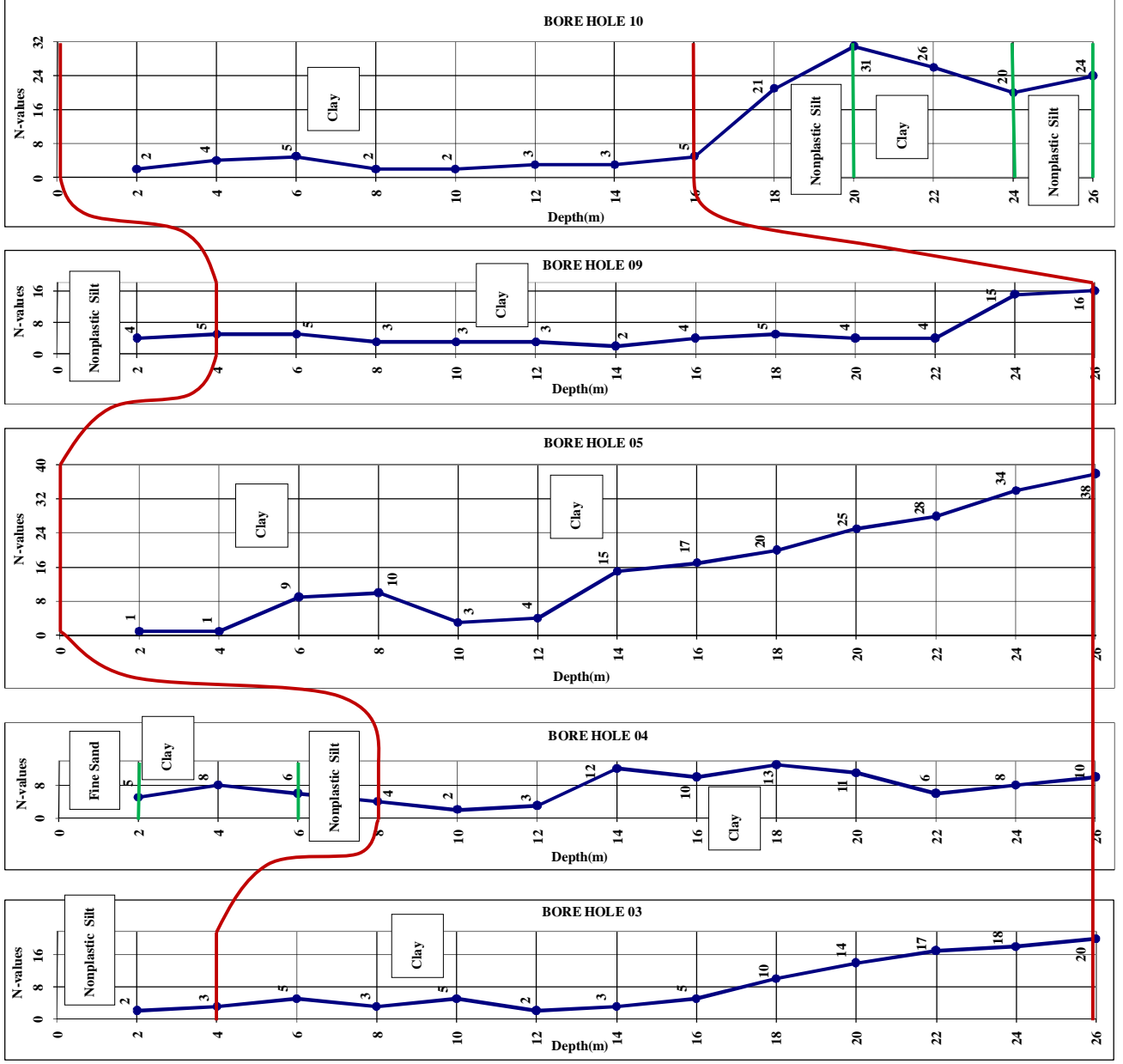


Figure 3.4: Geotechnical Characterization, Section-CC

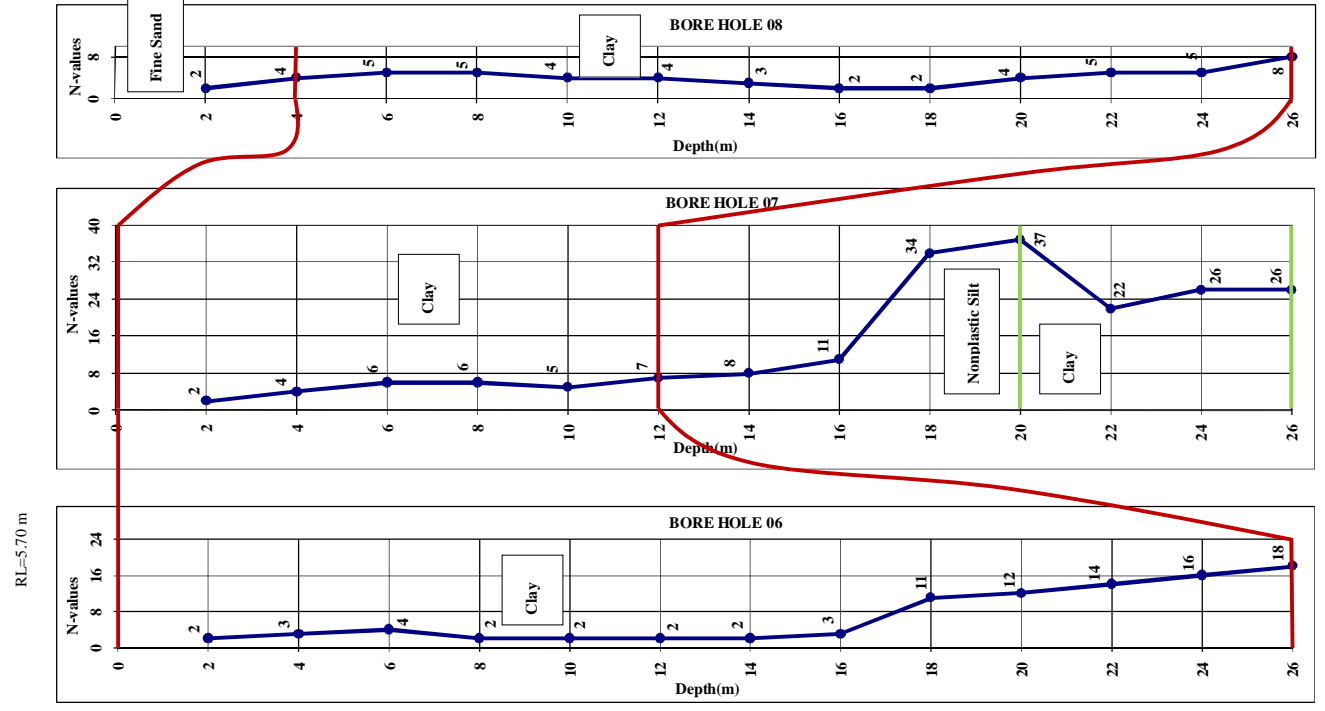


Figure 3.5: Geotechnical Characterization, Section-DD

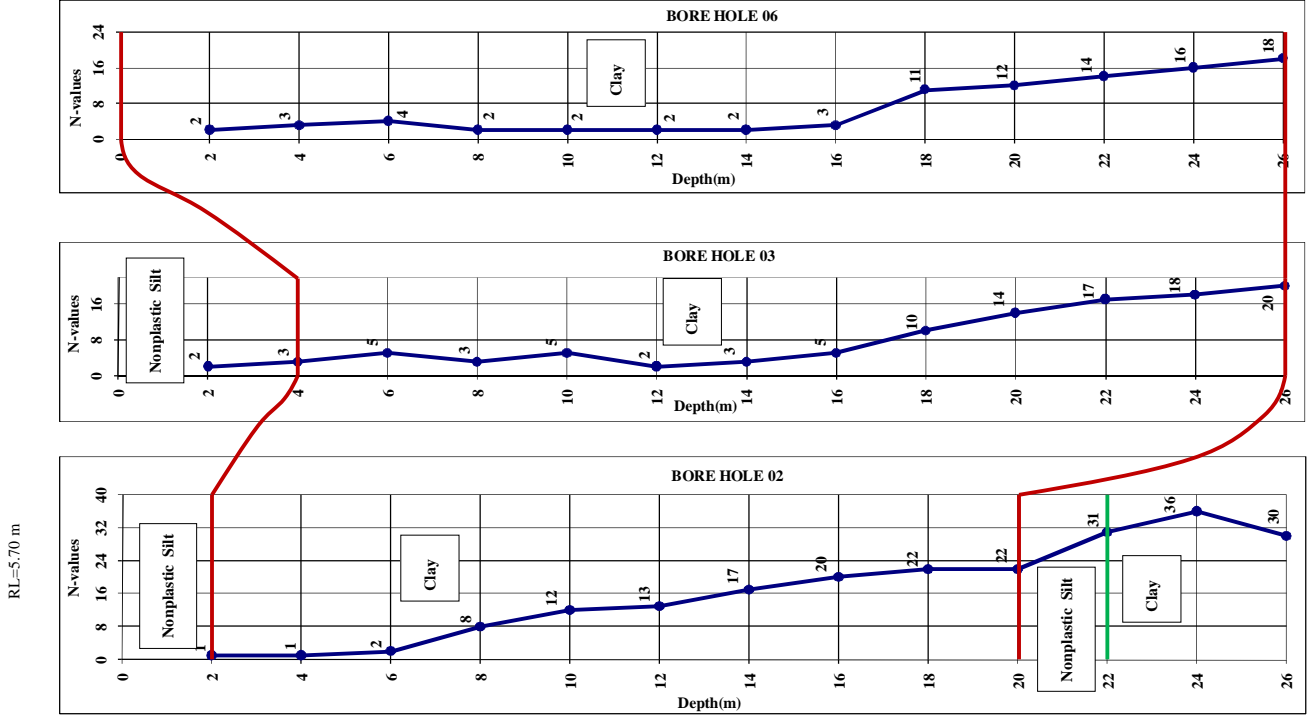


Figure 3.6: Geotechnical Characterization, Section-EE